Development of a dynamic tensioner device for joint gap stiffness during knee arthroplasty

by
Daniël Jacobus Wium

Thesis presented in partial fulfilment of the requirements for the degree of Master of Engineering (Mechanical) in the Faculty of Engineering at Stellenbosch University

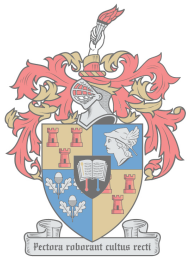

Supervisor: Dr J.H. Müller

March 2018

Declaration

By submitting this thesis electronically, I declare that the entirety of the work contained therein is my own, original work, that I am the sole author thereof (save to the extent explicitly otherwise stated), that reproduction and publication thereof by Stellenbosch University will not infringe any third party rights and that I have not previously in its entirety or in part submitted it for obtaining any qualification.

Date: March 2018

Abstract

Correct knee alignment and soft tissue tensions can relieve pain, improve knee function and increase the durability of the prosthesis after knee arthroplasty. Knee alignment and soft tissue tensions relate to the joint gap stiffness. The joint gap stiffness is a measure of the tension in the ligaments and the distance between the femur and the tibia. The joint gap stiffness of the knee is typically assessed with the knee in 0° and 90° knee flexion. Guidelines for the tension of the ligaments and the distance between the femur and the tibia have not yet been defined for knee flexion between these angles. The aim of this study is to provide a proof of concept for a dynamic knee tensioning device capable of measuring the joint gap stiffness at all angles between 0° and 90° knee flexion during unicompartmental knee arthroplasty. In this study, two prototypes were developed which quantify the joint gap stiffness in terms of the tibiofemoral force and the gap distance. The prototypes are capable of either measuring the tibiofemoral force at a constant gap distance or measuring the gap distance at a constant distraction force. Three *in-vitro* tests were conducted in which the prototypes were used to measure the joint gap stiffness of cadaver knees. The joint gap stiffness was measured in the native knee (intact femur) as well as in the resurfaced knee. The results have proven that the knee tensioners developed in this study can provide insight into certain characteristics of the knee, which include knee stiffness, spatial geometry, and articulating surface geometry of either the medial or the lateral compartments. The knee tensioners assess the outcome of soft tissue balancing on a quantitative level which can be correlated to postoperative results. This may lead to the standardisation of soft tissue balancing. The knee tensioners developed in this study provide a concept for the design of a dynamic knee tensioner to be used during clinical unicompartmental knee arthroplasty as well as in clinical total knee arthroplasty.

Opsomming

Korrekte knie-belyning en sagteweefsel-spanning kan die funksie van ‘n knie verbeter en die duursaamheid van ‘n prostese verleng na afloop van ‘n knievervangingsoperasie. Knie-belyning en sagteweefsel-spanning hou verband met die kniegewrig-gaping-styfheid. Die kniegewrig-gaping-styfheid is ‘n funksie van die spanning in die knieligamente en ‘n funksie van die afstand tussen die femur en die tibia. Die kniegewrig-gaping-styfheid word tipies geassesseer met die knie in 0° en 90° fleksie. Daar bestaan nog nie riglyne om die spanning in die knieligamente óf die afstand tussen die femur en die tibia tussen hierdie hoeke van knie-fleksie te bepaal nie. Die doel van hierdie studie is om ‘n konsepbewys te lewer vir ‘n nuwe dinamiese knietoestel wat die gewrig-gaping-styfheid kan meet by alle hoeke van knie-fleksie tussen 0° en 90° tydens ‘n halwe knievervangingsoperasie. In hierdie studie is twee prototipes ontwikkel wat die kniegewrig-gaping-styfheid kwantifiseer in terme van die spanning in die knieligamente en die afstand tussen die femur en die tibia. Die prototipes kan óf die tibiofemorale krag meet met ‘n konstante gaping-afstand óf die gaping-afstand meet met ‘n konstante tibiofemorale krag. Drie *in-vitro* toetse, waartydens die gewrig-gaping-styfheid van kadawer knieë gemeet is, is uitgevoer. Die gewrig-gaping-styfheid is gemeet in die oorspronklik knie met die ongeskonde femur en ook in die knie waarby prostetiese femurs ingevoeg is. Die *in-vitro* toetse het insiggewende resultate rakende die styfheid van die knie, die geometrie van die knie ruimte, en die geometrie van die kontakoppervlakte van die bene in óf die laterale óf mediale kompartemente gelewer. Die knietoestelle assesseer die uitkoms van sagteweefsel-balansering tydens ‘n knievervangingsoperasie op ‘n kwantitatiewe vlak wat met resultate verkry na ‘n operasie gekorreleer kan word. Dit mag lei tot die standaardisering van sagteweefsel-balansering. Die knietoestelle in hierdie studie lewer ‘n konsep vir die ontwerp van ‘n dinamiese knietoestel wat in ‘n kliniese halwe knievervangingsoperasie en in ‘n kliniese totale knievervangingsoperasie gebruik kan word.

Acknowledgements

The author would like to thank Dr JH Müller for his supervision and guidance throughout the course of this study. Furthermore, the author would like to thank Dr Willem van der Merwe for his advice and suggestions for the research of this thesis and his participation in the tests that were conducted. The organisation of cadaver tests by Mrs L Burger is also greatly appreciated.

Lastly, the author would like to thank his fellow BERG colleagues for the camaraderie and his family, friends and girlfriend for their reliable support and advice throughout this study.

Table of contents

List of figures

List of tables

Nomenclature

Abbreviations

ACL	Anterior Cruciate Ligament
ADC	Analog to Digital Converter
CAD	Computer-aided Design
CAS	Computer Assisted Surgery
CR	Cruciate Retaining
DMP	Digital Motion Processor
FFT	Fast Fourier Transform
GND	Ground (electrical circuit)
GUI	Graphical User Interface
IDE	Integrated Development Environment
IMU	Inertial Measurement Unit
MAE	Mean Absolute Error
PCB	Printed Circuit Board
PCL	Posterior Cruciate Ligament
PS	Posterior Stabilised
RMS	Root Mean Square
SNR	Signal to Noise Ratio
TKA	Total Knee Arthroplasty
UKA	Unicompartmental Knee Arthroplasty
WOMAC	Western Ontario and MacMaster Universities Osteoarthritis Index

Symbols

σ	Bending stress	[Pa]
τ	Shear stress	[Pa]
Δ	Beam and plate deflection	[m]
A_{signal}	Amplitude of tibiofemoral force signal	[N]
A_{noise}	Amplitude of noise in tibiofemoral force signal	[N]
b	Width of femur plate	[m]
C	Capacitance	[F]
E	Modulus of Elasticity	[Pa]
F	Force on femur plate	[N]
H	Thickness of femur plate	[m]
I	Moment area of inertia	[m^4]
ℓ	Length of femur plate	[m]
n	Sample size	[-]
R	Electrical resistance	[Ω]
V_{in}	Input voltage of first-order analog filter	[V]
V_{out}	Output voltage of first-order analog filter	[V]
$V_{BridgeOut}$	Output voltage of Wheatstone bridge	[V]
V^{+}_{in}	Input of pin 6 of INA125 instrumentation amplifier	[V]
V^{-}_{in}	Input of pin 7 of INA125 instrumentation amplifier	[V]
$V_{Ref}Out$	Reference voltage of Wheatstone bridge	[V]

1 Introduction

In this study, a dynamic knee tensioning device which can potentially be used during knee arthroplasty was developed and tested. This research study was conducted for a Master's degree at Stellenbosch University's Mechanical and Mechatronic Engineering Department. In this introductory chapter, a brief background of the study is given, followed by the motivation for the study and the objectives that were to be achieved. This is followed by the methodology of the study and the layout of the contents of this thesis.

1.1 Background

Knee arthroplasty is a procedure that can relieve pain, correct instability during the gait cycle, and improve the range of motion of patients who either suffer from disease or deformity (Campbell, Schuster, Pfluger, & Hoffmann, 2010). Knee alignment and stability are important concepts in knee arthroplasty. A knee joint that is correctly aligned can not only relieve pain, but also improve knee function and longevity of the prosthesis after knee arthroplasty. In addition to the joint alignment, the tension of the ligaments in the knee should also be well-balanced mediolaterally (Kwak, Kong, Han, Kim, & In, 2012).

The alignment of the knee and the tension of the soft tissue relates to the joint gap stiffness of the knee. The joint gap stiffness of the knee is a measure of the tension in the ligaments and the distance between the femur and the tibia. It is assessed after the tibial and femoral resections have been made and before the prosthetic components have been inserted. During the assessment of the joint gap stiffness, a distraction force is typically applied between the tibia and the femur.

However, there are no set standards to which the distance between the bones or the tension of the ligaments must conform to. Instead, the outcome of the assessment of joint gap stiffness is very much dependant on a surgeon's subjective feel and experience (Nowakowski, Majewski, Müller-Gerbl, & Valderrabano, 2011).

1.2 Motivation

The tension of the ligaments, and the distance between the femur and the tibia have not been quantified as a function of all angles of knee flexion. Since the joint gap stiffness of the knee is typically assessed with the knee in 0° and 90° knee flexion, guidelines for the tension of the ligaments and the distance between the femur and the tibia have not yet been defined for all angles between 0° and 90° knee flexion. In past studies, knee tensioning devices have been developed in order to quantify the joint gap stiffness. However, these devices can only measure the joint gap stiffness at static angles of knee flexion. By quantifying the joint gap stiffness at all angles between 0° and 90° knee flexion, a profile for the stiffness of the knee can

be generated. The surgical community stand to benefit from datasets that report on the intact stiffness profile, since normative data can be derived against which resurfaced knees can be compared. With this information, knee arthroplasty morphology and surgical techniques can be optimised to ensure the restoration of the pre-arthritic knee or the correction of a deformity.

1.3 Aim and objectives

The aim of this study is to provide a proof of concept for a dynamic knee tensioning device capable of measuring the joint gap stiffness during knee arthroplasty at all angles between 0° and 90° knee flexion.

In order to quantify the joint gap stiffness, the distance between the tibia and the femur, as well as the distraction force applied between the tibia and the femur, must be measured simultaneously as a function of the angle of knee flexion.

The following objectives were identified that ensure the achievement of the aim of the study:

1. Perform a literature study on:

    a. Current techniques in the assessment of joint gap stiffness during knee arthroplasty.
    b. Previously developed knee tensioning devices.

2. Develop a knee tensioning device capable of:

    c. Applying a distraction force between the femur and the tibia.
    d. Measuring the distraction force.
    e. Measuring the distance between the femur and the tibia.
    f. Measuring all angles of knee flexion between 0° and 90°.
    g. Measuring the distraction force, the distance between the tibia and the femur, and the angle of knee flexion simultaneously.

3. Prove the functionality of the knee tensioning device by:

    h. Measuring and recording the distraction force, the distance between the femur and the tibia, and the angles of knee flexion between 0° and 90° in a human knee.
    i. Presenting the measured joint gap stiffness as a function of the angle of knee flexion.

1.4 Methodology

Before concepts for the knee tensioning device were generated, a literature study was done on the assessment of joint gap stiffness and how previously developed devices have been used to quantify it. Different concepts for the knee tensioning device were then generated and a final concept was chosen as the design for the manufactured knee tensioner.

After the design of the knee tensioning device was finalised, a prototype was manufactured. An *in-vitro* test was conducted in which the prototype was used to measure the joint gap stiffness of a cadaver knee. The prototype was used with the native knee (intact femur) as well as with a femoral prosthetic component.

After the first *in-vitro* test, shortcomings of the design were identified and a second prototype was manufactured which improved on the design of the first prototype. Two more *in-vitro* tests were conducted with the second prototype in which the joint gap stiffness of cadaver knees was measured with the native knee as well as with different femoral prosthetic components. All measurements during the *in-vitro* tests were recorded and the joint gap stiffness was presented as a function of the angle of knee flexion.

1.5 Report layout

Before the development of the knee tensioning device is discussed in this report, a literature review is given in Chapter 2. In this literature review, knee arthroplasty is explained and more specifically a technique in which the soft tissue is assessed, which addresses the need for the knee tensioning device that was developed for this thesis. Chapter 3 follows with a description of the design of the knee tensioner, including the concepts that were considered, the design considerations, and the technical issues related to it. The *in-vitro* tests are described in Chapter 4 and the results of the tests are presented in Chapter 5. A discussion of the results is then given in Chapter 6.

2 Literature study

2.1 Introduction

A literature study was conducted to gain insight into the background of the thesis and to determine how the findings of the thesis influence the field of knee arthroplasty.

In this Chapter, a brief overview of knee arthroplasty is presented followed by a more in-depth description of one aspect of the knee arthroplasty technique. Since joint gap stiffness is quantified in this study, the factors that influence this were first studied. Subsequently, previous research on joint gap quantification and the tools developed for this purpose are presented. First, certain terms used in this thesis are explained.

2.2 Terminology

In this thesis, certain terms are used that are mostly used in the field of medicine and might therefore not be well known to some readers. In this section, these terms will be defined.

In order to define regions of the knee joint, the anatomical planes and directions of the body are used. Three planes that describe anatomical positions of the human body: The Sagittal plane, the Coronal plane and the Transverse plane. In Figure 1, these three planes are shown. The Sagittal plane divides the body into left and right sides. The Coronal plane is perpendicular to the Sagittal plane and divides the body into the front and back sides. The Transverse plane is perpendicular to both the Sagittal and Coronal planes and divides the body into the top and bottom halves (Body Planes and Sections, 2016).

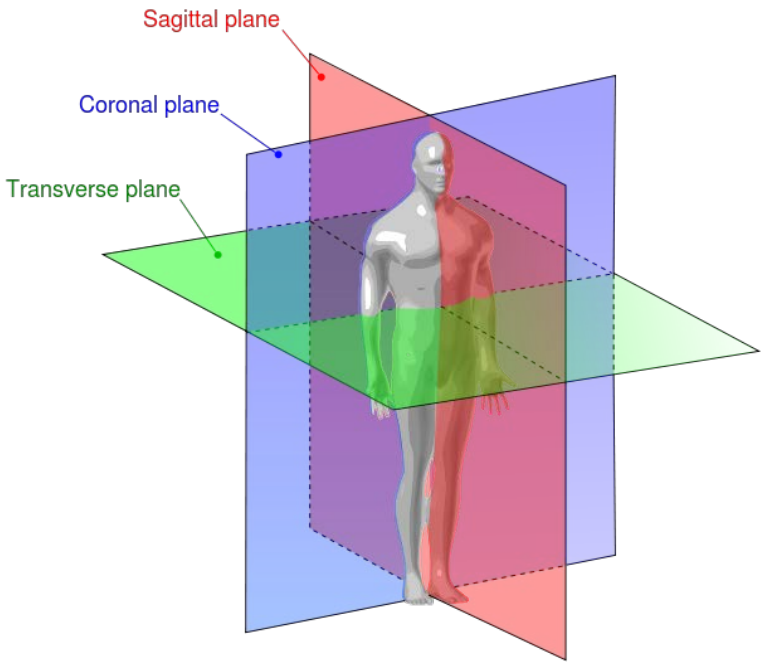

Figure 1: Anatomical planes of the human body (Body Planes and Sections, 2016)

The following pairs of directions are often used to describe locations of the body: Anterior and posterior, proximal and distal, and medial and lateral. Anterior means: In the direction of the chest side of the body, and posterior means: In the direction of the back of the body. The Coronal plane can also be seen as dividing the body into the anterior and posterior sides. Proximal and distal refer to a position on a limb with respect to the trunk of the body or the origin of the limb. Proximal refers to: Closest to the trunk or origin of the limb, and distal refers to: Furthest from the trunk or origin of the limb (Schmidler, Anatomy Terms, 2017). Medial and lateral refer to a position further and closer to the Sagittal plane, respectively. For example, the knee has a medial and lateral femoral condyle. The medial condyle is the condyle on the inner side of the leg and the lateral femoral condyle is the condyle on the outer side of the leg (Cheprasov, 2017).

Two other terms that will be used to describe the angle of the knee are varus and valgus. A varus-angled knee refers to the distal part of the lower leg being more medial than the knee joint, and a valgus-angled knee refers to the distal part of the lower leg being more lateral than the knee joint (Luijkx, 2017).

2.3 Knee arthroplasty

In this study, the joint gap stiffness of the knee is measured during knee arthroplasty. In this section, an overview of this surgical procedure is presented.

This overview provides insight into the field on which the results of this study has an impact. In this overview, the reason for the procedure, a description of the procedure itself, the implants, and the end-results of the procedure are given.

2.3.1 Background

The word “arthroplasty” refers to the replacement of a joint or the reconstruction of the joint using surgery. During knee arthroplasty, the articulating surfaces of the bones in the knee joint are replaced by prosthetic components. Either the entire knee joint can be replaced or only a certain compartment of the knee joint. Knee arthroplasty in which the entire knee joint is replaced is called total knee arthroplasty (TKA) and knee arthroplasty in which only one compartment of the knee is replaced is called unicompartmental knee arthroplasty (UKA). In cases where the underside of the patella and the groove on the femur with which it makes contact is damaged, these two surfaces can also be replaced during patellofemoral arthroplasty.

In Figure 2, the anatomy of a normal knee is shown. The knee joint is situated at the point where the distal end of the femur, the thigh bone, meets the proximal end of the tibia, the shin bone. These bones are connected by the collateral ligaments and the anterior and posterior cruciate ligaments. In between the distal femur and the proximal tibia lies the meniscus. The meniscus acts as a cushion for shock absorption and provides a surface on which the condyles of the femur can roll and slide. The articulating surface of the femoral condyles are covered in cartilage, which allows smooth movement over the meniscus. The patella, commonly known as the ‘kneecap’, is also part of the knee joint. The main function of the patella is to increase the lever arm of the patellar tendon (Fotheringham, 2016)

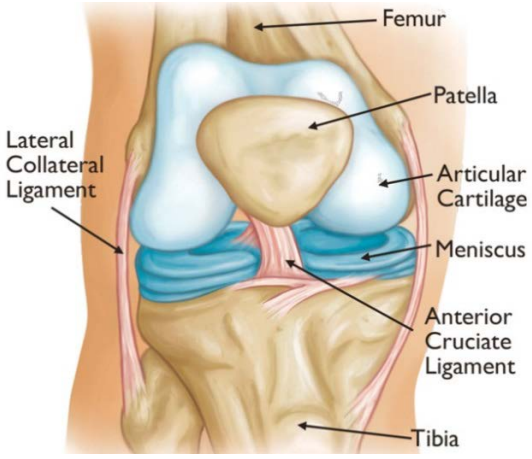

Figure 2: Anatomy of the normal knee (Foran, 2016)

Most patients who undergo knee arthroplasty suffer from arthritis. Arthritis is a disease that causes pain in the joints of the body and is most common in the knee. Patients who suffer from arthritis experience pain, stiffness and swelling in the knee

joint, which can make it difficult to bend or straighten the leg. There are three types of arthritis: osteoarthritis, rheumatoid arthritis and posttraumatic arthritis (American Academy of Orthopaedic Surgeons, 2016).

Osteoarthritis usually occurs in adults 50 years or older. In this type of arthritis, the cartilage on the articulating surface of the bone in the knee deteriorate and wear away. This exposes the bone surface and results in bone coming into contact with other bone in a grinding effect, which produces the pain. For instance, the surface of the femoral condyles presses against the proximal end of the tibia. Bone spurs then develop on the damaged surface.

Rheumatoid arthritis can target any joint in the body but is most common in the joint of the hand and feet. It is caused by a faulty immune system that attacks healthy tissue. The immune system releases chemicals that cause tissue to swell, most prominently the synovium membrane that covers the joint. The chemicals released by the immune system that cause inflammation also damage cartilage and ligaments resulting in pain and stiffness.

Posttraumatic arthritis is caused through the injury of a joint. Damaging bone or tearing of ligaments and menisci can cause bone surfaces to wear, which can lead to arthritis (American Academy of Orthopaedic Surgeons, 2016).

2.3.2 Replacement of the joint

Knee arthroplasty attempts to counter the effects of arthritis by removing the damaged surfaces of the bone and replacing them with prosthetic implants, which prevent bone on bone connections that cause pain, stiffness and instability. In TKA, the surfaces of the distal end of the femur and the proximal end of the tibia are replaced by metal implants and the meniscus is usually replaced by a polyethylene insert. In some cases, the patella is also resurfaced by replacing the surface in contact with the femur with a plastic button. In UKA, either the medial compartment or the lateral compartment is replaced (Greengard, 2012). In Section 2.3.3, the prosthetic implants of the knee are described.

Knee alignment and stability are important concepts in total knee arthroplasty. A tibiofemoral and patellofemoral joint that is correctly aligned can not only relieve pain, but also improve knee function and longevity of the prosthesis after TKA. In addition to the joint alignment, the soft-tissue surrounding the knee should also be well-balanced mediolaterally (Kwak, Kong, Han, Kim, & In, 2012). The balancing of the soft tissue is discussed in more detail in Section 2.4.

2.3.3 Implants

As mentioned in the previous section, the knee implant can consist of up to four components: The femoral component, the tibial component, the polyethylene spacer, and the patella component. In some cases, a tibial component is not inserted.

Instead, the polyethylene insert is attached directly to the resected proximal tibial surface. In Figure 3 and Figure 4, the components of an implant are shown after they have been inserted during TKA and UKA, respectively.

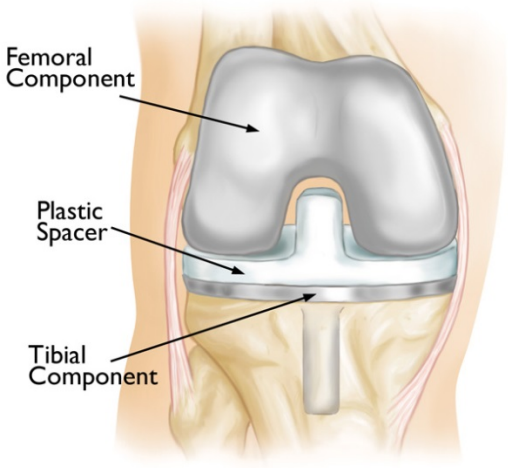

Figure 3: Components of the knee implant after TKA (Manner, 2016)

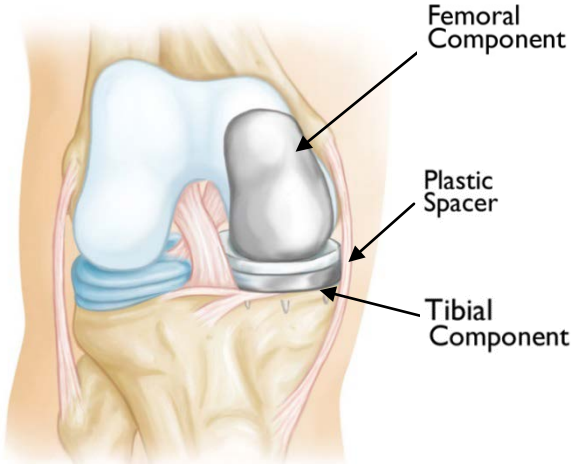

Figure 4: Unicompartmental knee implant in knee joint (Manner, 2016)

During TKA, the posterior cruciate ligament can either be removed or retained, depending on the condition of the posterior cruciate ligament. In both cases, the anterior cruciate ligament is sacrificed. A posterior stabilised implant design accounts for a posterior cruciate ligament that is removed, while a cruciate retaining implant design accommodates a retained posterior cruciate ligament (Manner, 2016). In Figure 5 and Figure 6, a posterior stabilising and a cruciate retaining implant design are shown, respectively. Figure 5 shows that the polyethylene insert of a posterior stabilising implant has a protrusion in the centre, which acts as a substitute for the posterior cruciate ligament by stabilising the knee (Manner, 2016).

Figure 5: Posterior stabilising implant design (Types of Total Knee Implants, 2017)

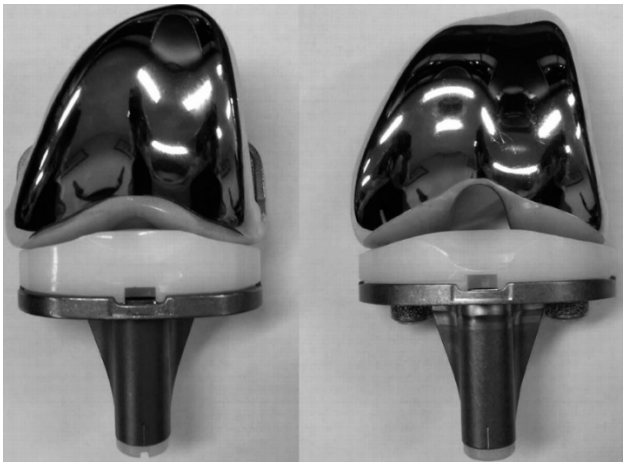

Figure 6: Two cruciate retaining implant designs (Park & Kim, 2011)

Implants can either be implanted into the knee joint by using quick hardening bone cement or by relying on the bone surrounding the implant to grow onto the implant without cement, thereby fixing it in place (Manner, 2016). Since the implants are required to last for as long as possible within the knee joint, the materials of the implants need to replicate the native bones by being strong and flexible enough to resist the forces and stresses acting upon it. In addition, the material must be biocompatible (Manner, 2016). Typically, the tibial component and femoral component would be made of cobalt-chromium alloys or titanium alloys. Both cobalt-chromium alloys and titanium alloys have high strength compared to other metal and are corrosion resistant and biocompatible. Titanium alloys are less dense than cobalt-chromium alloys, as well as less elastic, making it more similar to a natural knee joint (Knee Replacement Implant Materials, 2017).

2.3.4 Postoperative results

TKA and UKA have proven to yield excellent results. Based on the Western Ontario and MacMaster Universities Osteoarthritis Index (WOMAC), a study has shown that total knee arthroplasty reduces 53% of pain, 43% of stiffness and improves 43% of the physical function of the preoperative knee (Woolhead, 2005). Another study reported that UKA produces even better WOMAC outcomes for pain, stiffness and physical function (Noticewala, Geller, Lee, & Macaulay, 2012). However, TKA has proven better long-term survivorship and lower revision rates.

Two studies have found survival rates of 84% and 91% for UKA over 20 years, respectively, and between 92% and 100% survival rates for TKA in other long-term studies (Lyons, MacDonald, Somerville, Naudie, & McCalden, 2012). Failures leading to revision surgeries have been accredited to implant design, the fixation of the prosthesis, the over-active lifestyles of patients, and surgeon-related issues such

as poor preoperative planning, improper technique and damages made to the ligaments and articular cartilage during surgery (Marya & Thukral, 2013).

Part of the technique of TKA which influences the successful outcome of TKA, is soft tissue balance. Soft tissue balance relates to the alignment of the knee joint. In the next section, soft tissue balancing will be discussed in more detail.

2.4 Soft tissue balance

Since the aim of this study is to quantify the joint gap stiffness of the knee during knee arthroplasty, it is important to understand how it is influenced. Soft tissue balancing is a part of the technique of TKA that influences the stiffness of the postoperative knee joint. In this section, the concept of soft tissue balance will be explained in terms of its background, the motivation for its application and the methods used in relation to it.

2.4.1 Background

Soft tissue balance is an important aspect in the outcome of TKA. It has shown to have effects on patient satisfaction after TKA as well as clinical outcome scores (Meere, Schneider, & Walker, 2016). Soft tissue is described as the tissue that surrounds structures such as bones and organs and connects and provides support for these structures. Soft tissue includes ligaments, muscles, tendons, fat, blood vessels and nerves (Sports Medicine Australia, n.d.).

Soft tissue balance influences the alignment of the knee joint. The alignment of the knee joint not only has an effect on the durability and fastness of the implant, but also on the stability of the knee and on the range of motion. (Meere, Schneider, & Walker, 2016). Since the anterior cruciate ligament, the medial and lateral menisci, and in some cases the posterior cruciate ligament are resected during TKA, the stability of the knee relies on the soft tissue that remains and on the articulating surface geometries of the knee. By properly tensioning the collateral and capsular ligaments, varus-valgus and rotational stability can be achieved (Matsuda & Ito, 2015).

The primary cause of implant failure has been ascribed to incorrect soft tissue balance (Ries, Haas, & Windsor, 2003). It has been estimated that 40% of revision surgery soon after TKA could be avoided if the knee joint was balanced correctly (Meneghini, Ziemba-Davis, Lovro, Ireland, & Damer, 2016).

2.4.2 Methods

Soft tissue balance is usually assessed after the tibial and femoral resections have been made, and before the prosthetic components have been inserted. At this point, the alignment of the knee is assessed as well as the stiffness of the joint, in terms of

the distance between the femur and the tibia and also in terms of the tension in the collateral and capsular ligaments.

Various techniques are used to ensure the alignment of the knee joint. Mechanical alignment, kinematic alignment, and ligament balancing are all techniques that rely on different factors to ensure correct alignment and stability. Mechanical alignment is the most common technique and relies on the mechanical axis of the limb to align the knee neutrally, i.e. as a straight-line (Hutt, LeBlanc, Massé, Lavigne, & Vendittoli, 2016).

The mechanical axis of the limb is an axis originating from the hip joint which ends in the ankle joint, passing through the knee joint (Dosset, Swartz, Estrada, Lefevre, & Kwasman, 2012). This technique has been proven to ensure satisfactory long-term results (Hutt, LeBlanc, Massé, Lavigne, & Vendittoli, 2016). However, a study has shown that not every person has a pre-arthritic neutral (straight-line) mechanical axis. It was found that 98% of normal limbs do not have a neutral mechanical axis and 76% were found to have a deviation of larger than three degrees from neutral. Therefore, this technique does not correct normal joint alignment after TKA, but instead alters the native anatomy in most patients, leaving patients with limited knee function and dissatisfaction (Dosset, Swartz, Estrada, Lefevre, & Kwasman, 2012).

Kinematic alignment was introduced in 2006 with the goal of restoring the normal knee kinematics of the pre-arthritic knee by co-aligning the three kinematic axes of the knee (Dosset, Swartz, Estrada, Lefevre, & Kwasman, 2012). In comparison with mechanical alignment, the femoral component is usually placed in a more valgus orientation while the tibial component is placed in a more varus orientation. Kinematic alignment has proven to show better postoperative results in terms of range of motion and pain relief in comparison with mechanically aligned knees (Ishikawa, et al., 2015).

Ligament balancing, also known as gap balancing, attempts to counter the effects of arthritis, which causes deformity and osteophytes. The goal of ligament balancing is to create equal medial and lateral joint gaps in 90° knee flexion (90° between the upper leg and the lower leg) and 0° knee flexion (Ries, Haas, & Windsor, 2003). The joint gap should also not have medial or lateral tightness or laxity and must have correct varus or valgus alignment in 90° and 0° knee flexion. Correct ligament balancing can prevent ligament tightening or loosening which leads to valgus or varus deformity. It also improves tibiofemoral kinematics and decreases shear forces. A possible complication associated with ligament balancing is nerve injury during balancing due to nerve stretching (Babazadeh, Stoney, Lim, & Choong, 2009).

In order to determine the 90° and 0° knee flexion gaps, three techniques are commonly used: The spacer block technique, the tensor technique and the trial components technique (Kwak, Kong, Han, Kim, & In, 2012). When the spacer block technique is used, the 90° and 0° knee flexion gaps are assessed by inserting

spacers of variable thickness (usually of 2 mm increments) between the resected distal femur and the resected proximal tibia. The tensor technique utilises a laminar spreader to apply a distraction force between the resected distal femur and the resected proximal tibia, thereby tensioning the ligaments. The trial components technique involves the assessment of the knee kinematics throughout all angles of knee flexion with femoral, tibial and polyethylene trial components inserted (In, et al., 2009). In Figure 7, the three techniques are shown.

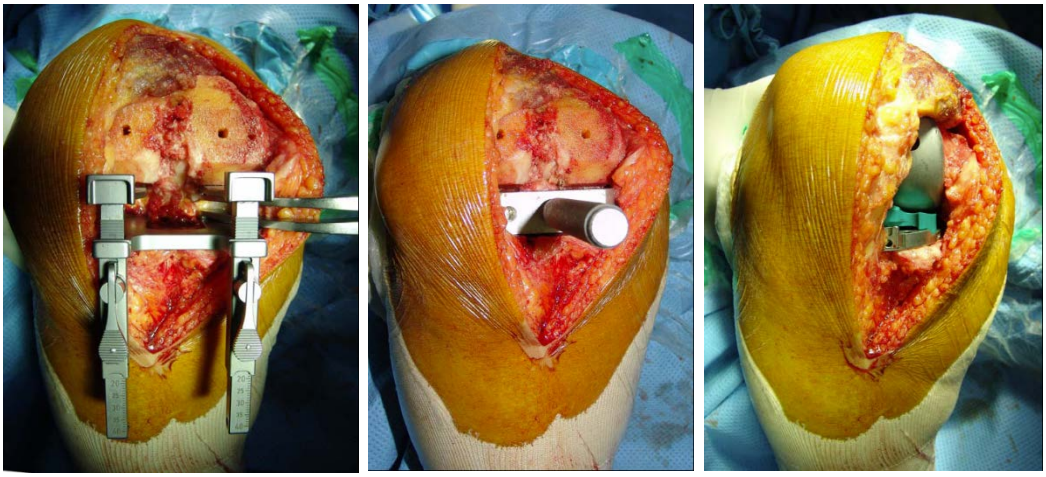

a. **b.** **c.**

Figure 7: a.) The femur and the tibia are distracted by use of a laminar spreader. b.) Spacer block inserted. c.) Femoral, tibia and polyethylene components inserted (In, et al., 2009).

Even though ligament balancing plays an important role in successful TKA, no set standards exist for the size of the joint gap, for the tension of the ligaments or for the distraction force. Instead, the outcome of ligament balancing is, to a great extent, dependant on a surgeon's subjective feel and experience (Nowakowski, Majewski, Müller-Gerbl, & Valderrabano, 2011).

2.5 Quantifying ligament stiffness: Past studies

Concerning the application of the distraction force between the distal femur and the proximal tibia, the majority of mechanical tensioning devices are only capable of applying the distraction force with the knee in 90° and 0° knee flexion. The lack of the continuous application of distraction forces between 0º and 90° knee flexion leaves the question as to what are appropriate tibiofemoral forces (tensions between the femur and the tibia) at all angles of knee flexion?

Attempts have been made to quantify the distraction force, even though mostly at 90° and 0° knee flexion. Kwak *et al*. (2012) measured the distraction force using a laminar spreader. Three surgeons were asked to apply the same amount of force to a force-measuring instrument as they would during TKA. In this study the mean

distraction force measured was 148 N. Kwak *et al*. (2012) used this information in the development of a pneumatic tensioning device for the application of a distraction force. In Figure 8, this pneumatic device is shown. The device used two pneumatic cylinders to distract the medial and lateral gaps after the bones have been resected. It also uses the gas pressure in the cylinder to measure the distraction forces. The cylinders applied the distraction force through plates that pushed against the resected surfaces of the femur and the tibia as shown in Figure 8. During cadaver tests, the device applied a constant distraction force of 150 N while the gap distances were measured. In order to measure the gap distance, scales on the cylinders measured the extension of the cylinders, which had to be recorded by reading the values off the scale. The device can also be used to measure the gap distances at angles between 90º and 0° knee flexion when a trial femoral component is inserted (Kwak, Kong, Han, Kim, & In, 2012).

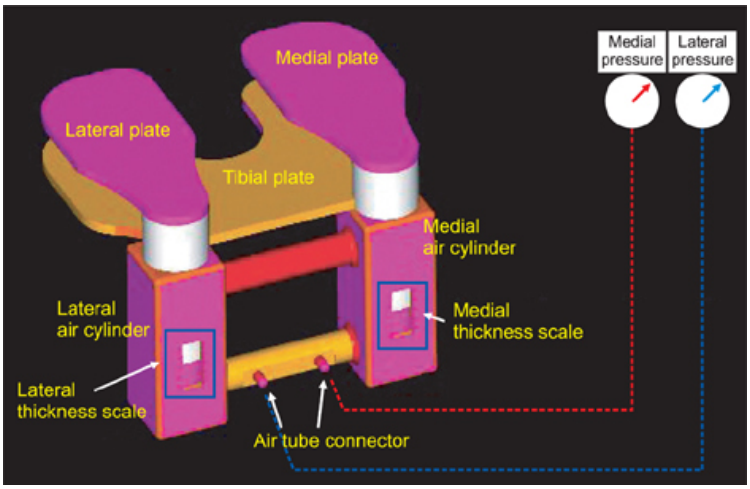

Figure 8: Pneumatic tensioner device by Kwak *et al* (2012)

Asano *et al.* (2008) used a torque driver to measure the distraction force applied by a tensioning device. However, the tension was only measured in 0° knee flexion.

Matsumoto *et al.* (2009) developed a knee tensioner capable of measuring the joint gap distance during soft tissue balancing at 0°, 10°, 45°, 90° and 135° knee flexion. The device was used *in-vivo.* The aim of the study was to compare the soft tissue tension in the case of 40 patients, half of whom received cruciate retaining (CR) TKA and the other half posterior stabilised (PS) TKA, both with the patella everted and reduced. This device also uses two plates, as shown in Figure 9, to distract the femur and the tibia. A top plate (A) pushes against the condyles of the femoral component, while the bottom plate (B) rests on the resected tibial surface. The top plate has a hinge at its centre allowing it to compensate for a difference in height between the two condyles. The device is actuated by applying a torque to a pinion (C) which is on a rack gear attached to the top plate. By using a torque driver, the pinion is turned to the desired distraction force.

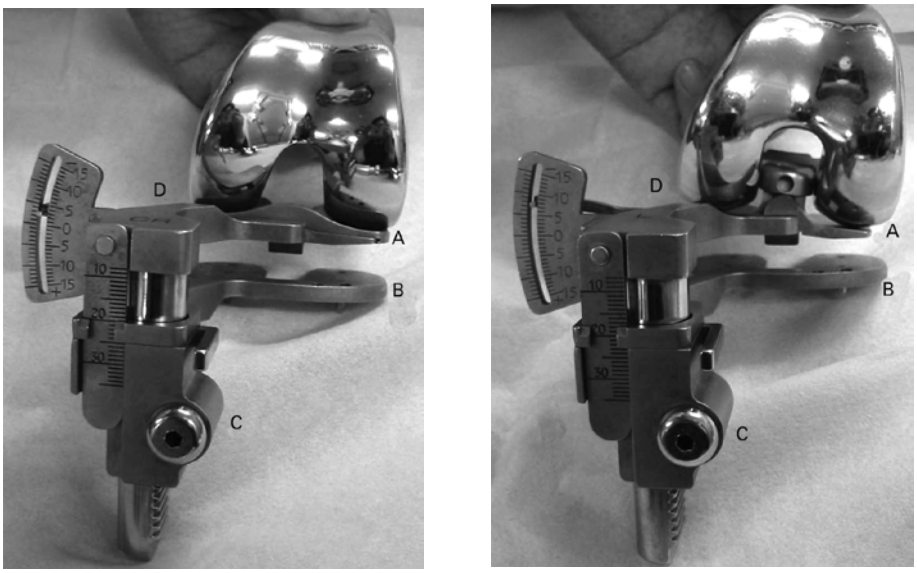

a. **b.**

Figure 9: The tensioner device developed by Matsumoto *et al.* (2009) configured for a.) cruciate retaining and b.) posterior stabilising TKA

A constant distraction force of 178 N was applied in the cases of all patients and the gap distance was measured, using a scale attached to the top plate as shown in Figure 9. The results of the study are shown in Figure 10, Figure 11, Figure 12 and Figure 13.

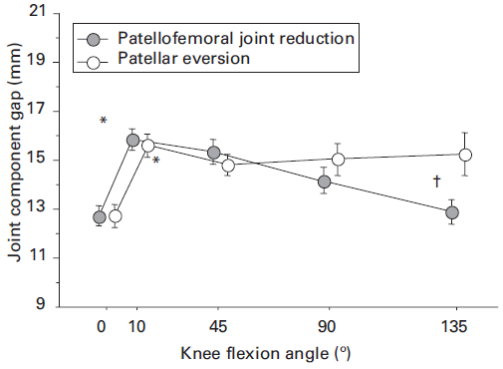

Figure 10: Joint component gap in cruciate retaining TKA (Matsumoto, et al., 2009)

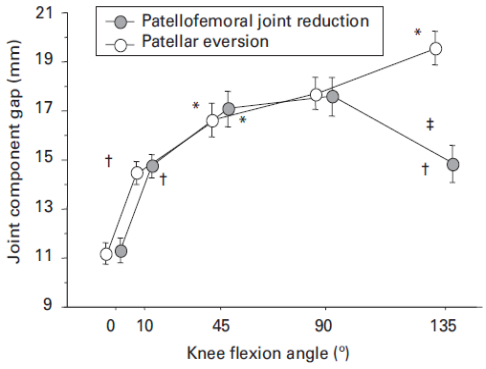

Figure 11: Joint component gap in posterior stabilising TKA (Matsumoto, et al., 2009)

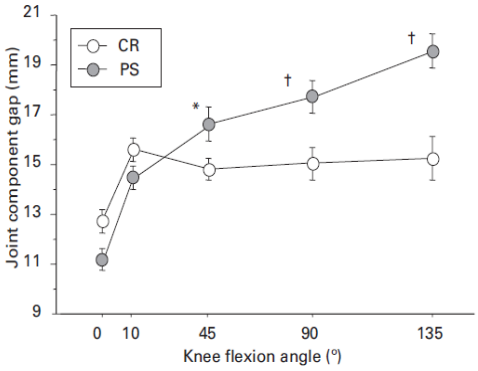

Figure 12: Joint gap component in TKA with patellar eversion (Matsumoto, et al., 2009)

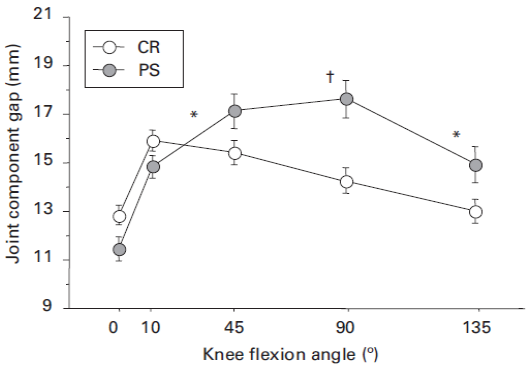

Figure 13: Joint gap component in TKA with patellar reduction (Matsumoto, et al., 2009)

Takayama *et al.* (2015) used a unicompartmental knee tensioner during UKA to measure the distance between the resected tibial surface and the prosthetic femoral condyle (component gap) in the medial compartment of the knee at four different distraction forces. The knee tensioner was similar to the knee tensioner developed by Matsumoto *et al.* (2009) with the difference of being designed to be inserted into the medial compartment of the knee. The results of this study are shown in Figure 14.

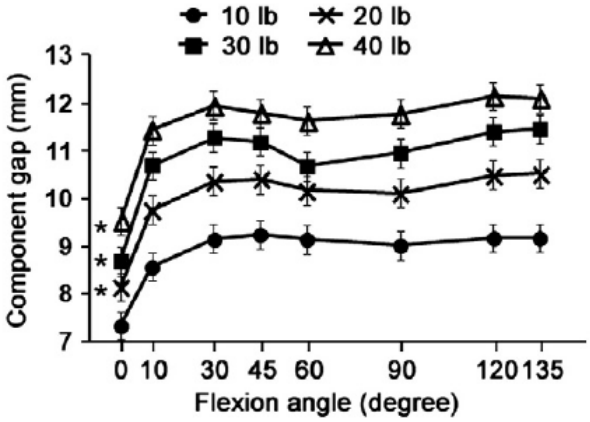

Figure 14: Component gap in the medial compartment (Takayama, et al., 2015)

In another study, a tensioning device was developed that measured the joint gap distances at 90° and 0° knee flexion before any bony resections were made. The tensioning device houses two springs, one for the lateral compartment and the other for the medial compartment, and the force is transmitted through Schanz screws in the femur and the tibia. To measure the joint gap, the distances between the screws were measured using a calliper. The idea behind the device is that the 90° and 0° knee flexion gaps would be measured under the preoperative condition of the bones (Nowakowski, Majewski, Müller-Gerbl, & Valderrabano, 2011). In Figure 15, the device is shown attached to the bones in both 90° and 0° knee flexion.

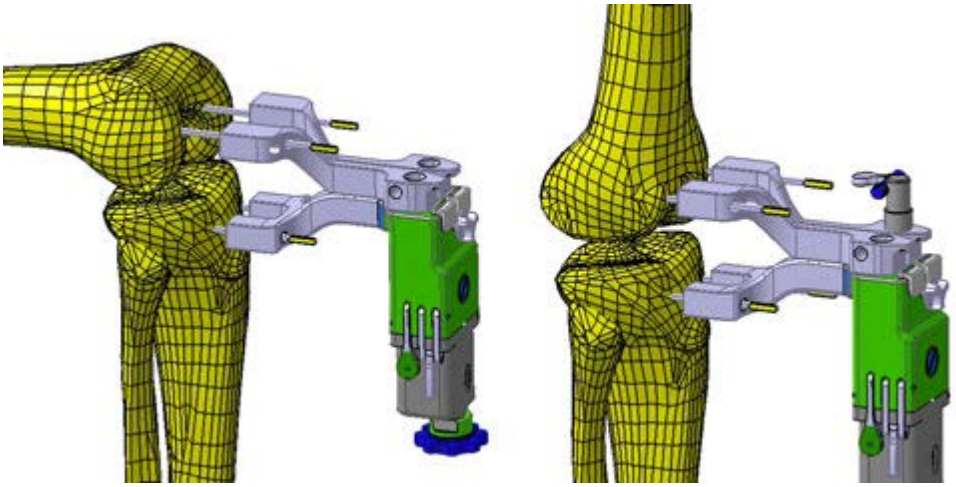

Figure 15: Tensioning device developed by Nowakowski *et al.* (2011) attached with Schanz screws to the femur and tibia

Viskontas *et al*. (2007) used computer assistance together with a tensioner, similar to the tensioner developed by Matsumoto *et al.* (2009). In this case, the tensioner was fitted with load cells, as shown in Figure 16, and used to compare two bone resection techniques of ligament balancing: The measured resection technique and the gap equalisation technique. The tensioner applied a distraction force between the distal femur and the proximal tibia, under simulated muscle loading, and measured the compartmental force using the load cells at 0°, 30°, 45°, 60° and 90° knee flexion.

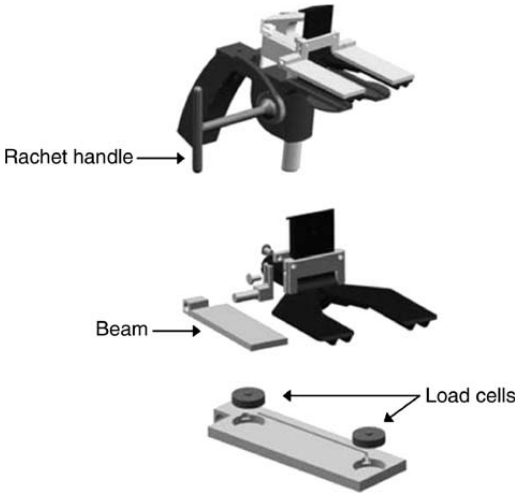

Figure 16: Tensioner fitted with load cell, developed by Visokantas *et al.* (2007)

In yet another study, load cells were incorporated in the measurement of compartmental force. D'Lima *et al.* (2007) developed a custom tibial component,

housing four force transducers that could measure the distribution of tibiofemoral loads. This device was tested in a cadaver knee after the prosthetic components had been inserted. The device therefore does not apply a distraction force, but purely measures the tibiofemoral forces once the knee has been replaced. D'Lima *et* al. (2007) used the device to determine whether the techniques of ligament balancing resulted in equal mediolateral and anteroposterior force distribution on the tibia.

The device consisted of a tibial tray, which housed the load cells, one in each quadrant, and a tibial insert, as shown in Figure 17. What made this device unique is that it could measure the forces at all angles between 90° and 0° knee flexion. The measurements were also transmitted wirelessly through an antenna in the tibial insert.

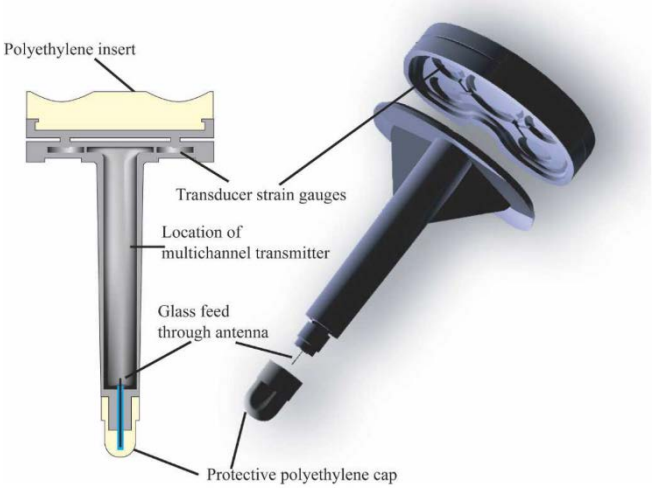

Figure 17: Custom tibia component with force transducers, developed by D'Lima *et al.* (2007)

More recently, computer navigation systems have been used in TKA. Computer navigation systems are useful in that they provide a very accurate and precise way of determining the correct bone resections and component positioning (Yoon, Jeong, & Yang, 2013). However, they are not yet capable of directly measuring the joint gap stiffness (D'Lima, Patil, Steklov, & Colwell, 2007). Another disadvantage of computer navigation systems is that they are costly and can increase operative time (Stephens, Hakki, Saleh, & Mihalko, 2014).

2.6 Conclusion

The knee tensioning devices that have been mentioned in this chapter are examples of devices that have been developed in the quest of determining the appropriate joint gap stiffness and distraction force, especially at angles between 90° and 0° knee flexion. Most of these devices either apply a distraction force or measure the

tibiofemoral compartmental forces at a few intermediate angles. In this study, these issues are addressed by developing a dynamic knee tensioning device that can investigate both the distraction force and the joint gap stiffness as a function of the angle of knee flexion. In the next chapter, the design of such a device is discussed.

3 Design of the knee tensioner

3.1 Introduction

After reviewing past research on the quantification of joint gap stiffness during knee arthroplasty, the requirements and specifications for a new concept for a dynamic knee tensioning device could be determined. In this thesis, the dynamic knee tensioning device will be referred to as the 'knee tensioner'.

In this chapter, the requirements and specifications are listed and the concepts that were investigated are discussed. The final design that was chosen for the knee tensioner is also discussed along with all the technical aspects related to it. The calibration and technical specifications of the physical knee tensioner is also discussed in this chapter.

3.2 Requirements

In addition to past research, the requirements were also determined after being conveyed by Dr Willem van der Merwe, a practising orthopaedic surgeon, through verbal discussion (Van der Merwe, 2016).

In this study, the objective is to measure the joint gap stiffness at all angles between 90° and 0° knee flexion, with the native femur and with different prosthetic femur designs. Since more than one prosthetic femur will be inserted, trial components will be used that can be removed once inserted. The stiffness of the joint gap will be defined in terms of the distraction force applied between the distal femur and the proximal tibia, and the distance between these two bones. The stiffness of both the medial and lateral compartments must be assessed to comply with the method of evaluating soft tissue balance in which a rectangular gap is to be achieved during TKA. This will also allow the knee tensioner to be used during UKA in which the lateral or medial compartment is assessed. Both the gap distance and the force distracting the knee joint must be presented as a function of the angle of knee flexion.

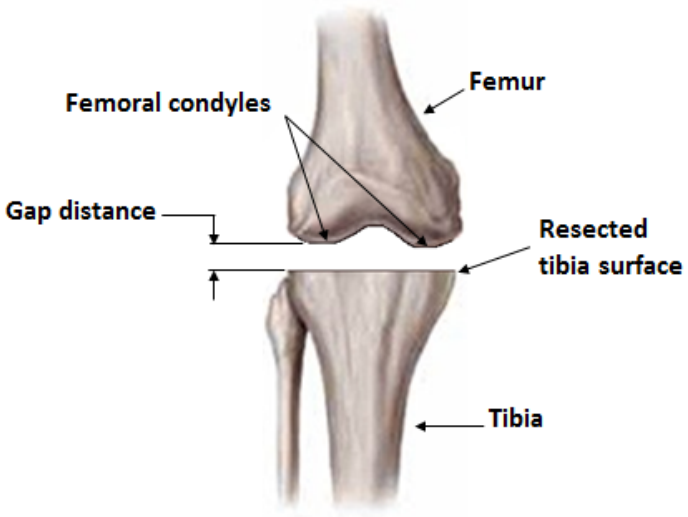

Figure 18: The knee joint after the tibial resections have been made (Knee Anatomy, 2017)

Soft tissue balance is typically assessed after the tibia and femoral resections have been made. However, in the case where the joint gap stiffness is to be assessed with the native femur still intact, only the tibia will be resected. In this case the gap distance, shown in Figure 18, is defined as the distance between the resected surface of the tibia and the articulating surface of the native or prosthetic femoral condyle. The distraction force is applied between these two bone surfaces. In the case where the joint gap stiffness is to be assessed with different prosthetic femur designs, tibial and femoral resections will be made for the implantation of the trial prosthetic femurs. As in the case of the native knee, the gap distance is measured from the resected surface of the tibia to the articulating surface of the trial prosthetic femur, and a distraction force is applied between these two surfaces. In order to measure the variation of the distraction force and the gap distance, the variable in question must be measured while the other is kept constant.

In order to obtain the information on the joint gap stiffness as described above, the knee tensioner must meet the following requirements:

1. The knee tensioner must exert a distraction force between the tibia and the femur in the knee joint.
2. The knee tensioner must measure the distraction force between the resected tibial surface and the native or prosthetic femoral condyle at all angles between 90° and 0° knee flexion while a constant distraction force is maintained.
3. The knee tensioner must measure the gap distance between the resected tibial surface and the native or prosthetic femoral condyle at all angles between 90° and 0° knee flexion while a constant distraction force is maintained.
4. The knee tensioner must measure the angle of knee flexion.

5. The knee tensioner must be able to accommodate different prosthetic femur designs.
6. The data measured by the knee tensioner must be stored.
7. The knee tensioner must stay fixed within the knee joint while measurements are taken.
8. The knee tensioner must not damage the knee.

3.3 Engineering specifications

Based on the requirements that were determined in the previous section, the specifications of the knee tensioner could be defined. These specifications were applied as a measure for the design of the knee tensioner, and they ultimately determined whether the knee tensioner that was developed succeeded in meeting the requirements.

The following specifications were defined:

1. The knee tensioner must be able to apply a distraction force over a range of 0 N to 150 N and measure the distraction force. The maximum value was determined after reviewing the research of Kwak *et al.* (2012) in which the mean distraction force, typically exerted by three surgeons, was found to be 148 N.
2. The knee tensioner must be able to measure a gap distance between 0 mm and 25 mm between the femoral condyle and the resected tibia. The maximum value was chosen after reviewing the research of Matsumoto *et al*. (2009) who measured a maximum gap distance of approximately 20 mm in knee arthroplasty patients with a distraction force of 178 N.
3. The knee tensioner must be able to measure all knee flexion angles between 90° and 0° knee flexion.
4. The device must be able to fit into a joint with a gap distance of 9 mm. The amount of bone removed from the tibia, measured from the top of the normal tibia plateau, is equal to the thickness of the tibial prosthetic component. Typically, this value would be 10 mm (Rossi, et al., 2012).
5. The knee tensioner must be able to measure the distraction force with an error of less than 10 %.
6. The knee tensioner must be able to measure the distraction force with a resolution of less than 5 N.

3.4 Concepts

3.4.1 Introduction

In this section, the concepts that were derived from the specifications, as presented in the previous section, are discussed. Each concept is first described and then evaluated with respect to criteria in a weighted evaluation matrix. Two methods for measuring the angle of knee flexion are also presented and evaluated. These two methods are applicable to all the knee tensioner concepts. Based on the evaluation, a specific concept was chosen as the final design for the manufacturing of the knee tensioner.

Since the stiffness of the medial and lateral compartments of the knee need to be quantified, the method in which the joint is distracted, and the gap distance and distraction force is measured, is identical in each compartment of the knee. In this study, a knee tensioner that can quantify the stiffness of one compartment was developed. This provided proof for a method for the quantification of the stiffness of both compartments during TKA, since two identical knee tensioners could be used for this purpose. In addition, the knee tensioner could also be used during UKA.

In generating concepts for the design of the knee tensioner, two main aspects, which influenced the physical layout of the device, were considered: The method of distracting the femur and the tibia, and the method of measuring the distraction force. Two methods of distracting the tibia and the femur were initially investigated: The use of an inflatable structure within the knee joint and the use of two plates, with one plate pushing against the articulating surface of the femoral condyle and the other pushing against the resected surface of the tibia. In Section 3.4.2, one concept using the former method is described and in Sections 3.4.3, 3.4.4 and 3.4.5, three concepts using the latter method are described. As mentioned before, the knee tensioner is required to measure the gap distance while a constant distraction force is maintained. Therefore, an automated method of distracting the femur and the tibia had to be conceptualised that relies on a feedback system which can track the distraction force and keep it constant.

3.4.2 Concept 1

As mentioned above, the use of an inflatable structure was considered for the distraction of the distal femur and the proximal tibia. A pressure gauge at the supply of the gas (inside the inflatable structure) would then have been used to measure the pressure inside the inflatable structure, which in turn could be used to quantify the force applied between the bones. In Figure 19, a simple illustration of the concept is given. As shown in Figure 19, the inflatable structure was placed beneath each femoral condyle with its base on the surface of the resected tibia. The gap distance could be measured by relating the deformation of the inflatable structure, under a load, to its height. The deformation of the structure could be measured using a strain gauge.

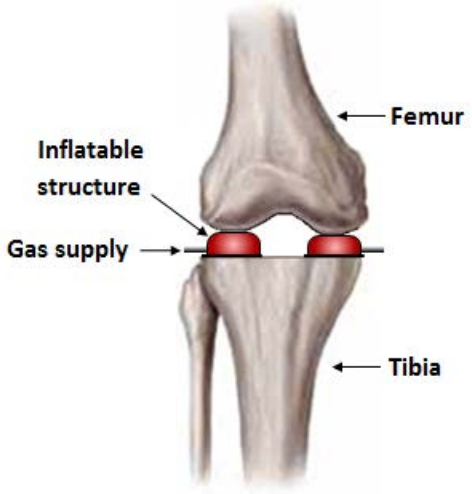

Figure 19: Concept 1 - Pneumatically inflatable structure

3.4.3 Concept 2

This concept incorporates the use of two plates in order to distract one compartment of the knee. These plates are both kept horizontally with one plate pushing against the articulating surface of the femur and the other pushing against the resected surface of the tibia. The top plate is actuated by use of pneumatic cylinders. In Figure 20, a CAD model of this concept is shown. Since a maximum gap distance of approximately 10 mm is provided within the knee joint (once the tibial resection has been made and the meniscus has been removed) the pneumatic cylinder has to be placed at the end of the plates. When the knee tensioner is inserted into the knee joint the pneumatic cylinder will then be positioned outside of the knee joint while the front end of the two plates is placed inside the knee joint. The guide rod, as shown in Figure 20, decreases the reaction moment within the pneumatic cylinder, ensuring smooth movement of the cylinder.

As in Concept 1, the distraction force is quantified using the air pressure inside the pneumatic cylinder. The pneumatic cylinder also ensures that the plate pushing

against the femur is always in contact with the femur, so that no lift off from the femur plate can take place. The gap distance is measured using a proximity sensor that detects the extension of the cylinder.

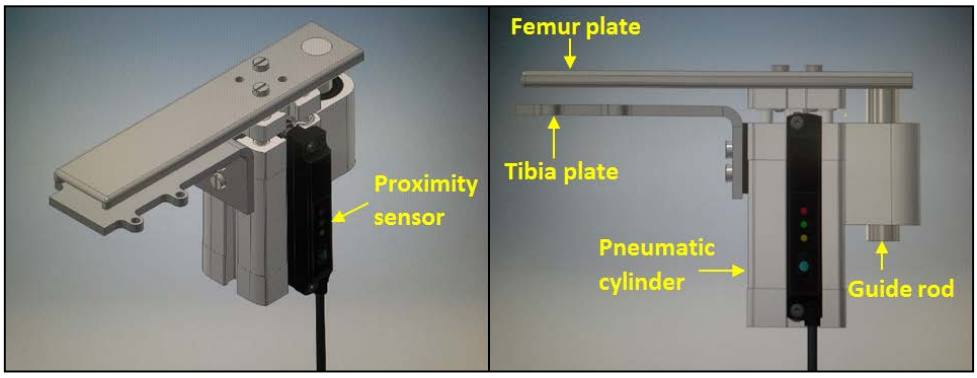

Figure 20: Concept - Pneumatically actuated plates

3.4.4 Concept 3

As in the case of Concept 2, Concept 3 also uses two plates to distract the femur and the tibia. In this concept, a linear stepper motor is used to actuate the top plate. The stepper motor has a threaded shaft that moves in and out of the motor as the motor turns. The shaft pushes the top plate (femur plate) up against the articulating surface of the femoral condyle. The femur plate is fitted with two guide rods, as shown in Figure 21, that slide in linear bearings in order to prevent any rotational movement of the plate and also to keep it horizontal. Theoretically, this also allows the motor shaft to apply 100% of its force to the femoral condyle, by means of the femur plate.

Since the force applied to the femoral condyle is equal to the force the shaft exerts on the femur plate, the distraction force can be measured by placing a load cell between the femur plate and the shaft of the stepper motor. The gap distance can be measured by counting the steps of the stepper motor and relating it to the distance travelled by the motor shaft.

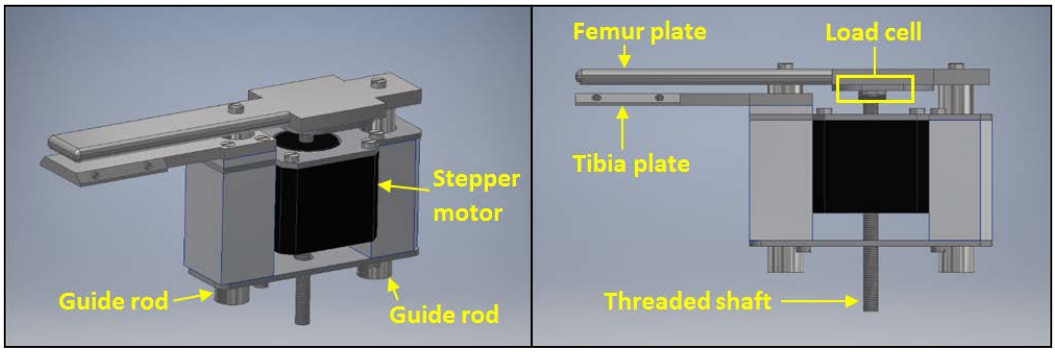

Figure 21: Concept 3 - Linear stepper motor with plates

3.4.5 Concept 4

Concept 4 also uses two plates and a motor to actuate the femur plate. However, in this concept a rack-and-pinion gear mechanism is used to actuate the femur plate. In Figure 22, a CAD model of the concept is shown. The pinion gear is located on the shaft of the motor and the rack gear is attached to the femur plate. This concept uses a DC electric motor. The current draw of the motor can be used to quantify the torque in the pinion gear. The torque can subsequently be used to quantify the distraction force. If the rack gear transmits a force of 150 N to a pinion gear of 10 mm diameter, the torque on the motor equals 0.75 N.m. The motor must therefore be able to deliver at least 0.75 N.m. The gap distance can be measured with a proximity sensor.

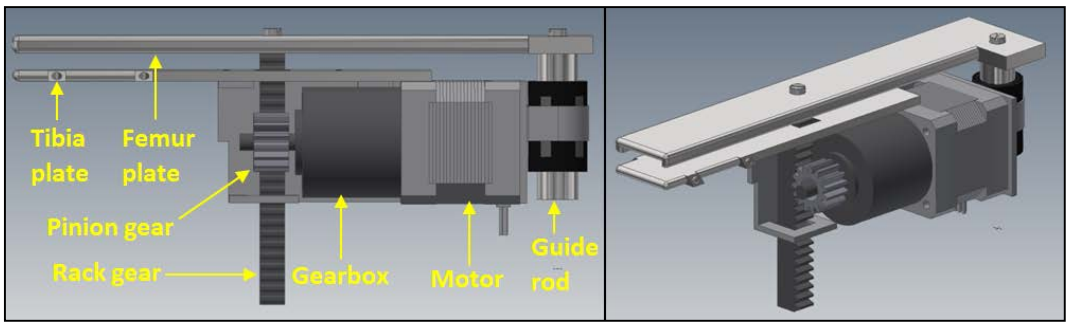

Figure 22: Concept 4 – Stepper/DC Motor with rack and pinion

3.4.6 Measuring the angle

Two apparatus were investigated for measuring the angle of knee flexion: A goniometer and an inertial measurement unit (IMU). In Figure 23, a digital goniometer is shown measuring the angle of knee flexion. In order to measure the angle of knee flexion, the goniometer uses the relative angle between its two arms, with one arm attached to the upper leg and the other attached to the lower leg. The goniometer uses a potentiometer to determine at which angle the two arms are with respect to each other.

Figure 23: A digital goniometer used to measure the angle between the upper and lower leg (Mediagauge, 2017)

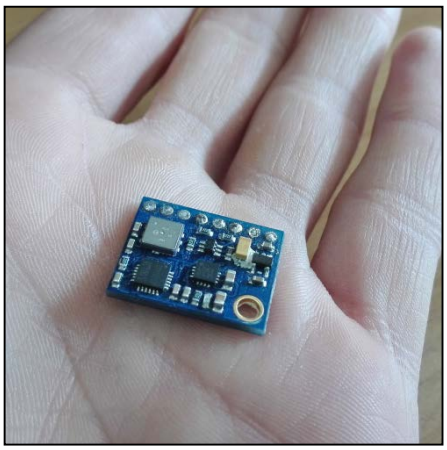

Figure 24: Inertial Measurement Unit printed circuit board

In Figure 24, an example of an IMU is shown. The IMU uses a gyroscope and accelerometer, both implanted on a single chip, to determine its orientation in three dimensions of space. The angles at which the IMU is orientated are measured with respect to the poles of the earth. If an IMU is placed on the lower leg, the orientation of the lower leg can be measured. Therefore, in order to measure the angle between the lower leg and the upper leg, the upper leg must be kept stationary while the change in the lower leg's orientation is used to calculate the difference in the angle as the lower leg is rotated about the knee.

3.4.7 Evaluation

In Table 1 and Table 2, a weighted evaluation matrix of the concepts of the knee tensioner and the methods of measuring the angle of knee flexion are given, respectively. In the two matrices, each criteria is given a weighting factor (W) ranging from one to five, with one being the least important and five the most important. Each Concept is given a score (S) based on how well the concept meets the criteria. A score ranging from one to five is given, with one being the worst

satisfied and five being the best satisfied. A total (T) is calculated for each concept with regards to each criteria by multiplying the weighting factor with the score.

Table 1: Weighted evaluation matrix of knee tensioner concepts

Criteria	Concept											
	1			2			3			4		
	W	S	T	W	S	T	W	S	T	W	S	T
Exert a distraction force between the tibia and the femur	5	2	10	5	2	10	5	5	25	5	5	25
Measure distraction force	5	4	20	5	4	20	5	5	25	5	3	15
Measure gap distance	5	1	5	5	5	25	5	4	20	5	5	25
Accommodate different prosthetic femur designs	4	5	20	4	4	16	4	4	16	4	4	16
Device can stay fixed within joint gap	5	5	25	5	4	20	5	4	20	5	4	20
Maintain constant gap distance	5	2	10	5	2	10	5	4	20	5	4	20
Maintain constant distraction force	5	1	5	5	1	5	5	4	20	5	1	5
Device does not damage the knee	4	4	16	4	4	16	4	4	16	4	4	16
Total			111			122			162			142

Table 2: Weighted evaluation matrix of angle measurement methods

Criteria	Concept					
	Goniometer			Inertial measurment unit		
	W	S	T	W	S	T

Use within operation setup	5	3	15	5	5	25
Integration with knee tensioning device	5	2	10	5	5	25
Accuracy	5	4	20	5	4	20
Functionality	5	2	10	5	5	25
Total	40					70

When looking at the total scores of the knee tensioner concepts, Concept 3 has the greatest total score. Concept 3 is superior in measuring the distraction force by use of a load cell and in maintaining a constant distraction force as the knee is rotated. The load cell provides a more accurate method of measuring the distraction force without delays such as that which could arise with the use of pneumatics. The holding torque of the stepper motor is greatly advantageous in maintaining a constant distraction force and can adjust the gap distance with a greater resolution than typical DC or servo motors and pneumatic cylinders. Therefore, Concept 3 was chosen as the final concept for the knee tensioner that was manufactured.

The IMU has a greater total score than that of the goniometer. Even though both methods are deemed to be similar in accuracy, the size of the IMU allows it to be fixed to the knee tensioner. It does not pose as an obstacle to the operation setup as it is contained within the knee tensioner. Its disadvantage of only being capable of only measuring its own orientation can easily be addressed by keeping the upper leg or lower leg stationary during tests. The IMU was chosen above the goniometer as the method of angle measurement.

In the next section, a detailed description of the physical model of the knee tensioner, based on Concept 3, is presented.

3.5 Final concept

3.5.1 Introduction

In Section 3.4, four different concepts for the knee tensioner were described and evaluated by use of the weighted evaluation matrix. Concept 3 was chosen as the best concept for the knee tensioner and was used for the first prototype of the knee tensioner, which will be referred to as Prototype 1. In Figure 25, the physical model of Prototype 1 is shown.

After the manufacturing and testing of Prototype 1, certain aspects of its design that could be improved were identified. The improvements that were made resulted in a second knee tensioner prototype, which will be referred to as Prototype 2.

In this section, a detailed description of Prototype 1 is given. The description includes the following aspects of the knee tensioner: The mechanical design, the development of its electronics, the method in which the stepper motor is controlled, the measuring of the gap distance, distraction force and angle of knee flexion, the control system, the graphical user interface, the software algorithms, and the configuration of the electrical components. The improvement that were made to Prototype 1 and which lead to the design of Prototype 2, are discussed in Section 3.6.

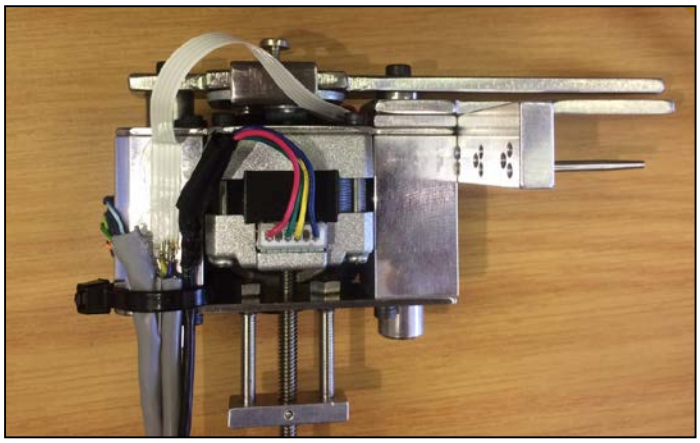

Figure 25: The physical model of Prototype 1

3.5.2 Mechanical design

In this section, the main mechanical aspects of Prototype 1 will be discussed. In Figure 26, the aspects that are discussed are annotated on a picture of the knee tensioner showing the parts without any electronic wiring. All parts of the knee tensioner were designed in the CAD software Autodesk Inventor (Version: Professional 2016, San Rafael, 2015) and the layout of the knee tensioner assembly was determined using this software. In Appendix B the engineering drawings for the manufacturing of the knee tensioner are given.

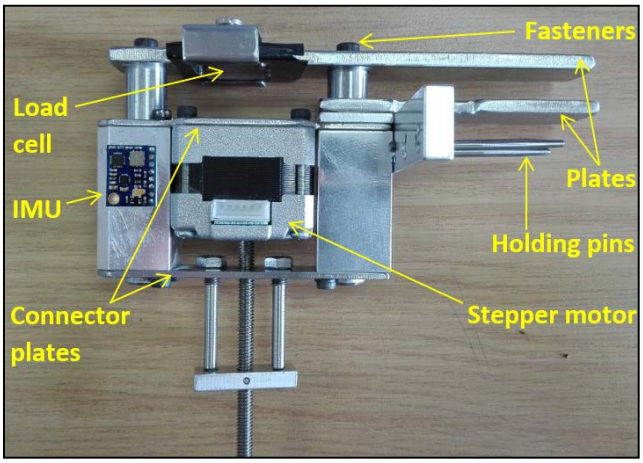

Figure 26: Mechanical design aspects of the knee tensioner

3.5.2.1 Plates

In the illustration shown in Figure 27, the knee tensioner is inserted into the knee joint between one prosthetic femoral condyle and the resected surface of the tibia. The gap that is created after the tibia has been resected and the meniscus has been removed, is approximately 10 mm. This leaves little space inside the knee joint, which means that the stepper motor, load cell and IMU must be located outside the knee joint when the knee tensioner is inserted.

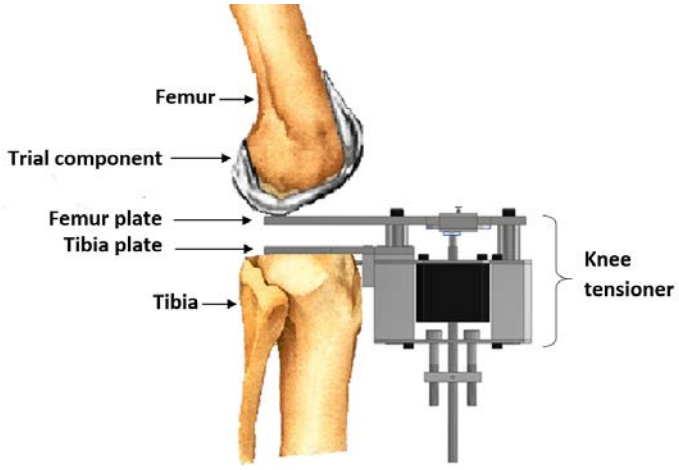

Figure 27: Side view of the knee tensioner inserted into the knee joint (Schmidler, Knee Replacement Surgery, 2017)

The femur plate is subject to two forces: A force exerted by the femoral condyle at the end of the plate and a force exerted by the stepper motor shaft at the other end of the plate. These two forces force the plate to rotate in the direction as shown in Figure 28.

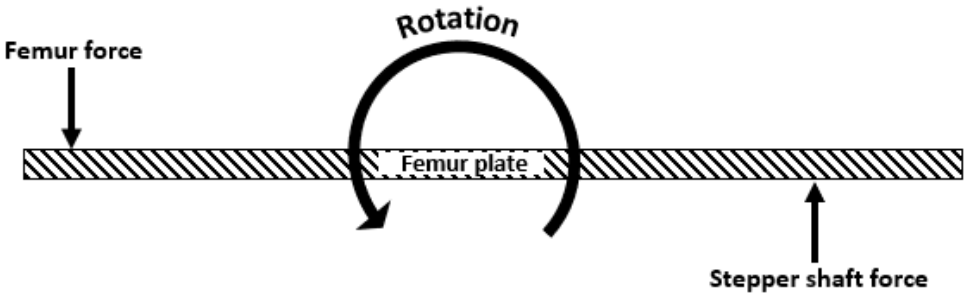

Figure 28: Forces acting on the femur plate

To counter the rotational movement, it was decided to attach two vertical guide rods to the femur plate, which keeps the femur plate horizontal at all times. A guide rod was placed both sides of the stepper motor shaft. In Figure 29, a cross-sectional view is shown of the knee tensioner, indicating the guide rods. The lengths of the guide rods were chosen to allow a minimum distance of 25 mm to be achieved between the top surface of the femur plate and the bottom surface of the tibia plate. The guide rods slide in plain linear bearings made of vesconite. Vesconite was chosen for its low coefficient of friction. Low friction was necessary to ensure that a micron of vertical movement could be measured by the load cell and translated to a force on the femur plate. The plain linear bearings are housed in aluminium blocks, indicated in Figure 29 as 'bearing blocks', both sides of the stepper motor.

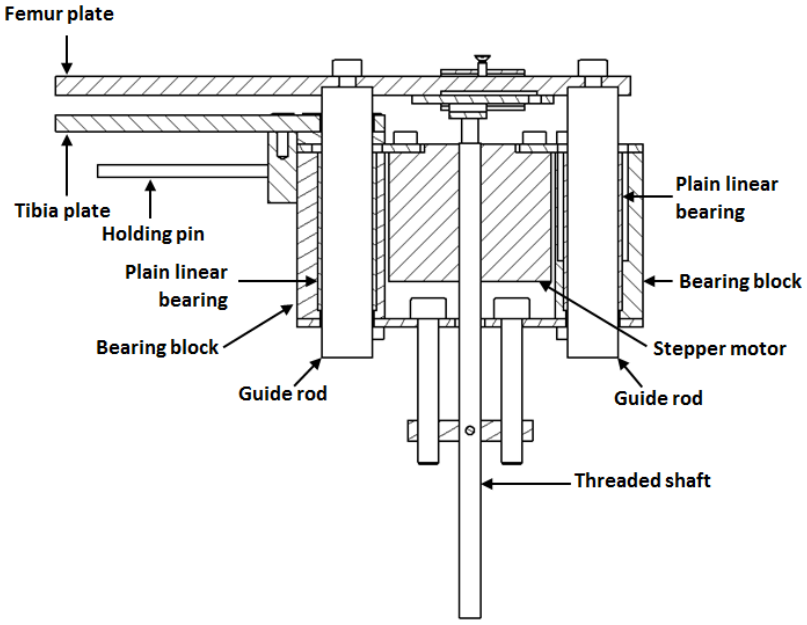

Figure 29: Cross-sectional view of the CAD model of the knee tensioner

The tibia plate is fixed to the aluminium block closest to the knee and when the knee tensioner is inserted into the knee joint, it rests on the resected surface of the tibia. Both the femur plate and the tibia plate are made of stainless steel. Stainless

steel was chosen due to its resistance to corrosion and its biocompatibility (not causing harm to living tissue). Aluminium was chosen for the bearing blocks to keep the weight of the device low.

The length and width of the femur plate was chosen so that the femoral condyle is always in contact with the femur plate throughout all angles of knee flexion. The width and length of the tibia plate was chosen so that it could rest on as much area of the resected tibial surface as possible, for better force distribution. The results of an investigation of the relationship between the dimensions of the knee by Seedhom *et al.* (1972) and the dimensions of the prosthetics of the manufacturers Zimmer (Zimmer, 2017) and Smith & Nephew (Smith & Nephew, 2017), were used to calculate a mean value for the dimensions of the knee. A mean value for the width of a femoral condyle was calculated to be 25 mm. Since the femoral condyles are convex in the Coronal plane, the point of contact between the condyle and the femur plate will vary within the mean width of the condyle. To account for the lateral movement of the point of contact, the width of the Femur plate was chosen to be 20 mm.

In order to determine the length of the femur plate, the results from a study by Iwaki *et al.* (2000) on tibiofemoral movement was used. According to Iwaki *et al.* (2000) the articulating surface of the medial femoral condyle is in contact with the medial tibial condyle over a range of 27 mm, starting at a distance of 9 mm from the most anterior edge of the tibial condyle, on average. The articulating surface of the lateral femoral condyle was found to range over a distance of 24 mm, starting at a distance of 11 mm from the anterior edge of the tibial condyle. Since the knee tensioner is to be used in the medial and lateral compartments, the length of the plate is chosen to suit the lateral compartment, which has the largest distance between the anterior edge of the tibial condyle and the end of the area of contact between the femur and the tibia. This requires the femur plate to extend a minimum distance of 36 mm into the knee, measured from the anterior surface of the tibia to within the knee joint. To account for outliers, it was decided to have the length of the plate extend 50 mm into the knee.

A finite element analysis was performed to determine the deflection of the femur plate and the stresses within the plate, for a certain thickness of the plate. The finite element model of the femur plate was set up in the pre-processing software Patran (Version: 2014.0.1, Newport Beach, 2014) and the model was analysed in the finite element solver Nastran (Version: 2014.0.1, Newport Beach, 2014). A thickness of 4.5 mm was first analysed. 4.5 mm was chosen so that together with a 5 mm thickness tibia plate, the combined thickness of the plate is 9.5 mm, which will allow the knee tensioner to fit into most knee joint gaps. As shown in Figure 30, the model of the plate was created with the guide rods attached to it. A tetrahedral mesh was applied to the model with element lengths of 0.002 mm.

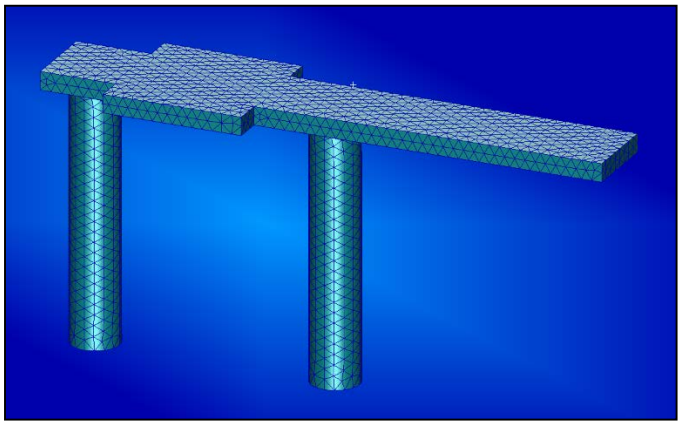

Figure 30: Finite element model of femur plate in Patran

The guide rods were included in the model to account for the deformation of the guide rods in the total displacement of the tip of the femur plate, as indicated by an 'X' in Figure 31.

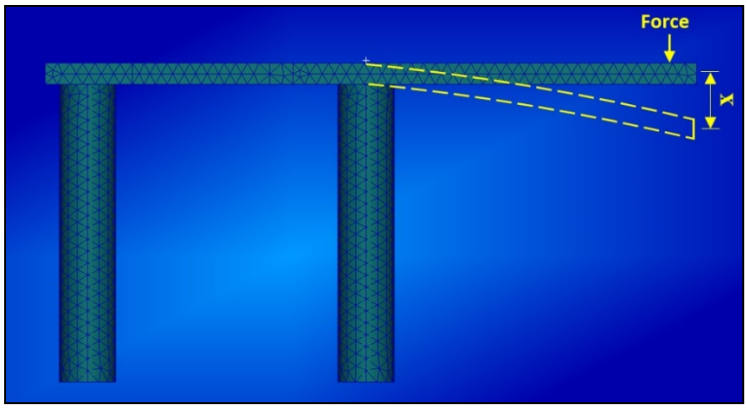

Figure 31: Total displacement of the tip of the femur plate

The surface of the guide rods in contact with the plain linear bearings were constrained in the position where the distance between the top of the femur plate and the bottom of the tibia plate is 20 mm. The constraint on this surface allowed the guide rods to displace only in the vertical direction. A point on the femur plate, at which the centre of the load cell is located, was constrained in all degrees of freedom. A force of 150 N, the maximum force expected during *in-vitro* tests, was applied at the end of the plate. The force was distributed over five nodes in the area where the femoral condyles are expected to make contact with the femur plate. In Figure 32, the constraints on the guide rods are shown as well as the distributed force on the end of the plate.

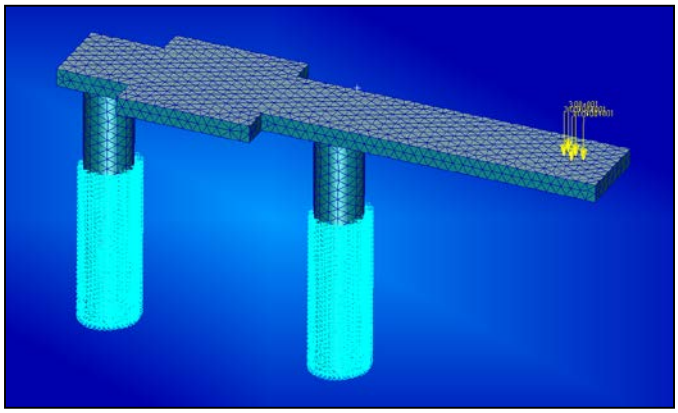

Figure 32: Constraints and forces on finite element model in Patran

In Figure 33, the results of the finite element analysis are depicted. The tip of the femur plate displaced 0.46 mm while the maximum stress in the plate was 158 MPa. The results of the deflection and the maximum stress were also verified with analytical calculations, which are given in Appendix F. With the analytical calculations the deflection was calculated to be 0.56 mm. Tresca's Maximum Shear Stress failure theory was applied, and it was found that yielding will not occur. Since this displacement was obtained under the extreme case of a force of 150 N, a displacement of 0.462 mm is considered negligible. The yield strength of steel is approximately 215 MPa, which is well above the maximum stress of 158 MPa, which was determined computationally, in the plate. Therefore, a thickness of 4.5 mm is an acceptable thickness for the femur plate and a thickness of 5 mm is subsequently acceptable.

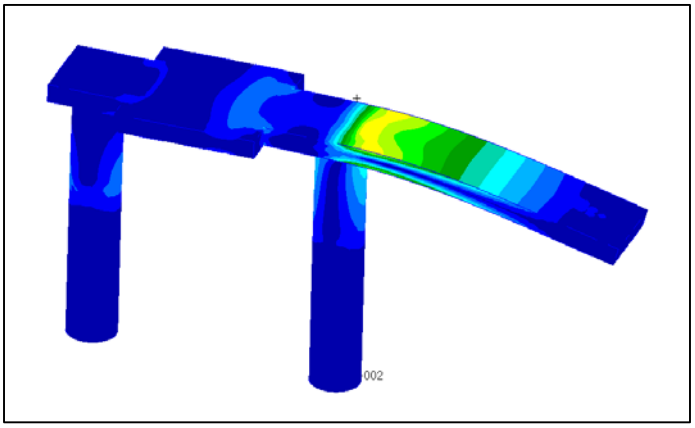

Figure 33: Results of finite element analysis: Deformation of plate with stress fringe in Patran. Yellow indicates high stress and blue indicates low stress

3.5.2.2 Connector plates

Two 2 mm thick stainless steel plates connect the two linear bearing blocks with each other at the top and the bottom, as shown in Figure 26. The stepper motor is also fastened to the connector plate at the top of the knee tensioner.

3.5.2.3 Load cell

In Figure 34, the load cell is shown. The load cell is located underneath the femur plate, between the two guide rods, so that the shaft of the stepper motor can push against it and transfer the force to the femoral condyles by means of the femur plate. The load cell is fixed to the femur plate with a clamp, as shown in Figure 35. The clamp consists of a steel plate bent around the femur plate and onto the load cell. The clamp is tightened with a screw at the top of the femur plate. The load cell is discussed in more detail in Section 3.5.5.

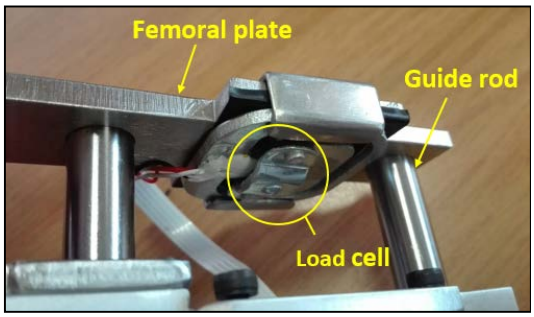

Figure 34: Load cell under femur plate

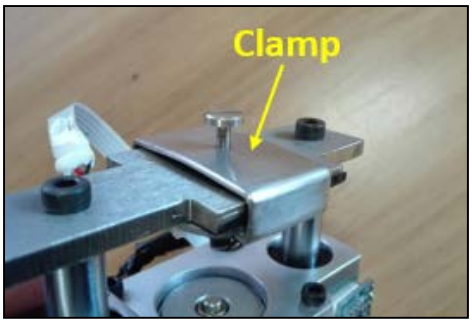

Figure 35: Clamp holding the load cell to the femur plate

3.5.2.4 Stepper motor

The stepper motor used in the knee tensioner is a NEMA 32 size stepper motor. The specification sheet of the stepper motor can be found in Appendix A. The stepper motor has a threaded shaft that moves linearly through the motor. As the shaft moves upwards, it pushes against the load cell and actuates the femur plate. In order to ensure linear motion of the shaft, the shaft must be prevented from turning. Therefore, a small rectangular block is attached to the shaft, as show in Figure 36, which slides on a guide pin on either side of the shaft and prevents any twisting motion.

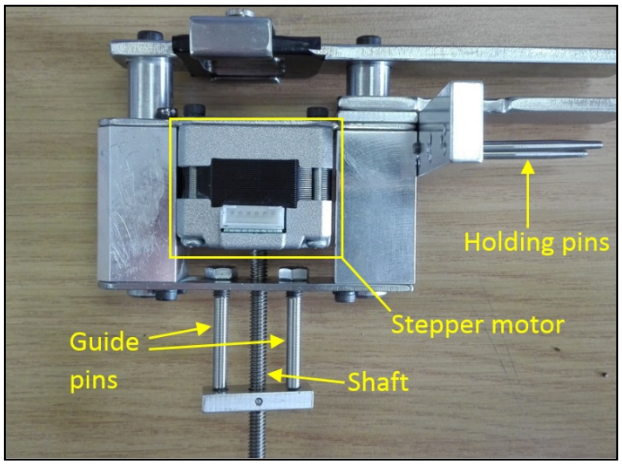

Figure 36: Linear stepper motor system

3.5.2.5 Holding pins

In order to prevent the device from detaching from the knee joint, the device is fixed to the tibia with holding pins that penetrate the tibia. The holding pins are shown in Figure 36. The size of the holding pins were based on pins used with a TKA tibia cutting block. The tibia cutting block is fixed to the tibia with the same holding pins. Therefore, after the tibia has been resected the existing holes made by the tibia cutting block can be used by the knee tensioner. The holding pins are fixed to an aluminium block and spaced similar to the pins on the tibia cutting block.

3.5.2.6 Inertial measurement unit (IMU)

In Figure 37, the IMU is shown attached to the side of the knee tensioner. In this position, the IMU is parallel to the Sagittal plane, when the knee tensioner is inserted into the knee joint. This allows the IMU to measure the angle between the upper and lower leg in the Sagittal plane.

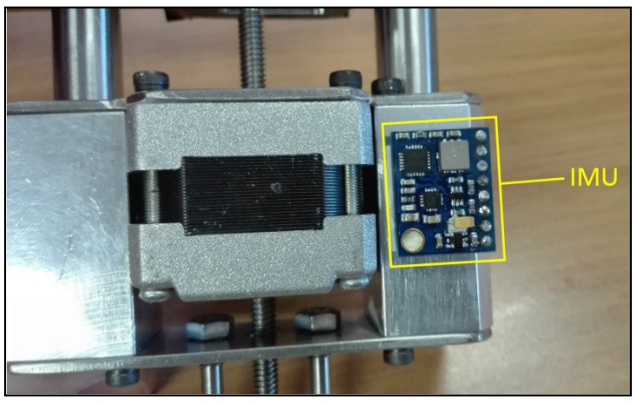

Figure 37: Location of IMU on the knee tensioner

3.5.2.7 Fasteners:

Allen key cap screws are used to connect all parts of the knee tensioner. The screws were chosen for quick loosening and fastening by use of an Allen key.

3.5.3 Electronics development

A system had to be developed that could control the distraction force applied by the knee tensioner in the knee joint and integrates the sensors on the knee tensioner. For this application, it was decided to use a microcontroller with analog and digital input and output pins that can send commands to the knee tensioner and receive signals from the load cell and from the IMU. An algorithm can be uploaded to a microcontroller, which continuously controls signals going to and coming from the knee tensioner. An Arduino microcontroller was chosen due to its wide availability of resources and open source tools for the development of electronic systems (Arduino, 2017). In order to keep the space occupied by the microcontroller to a minimum, an Arduino Nano microcontroller is used. The Arduino Nano specification sheet is given in Appendix A.

An algorithm was developed that controls the stepper motor, processes the signals from the load cell and IMU, and calculates the gap distance. This algorithm is called the Knee Tensioner Algorithm and was developed in the Arduino software (Version: 1.6.11, 2016), which is an integrated development environment (IDE). The algorithm is coded in the IDE on a PC and then uploaded to the Arduino Nano via a USB cable. The structure of the Knee Tensioner Algorithm is given in Section 3.5.10.

In order to command the Knee Tensioner Algorithm to perform specific tasks and record the data it produces, an additional algorithm was developed in the program Processing (Version: 3.2.4, 2016), which is also an IDE. With Processing, the user of the knee tensioner can control the device by means of a graphical user interface (GUI) on a PC and record the data the knee tensioner provides. Unlike the Knee Tensioner Algorithm, which is uploaded to the Arduino Nano, this algorithm operates from the Processing IDE on a PC. This algorithm is referred to as the GUI Algorithm. In Section 3.5.10, the structure of the GUI Algorithm is given along with a description of its communication with the Knee Tensioner Algorithm.

The two main functions of the knee tensioner are Distance Control and Force Control. Under Distance Control, the gap distance in the knee joint is kept constant, while under Force Control the distraction force in the knee joint is kept constant. Under each of these functions, two methods of specifying the starting value for the function are available and are shown in Figure 38. These methods will be referred to as Modes. In the GUI it is clearly indicated in which field the values for each Mode must be submitted.

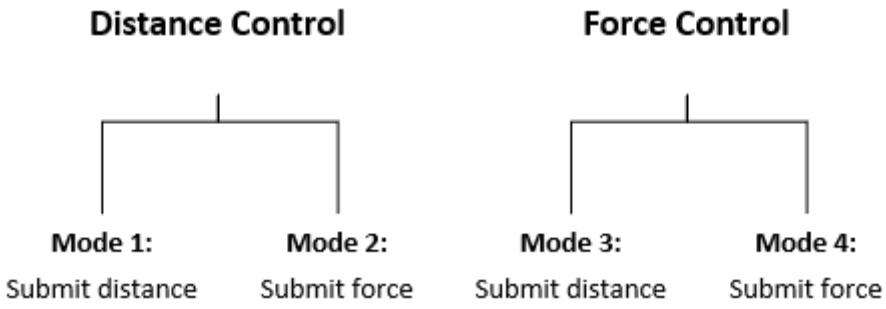

Figure 38: Methods of function input

The following is a description of each Mode:

Mode 1: A distance is specified by the user that the knee tensioner will keep constant through all angles of knee flexion.

Mode 2: A force is specified by the user and the distance at the specific force, while the knee is still stationary, is used to determine which distance will be kept constant through all angles of knee flexion.

Mode 3: A distance is specified by the user and the force at the specific distance, while the knee is still stationary, is used to determine which force will be kept constant through all angles of knee flexion.

Mode 4: A force is specified by the user that the knee tensioner will keep constant through all angles of knee flexion.

3.5.4 Controlling the stepper motor

In the Arduino IDE, a library is used in which the stepper motor is controlled with two parameters: The speed of the stepper motor, in revolutions per minute, and the number of steps it turns, both of which are specified in the Knee Tensioner Algorithm.

Even though greater speed would lessen the time it takes to distract the knee joint, there exists an inverse relationship between the torque of the stepper motor and the speed. Therefore, a speed was chosen that ensures the knee tensioner can exert a maximum force of 150 N.

The steps of the stepper motor is discussed in Section 3.5.7. The stepper motor requires 12V to operate. This is provided through a 12V power adapter, which is plugged into a wall socket.

3.5.5 Measuring the force

In Figure 39, the load cell is shown. The load cell consists of two strain gauges placed on a deformable element. The shaft of the stepper motor makes contact with the load cell at the point indicated in Figure 39. This point of contact is on the deformable element, which bends under force. The perimeter of the load cell is in contact with the femur plate, while the deformable element is above an indentation in the femur plate, providing space for the element to displace. The load cell can be modelled as a cantilever beam having a fixed end, with the deformable element representing the beam. The strain gauges are at the fixed end of the element and measures the strain of the element under load. The force of the stepper motor is transferred from the shaft of the stepper to the femur plate through the load cell. The strain that is measured by the strain gauges is then converted to a force.

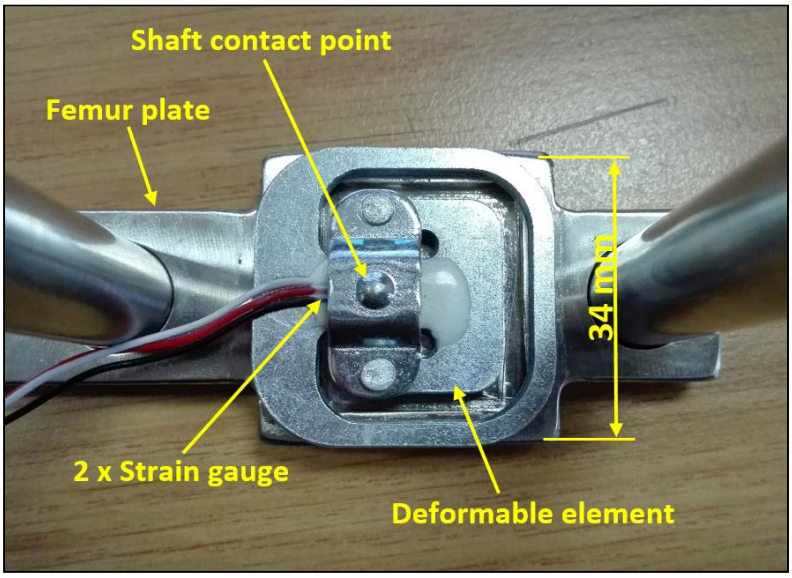

Figure 39: Load cell

A strain gauge is a conductive flat metallic pattern that can measure the strain of an element. As the element deforms under a force, the strain gauge also deforms causing the electrical resistance of the strain gauge to change. The change in strain of the element is proportional to the change in electrical resistance of the strain gauge. When a current is generated in the strain gauge the change in voltage across the strain gauge can be used to quantify the force applied to the element.

In order to measure the strain of the deformable element, the strain gauges are connected in a Wheatstone bridge configuration as shown in Figure 40 in which R represents the resistance of each strain gauge. As shown in Figure 40, the Wheatstone bridge is completed by connecting two identical load cells. Load cell 1 is used in the knee tensioner and Load cell 2 is passively connected to the Wheatstone bridge circuit.

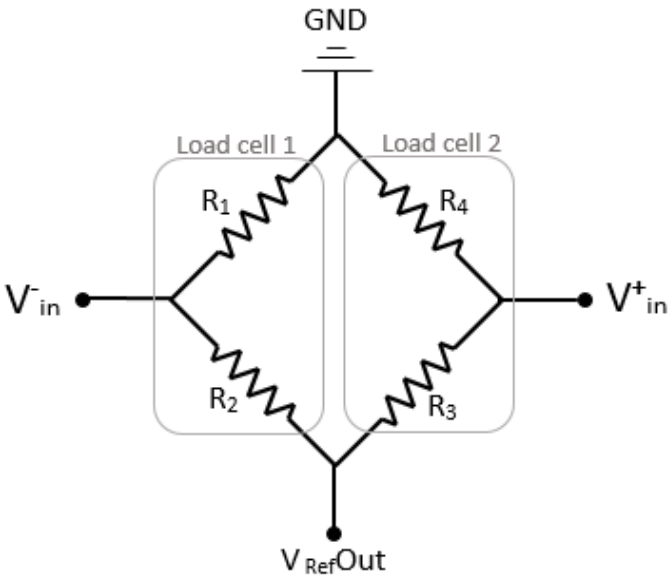

Figure 40: Wheatstone bridge configuration of the strain gauges in the load cells.

The labels $V_{Ref}Out$, V^{+}_{in}, and V^{-}_{in}, in Figure 40, correspond to the pins on the amplifier, which is discussed below. The circuit is excited by applying a 5 V voltage across $V_{Ref}Out$ and ground (GND) and the output of the circuit is measured across V^{-}_{in} and V^{+}_{in}. When no load is applied to Load cell 1, the measured output voltage ($V_{BridgeOut}$) across V^{+}_{in}, and V^{-}_{in} is 0 V. When a load is applied to Load cell 1, the output is a nonzero voltage proportional to the magnitude of the force. V_{out} is calculated using the following formula (National Instruments, 2016):

$$\boldsymbol{V_{BridgeOut} = V_{in}^{+} - V_{in}^{-} = \left(\frac{R_1}{R_1+R_2} - \frac{R_4}{R_3+R_4}\right) \times V_{Ref}Out} \quad (1)$$

In order to measure the voltage across the strain gauge an Arduino microcontroller is used. The Arduino has multiple analog inputs which measures the magnitude of an analog signal. The Arduino has an analog-to-digital-converter (ADC), which converts the measured voltage to a digital value and sends these values via USB to a PC. For this application an Arduino Nano microcontroller PCB is used, which is shown in Figure 50. The Arduino Nano measures a voltage between 0 and 5 volts and presents the measured voltage as a digital value ranging over 1023 integers. Therefore, the analog resolution of the Arduino Nano is 4.89 mV, which is calculated by dividing 5 V by 1023 integers.

The specification sheet of the load cell is given in Appendix A. The load cell in the knee tensioner has a capacity of 50 kg and an output sensitivity of 1±0.1 mV/V. The output sensitivity of the load cell indicates that if the load cell is excited by a voltage of 5 V, the output of the load cell under a load of 50 kg will be 5mV. The knee tensioner is designed for a maximum force of 150 N (~15 kg). Therefore, the

expected maximum output of the load cell is 1.5 mV. Since the resolution of the Arduino Nano is 4.89 mV, the signal from the load cell must be amplified significantly in order to detect a change in voltage over the strain gauges for loads in the range of 0 to 150 N.

An INA125 instrumentation amplifier is used to amplify the signal from the load cell. In Figure 50, the amplifier is shown. In Appendix A the specification sheet of the amplifier is given and in Appendix D the schematic of the circuits shows how the amplifier is connected to the load cell and the Arduino Nano. The gain of the amplifier is set with an external resistor (R_G) between pins 8 and 9, and is calculated using the following formula:

$$\boldsymbol{Gain = 4 + \frac{60\ k\Omega}{R_G}} \qquad (2)$$

An external resistance of 180 Ω was chosen. With R_G = 180 Ω, the gain is 337.33. This increases the output voltage of the load cell to 506 mV under a load of 150 N. With this gain, the force resolution is 1.45 N. Increasing the gain results in a higher force resolution, however, this also increases the amplitude of the noise in the signal. Therefore, there exists a trade-off between the resolution of the force and the noise in the signal. In order to decrease the noise, certain methods were used to filter the signal, which will now be discussed.

Shown in Figure 41 is a sample of the unfiltered signal from the load cell. Note that the signal was sampled before the load cell was calibrated in terms of Newton force. The low frequency oscillation was created to replicate the expected frequency of the measured force during *in*-vitro tests. It can also be seen that there are high frequency changes in the signal, which is known as noise. Noise in a signal can have the effect that it prevents meaningful changes in the magnitude of the signal from being detected. The noise in the signal is caused by the strain gauge, stepper motor and IMU sharing the same ground and causing a ground loop. Unwanted current is introduced into the loop through electromagnetic induction, which is observed as noise in the signal to be measured (Engdahl, 2013). It is expected that the change in force measured during experimentation will have a frequency significantly lower than the frequency of the noise.

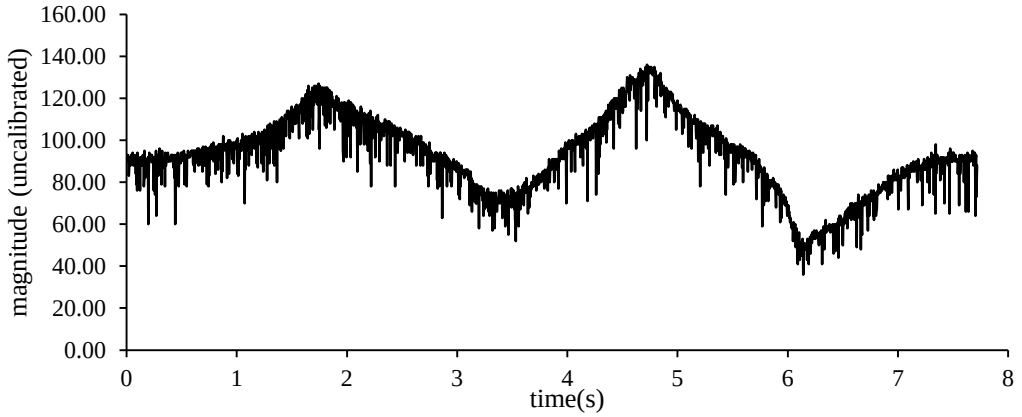

Figure 41: Sample of unfiltered signal from load cell

In order to determine which frequencies represent the noise in the signal, the amplitude of the signal is analysed in the frequency domain. By applying a fast Fourier Transform (FFT) algorithm to the sample signal, the signal was converted from a signal in the time domain to a signal in the frequency domain. The signal was converted using MATLAB (Version: R2016b, 2016) and the code for this conversion is provided in the attached CD. In Figure 42, the single-sided amplitude spectrum of the unfiltered signal is given. It was determined that the signal representing the change in force exists below a frequency of 100 Hz and that all signals above 100 Hz represent the noise (during calibration of the knee tensioner the frequency above which noise existed was found to be much lower).

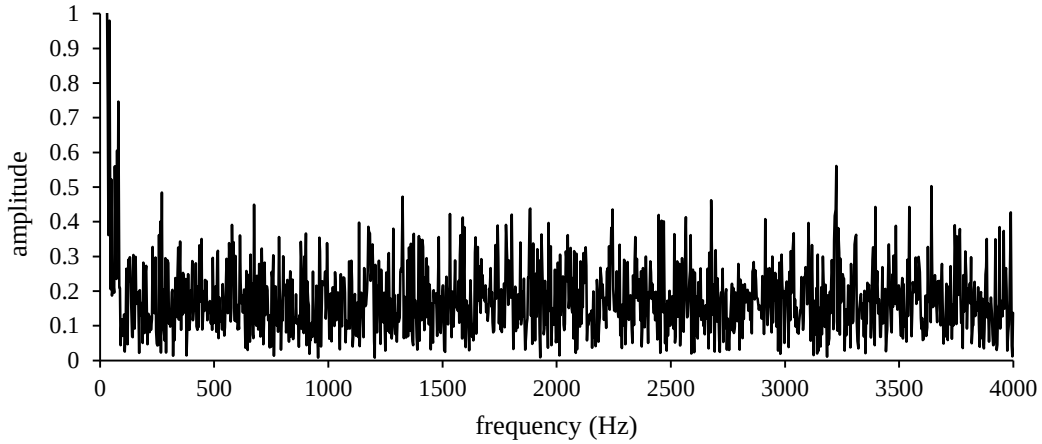

Figure 42: Single-sided amplitude spectrum of unfiltered signal

In order to filter the signal so that signals with frequencies below 100 Hz is retained and signals with frequencies higher than 100 Hz is blocked, a low pass filter is required. A low pass filter allows all signals with frequencies below a cut-off frequency (f_c) to pass through the filter and blocks the rest. In this case, the cut-off frequency is 100 Hz. An analog and digital first-order low pass filter was incorporated. An analog first-order low pass filter consists of a resistor and a

capacitor connected in series, as shown in Figure 43, with input signal V_{in} and output signal V_{out} (Electronic Tutorials, 2017).

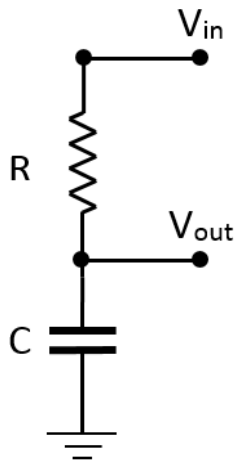

Figure 43: Analog first-order low pass filter

The values for the resistor and the capacitor are determined using the following formula (Electronic Tutorials, 2017):

$$\boldsymbol{f_c = \frac{1}{2\pi RC}} \quad (3)$$

A combination of resistor and capacitor values were chosen to satisfy a cut-off frequency of 100 Hz. However, after the combination was tested practically there was still significant noise on the signal. Through an iterative process, the cut-off frequency was lowered through different resistor and capacitor values until an acceptable amount of noise was removed without removing the signal representing the change in force. The resistor and capacitor values settled on was 20 Ω and 100 µF respectively, which results in a cut-off frequency of 79.58 Hz. However, for the final *in-vitro* test in which Prototype 2 was used, the cut-off frequency was lowered to 18 Hz with 88 Ω resistance and 100µF capacitance, in an attempt to reduce noise further.

A digital filter was also incorporated due to the presence of noise after the implementation of the analog filter. The transfer function of a first order low pass filter is given in Equation 4 (HowToDoIt, 2015).

$$\boldsymbol{H(s) = \frac{2\pi f_c}{s+2\pi f_c}} \quad (4)$$

In order to use the equation in the Knee Tensioner Algorithm, it must be converted from continuous-time form to discrete-time form. This conversion was done in MATLAB and the code for this conversion can be found in the attached CD. After the transfer function was converted to discrete-time form, it was written into the

Knee Tensioner Algorithm code, which is given in the attached CD. Again, the transfer function was calculated with a cut-off frequency of 100 Hz. However, after practical implementation it was found that a cut-off frequency of 1 Hz was more suitable for the digital filter, as will be explained in Section 3.7.4. In Figure 44, a sample of the signal is given after analog and digital filtering is applied. Compared to the signal in Figure 41, the filtered signal does not contain observable noise. In Figure 45, the filtered signal is shown in the frequency domain, after a FFT algorithm was applied. It is clear that most of the high frequency noise was reduced to zero. In Section 3.7, the remaining noise in the filtered signal after the knee tensioner was calibrated is quantified along with the signal-to-noise ratio and the response time of the load cell.

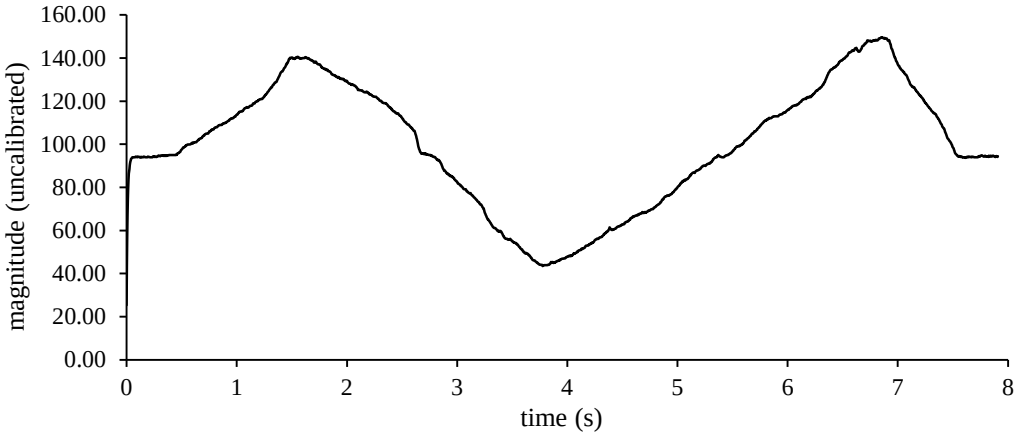

Figure 44: Sample of filtered signal from load cell

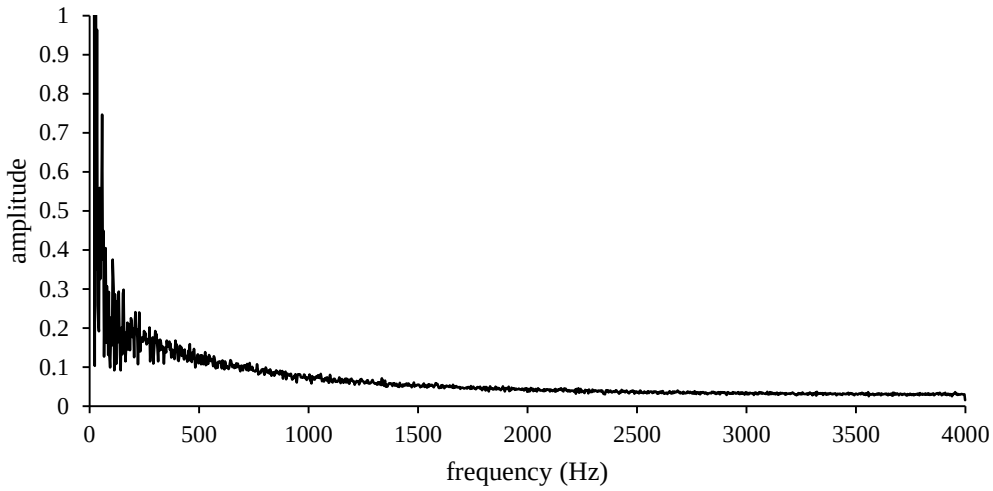

Figure 45: Single-sided amplitude spectrum of filtered signal

The Arduino software (Version: 1.6.11, 2016) was used to monitor the amplified signal, after being converted to a digital value by the Arduino Nano. The Arduino IDE can be used to monitor the serial port through which the Arduino Nano

communicates with the PC. The digital values sent through the serial port can be viewed in real-time using the IDE.

3.5.6 Measuring the angle

The IMU, shown in Figure 24 and Figure 37, uses an InvenSense MPU-6050 sensor (TDK InvenSense, 2017) that incorporates a gyroscope and an accelerometer, each measuring in 3-axes. The gyroscope measures the IMU's orientation and the accelerometer measures the acceleration of the IMU, both in 3-dimensional space. The sensor is capable of measuring the angles and accelerations in all the axes simultaneously and has a 16-bit analog to digital converter. In order to communicate with an Arduino microcontroller, the MPU-6050 uses an I2C-bus. The MPU-6050 sensor has a Digital Motion Processor (DMP), which can do calculations with the raw values measured by the sensor to produce values that can be interpreted as angles and accelerations (Arduino, 2017). In Appendix A, the specification sheet of the InvenSense MPU-6050 is given.

In order to use the DMP to calculate meaningful information regarding the IMU's orientation and acceleration an Arduino library is used in the Arduino IDE together with an Arduino 'sketch' (Arduino code), both of which were written by Jeff Rowberg and made publically available to use without limitations (Rowberg, 2017). This library and the code within this sketch, after being modified, were incorporated in the Knee Tensioner algorithm. The sketch, as written by Jeff Rowberg, enables the IMU to give the orientation of the IMU in terms of either rotation quaternions, Euler angles or angles representing the yaw, pitch and roll of the IMU. For this application the yaw, pitch and roll angles were used to describe the orientation of the IMU since the orientation of the knee tensioner is measured with respect to a starting orientation (the orientation of the tibia before the knee is flexed). The IMU is placed on the tensioner parallel to the Sagittal plane. The pitch angle is then used to measure the rotation of the tibia in the Sagittal plane.

The original sketch was modified by removing all *Serial.print()* statements that do not display information regarding the orientation of the IMU. This was done to increase the speed at which the sketch is executed. Furthermore, for the use of the code in the Knee Tensioner Algorithm, the statements that cause the sketch to wait for a character to be sent through the serial port to start the measurements were removed to allow the MPU-6050 sensor to initialize as soon as the Knee Tensioner Algorithm is executed. The original "MPU6050_6Axis_MotionApps20.h" library file was also modified to allow the sensor to give angles between 0° and 180°, and not the original range of 0° to 90°. A range of 0° to 180° is required since the knee is capable of flexing beyond 90° knee flexion and valuable information regarding the joint gap stiffness beyond 90° knee flexion can then be obtained.

The sampling rate of the MPU-6050 sensor can also be set in the "MPU6050_6Axis_MotionApps20.h" library file. The sampling rate of the IMU

was set to 25 Hz for Prototype 1 and was increased to 100 Hz for Prototype 2 in an attempt to increase the sampling rate of the Arduino.

A crucial error was encountered when using the sketch as written by Jeff Rowberg. The error caused the Arduino Nano to freeze after an arbitrary amount of time. The solution to this problem was found in an online forum in which similar cases were reported. A solution was presented in a comment (109JB, 2015) on an issue a user of a MPU-6050 sensor had in which the Arduino Nano would also freeze after a while (Lage, 2015). The Arduino Nano reads the values from the MPU-6050 sensor from a FIFO (first-in, first-out) buffer once an interrupt signal is detected. By connecting the interrupt pin on the IMU, labelled "INT" in Figure 46, the Arduino Nano can make use of interrupt signals. The solution to the issue is to disregard the use of an interrupt signal and thus the use of the interrupt pin on the IMU. Thus, the "INT" pin was disconnected from the Arduino Nano and a modified sketch was used that was given in the comment presenting the solution (109JB, 2015). This solved the problem of the Arduino Nano freezing after certain amount of time.

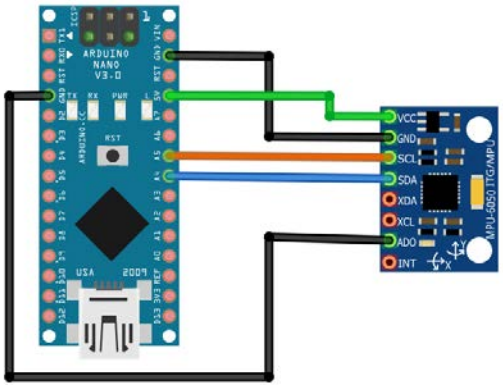

Figure 46: IMU to Arduino connections

3.5.7 Measuring the gap distance

The gap distance of the knee joint is measured between the surface of the femur plate in contact with the femoral condyle and the surface of the tibia plate in contact with the resected surface of the tibia. The number of steps the stepper motor turns is used to measure the distance the shaft displaces in the axial direction of the shaft. Using the Arduino IDE, the stepper motor can be commanded to turn a certain number of steps when prompted to do so. Since the number of steps can be controlled, the displacement of the shaft can be controlled which relates to the change in the distance between the articulating surfaces of the femur plate and the tibia plate.

The thread on the shaft of the stepper motor has a pitch of 2 mm. This means that if the stepper motor does one rotation, the shaft will displace 2 mm in the axial direction. In addition, one rotation of the stepper motor equals 200 steps, giving the

knee tensioner a resolution of 0.01 mm per step. Thus, the change in gap distance is calculated using the following equation:

$$\Delta \textbf{ gap distance} = \textbf{0.01 mm} \times \textbf{steps} \quad (5)$$

However, Equation 5 is for an ideal situation. In practice, the stepper motor is prone to skip steps or not execute them when commanded to turn a number of steps ranging in the thousands. To account for this irregularity a calibration test was done to find a more suitable equation for the required range of steps. The stepper motor was commanded to turn a number of steps starting from zero and ending at 6000, each time increasing the number of steps by a 1000. The gap distance was then measured using a Vernier Calliper after each set of steps was executed. In Figure 47, the result of this test is shown.

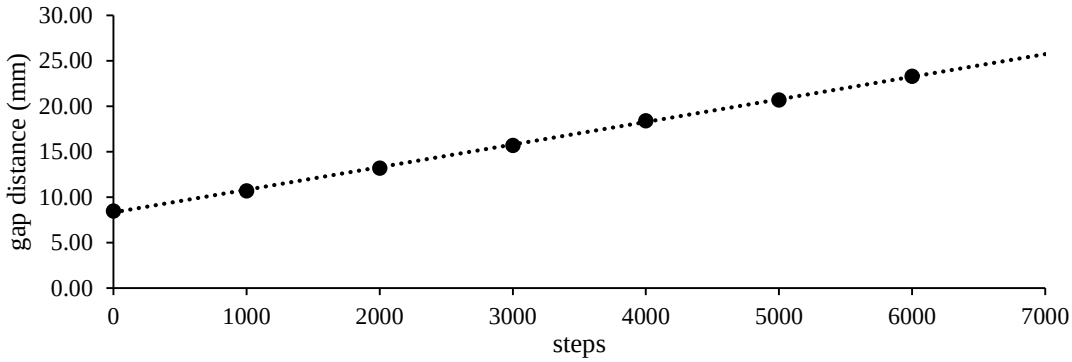

Figure 47: Results from stepper motor calibration test

A linear trend line was then fitted to the data and the equation of this trend line used as the new relationship between the number of steps and the gap distance, which is as follows:

$$\textbf{\textit{gap distance}} = (\textbf{0.0025 mm} \times \textbf{\textit{steps}}) + \textbf{8.5} \quad (6)$$

The minimum gap distance the knee tensioner can provide is 8.5 mm, due to the thickness of the plates. Therefore, the user of the knee tensioner must always provide a minimum value of 8.5 mm for the required gap distance. In the knee tensioner algorithm, the number of steps the stepper motor must turn to create a certain gap distance (mm) is calculated using the following equation:

$$steps = round\left(\frac{gap\ distance - 8.5}{0.0025}\right) \quad (7)$$

The *round()* function in Equation 7 rounds a value to the nearest integer.

In the Knee Tensioner Algorithm code, the number of steps the stepper motor turns after each loop was set at 20 steps for the Distance Control function and 10 steps for the Force Control function. This relates to 0.2 mm and 0.1 mm respectively. Even though there is no feedback regarding the number of steps the stepper motor turns, the steps are monitored by assigning a variable to it in the Knee Tensioner

Algorithm code, which is updated by the number of steps the stepper motor turns each time it is commanded to turn.

3.5.8 Control system

The Force Control function of the knee tensioner requires a control system to enable the knee tensioner to maintain a constant distraction force in the knee joint for all angles of knee flexion between 0° and 90°. Therefore, a control system was implemented in the Knee Tensioner Algorithm. The algorithm maintains the desired distraction force by commanding the stepper motor to decrease the gap distance when the measured force is above the desired distraction force and increasing the gap distance when the measured force is below the desired distraction force.

In the algorithm, the gap distance is adjusted in increments of a constant number of stepper motor steps, as mentioned above, and at a constant speed (stepper motor turning speed) until the measured force is within a certain tolerance of the desired distraction force. The tolerance on the measured force is 2.5% above and below the desired distraction force.

3.5.9 Graphical user interface (GUI)

The GUI was developed in the Processing IDE. In Appendix C, a screenshot of the GUI is shown. The GUI provides the user of the knee tensioner with four input fields to submit values for the required gap distance and force to the knee tensioner, depending under which two functions it should operate. There is also a button to calibrate the force and angle, a button to start the recording of the data, a button to stop the recording, and a button to return the knee tensioner to zero gap distance.

When the knee tensioner is inserted into the knee joint, the load cell must be calibrated by clicking on the ‘Calibrate’ button. This zeroes the force measurement before the knee tensioner distracts the knee joint. The Calibrate button also zeroes the angle measurement, so that the initial angle of knee flexion can be used a reference for other angles of knee flexion. The ‘Record’ and ‘Stop Record’ buttons start the logging of the data and saves it, respectively. In order to return the plates of the knee tensioner to a zero gap distance, the ‘Return’ button must be clicked on.

In the following section, the structures of the Knee Tensioner Algorithm and the GUI Algorithm are given and discussed.

3.5.10 Software algorithm

In this section the Knee Tensioner Algorithm and the GUI Algorithm is discussed in terms of their structure, their interaction with each other and their implementation into the hardware.

The Knee Tensioner Algorithm was developed in the Arduino IDE. The Knee Tensioner Algorithm consists of C and C++ programming language functions. Once the algorithm is compiled by the Arduino IDE, it is uploaded to the Arduino Nano from which it operates. The Knee Tensioner Algorithm has the following functions:

- Receives commands from the GUI Algorithm.
- Receives data from the load cell and IMU.
- Sends commands to the stepper motor.
- Sends data regarding force, angle and gap distance to the GUI Algorithm.

In Figure 48, the Knee Tensioner Algorithm is represented by a flow diagram of signals in which it is shown how the GUI Algorithms sends and receives data. For both the Distance Control and the Force Control functions, either an input with a distance or an input with a force is given.

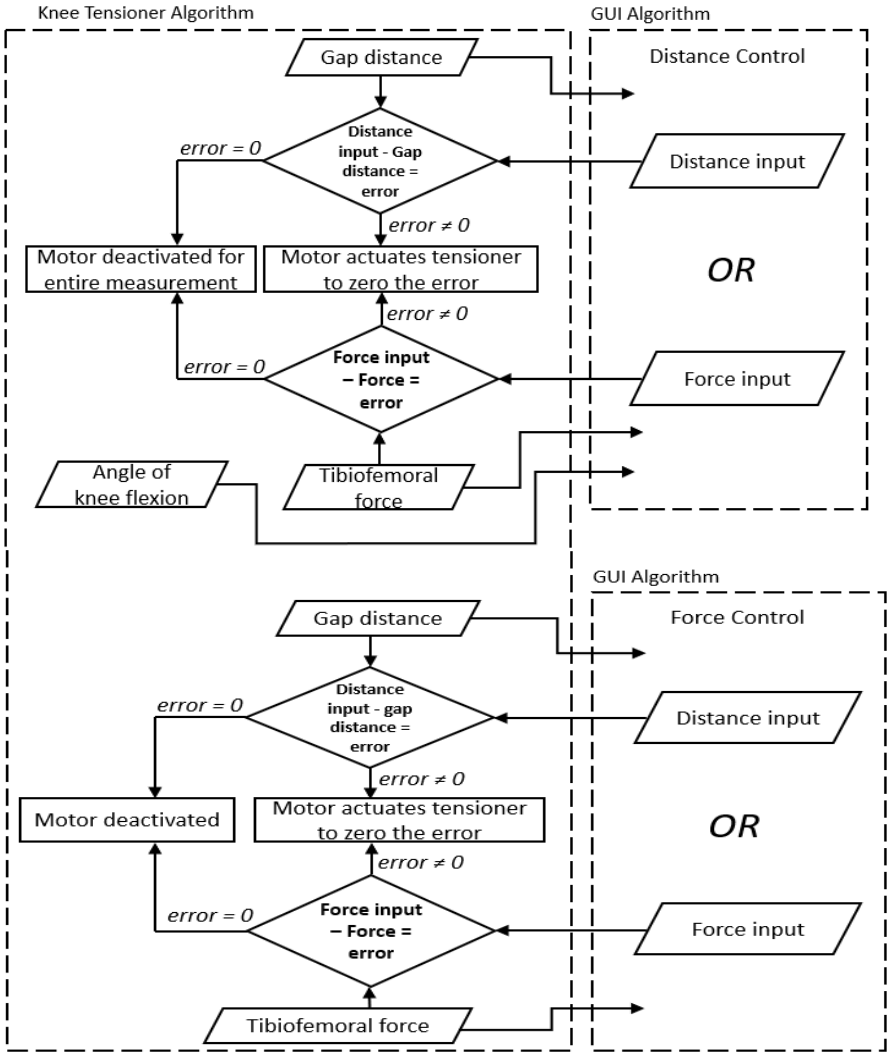

Figure 48: Knee Tensioner Algorithm flow diagram

In Figure 49, the GUI Algorithm is also represented by a flow diagram of data. Note that when the user clicks on the 'Record' button in the GUI, a file with a .csv extension is created wherein the values of force, angle and gap distance will be saved. A .csv file can be viewed and edited in Microsoft Excel.

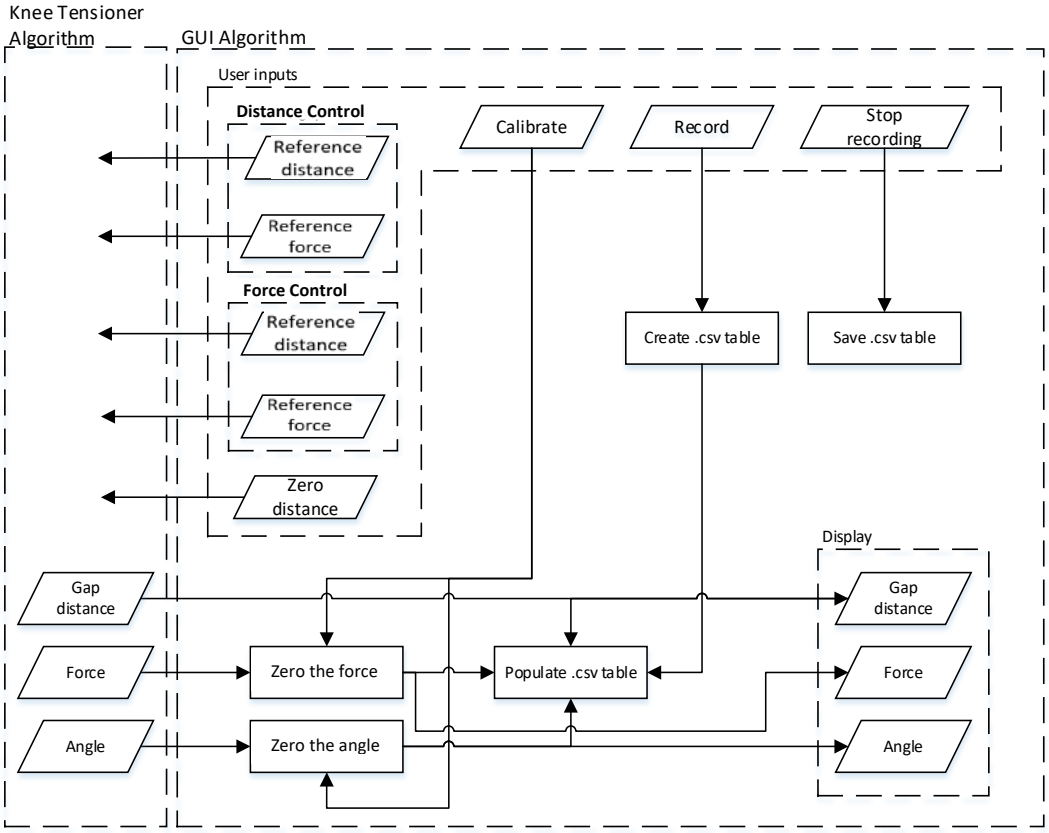

Figure 49: GUI Algorithm flow diagram

Data is exchanged between the Knee Tensioner Algorithm and the GUI Algorithm through serial communication. Serial communication is made possible by connecting the Arduino Nano to the PC with a USB cable.

3.5.11 Electrical configuration

In order to allow the knee tensioner to move freely during experimentation within the testing area, the electronic components that are not attached to the knee tensioner were placed on a PCB, which is connected to the knee tensioner via a 3 m long cable. Initially, a breadboard was used to connect the electronic components with each other, in order to determine the correct configuration and test different analog filters. After the correct circuit configuration was determined, a PCB was designed and manufactured. It was decided to manufacture a PCB due to its compact size and secure connections.

The main electronic components on the PCB include the following: The Arduino Nano, the stepper motor drive chip and the INA125 amplifier. In Appendix D, a full list of the PCB components is given along with the schematic of the circuits. In Figure 50 the PCB is shown. A plastic enclosure for the PCB was printed by a 3D printer, which protects the PCB. The enclosure containing the PCB is called the Control Box and is shown in Figure 51. The dimensions of the Control Box are included in the attached CD.

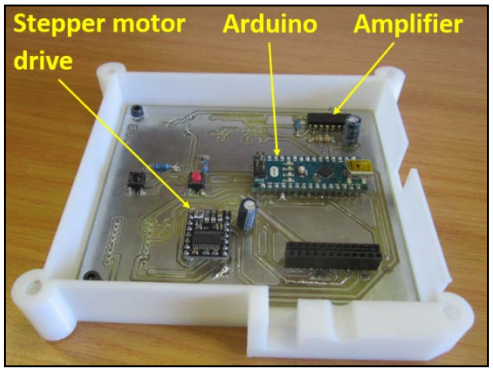

Figure 50: PCB inside the Control Box

Figure 51: Control Box

Three cables connect to the Control Box: A USB connecting the Arduino Nano to the PC, a 12 V power adapter cable connecting to a wall socket, and the cable connecting to the knee tensioner containing the wires of the load cell, the IMU and the stepper motor. In Figure 52, a schematic of the connections between the PC, the Control Box and the knee tensioner is shown.

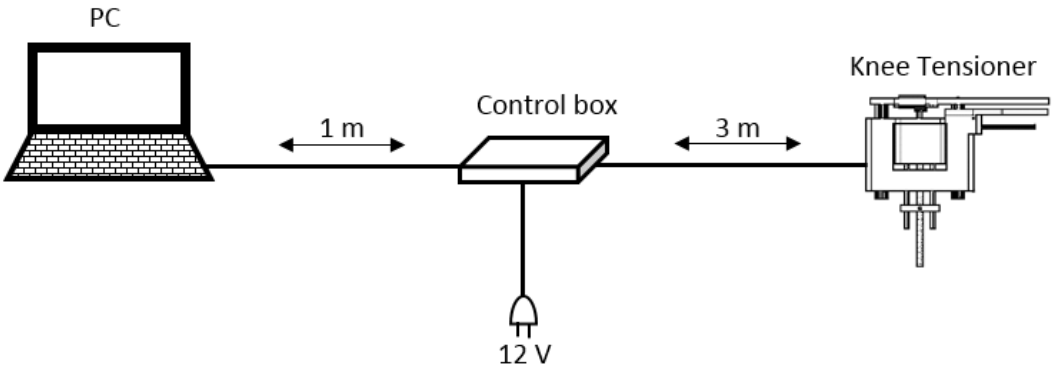

Figure 52: Schematic of wiring

3.6 Design modifications

After Prototype 1 was manufactured, four aspects were identified which could be improved. They include the following:

1. The assembly of the knee tensioner body, which includes the two bearing blocks and the top and bottom connector plates.
2. The plain linear bearings wherein the guide rods slide.
3. The holding pins.
4. The control system.
5. The position of the IMU.

In this section, these five aspects and their improvements are discussed. After the improvements were made, the new knee tensioner model that resulted was named Prototype 2.

3.6.1 Knee tensioner body assembly

The body assembly of Prototype 1, consisting of the bearing blocks and the two connector plates, can be viewed in Figure 29. In order to allow the two guide rods to slide with as little friction as possible within the plain linear bearings, both the two guide rods and the two plain linear bearings all have to be parallel to allow equal spacing around the surface of the guide rods. Since the two bearings blocks are fixed to the connector plates with screws, they pose the risk of misaligning after the body has been disassembled and reassembled. This potential risk exists due to the spaces created by the tolerances on the screw holes, which cause the bearing blocks to shift relative to each other.

To avoid this risk, a new body was designed consisting of one part, preventing the bearing blocks from moving with respect to each other. This part was manufactured from aluminium and is shown in Figure 53.

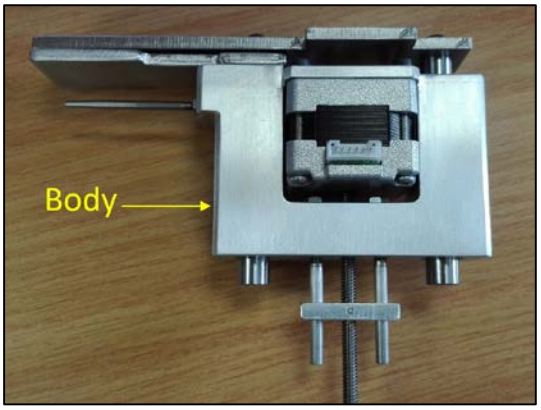

Figure 53: The physical model of Prototype 2 excluding the load cell, the IMU and electrical wiring

3.6.2 Plain linear bearings

As explained in Section 3.5.2, a moment is created in the femur plate when the femoral condyles exert a force on the plate. The moment causes the guide rods to rotate within the plain linear bearings, pushing them with a reaction force against the inner surface of the bearings. Due to the increased force on the surface of the guide rods, the friction between the rods and the bearing increase. This prevented the knee tensioners from exerting a distraction force of more than 80 N. If the force of the femoral condyles is too large, the friction force causes the guide rods to "lock", preventing the stepper motor from actuating the femur plate.

In order to reduce the amount of friction, the plain linear bearings were replaced with linear ball bearings. Linear ball bearings contain rows of steel balls that line the inner surface of the bearing. This significantly reduces the friction between the guide rods and the bearings and the knee tensioner was capable of exerting a distraction force of 160 N, as specified in Section 3.3. In Figure 54, the linear ball bearings are shown in a cross-sectional view of the body of Prototype 2.

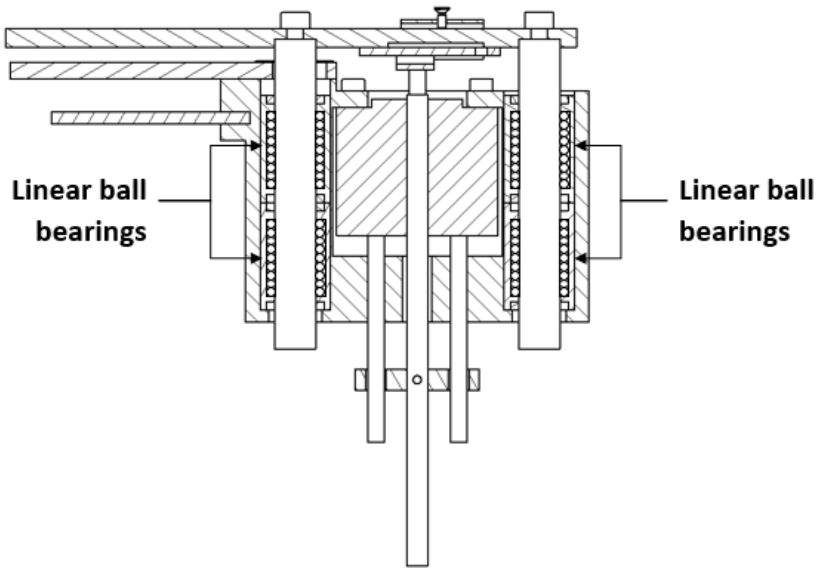

Figure 54: Cross-sectional view of CAD model of Prototype 2

3.6.3 Holding pins

Two holding pins were fixed to Prototype 1. It was found that one holding pin was sufficient. Therefore, Prototype 2 was fitted with one holding pin, as shown in Figure 53 and Figure 54.

3.6.4 Control system

The control system was modified by incorporating proportional control. With proportional control, the distance (or stepper motor steps) and speed (stepper motor

turning speed) of the increments by which the gap distance is adjusted, is proportional to the difference between the measured force and the desired distraction force. However, when the difference between the measured force and the desired force is equal to or larger than 5 N, the distance and speed of the increments are limited to 0.2 mm (20 stepper motor steps) and 1.67 mm/s (50 rpm stepper motor rotation speed), respectively.

3.6.5 IMU position

IMU measures angles describing its orientation in terms of yaw, pitch and roll (see Section 3.5.6). In the orientation and position of the IMU on the knee tensioner, as shown in Figure 37, the IMU at times failed to measure any change in the angle of knee flexion with the IMU's pitch angle. This happened due to the occurrence of gimbal lock in which the detection of one degree of freedom in the three-dimensional space is lost when two axes of rotation align (Jones & Fjeld, 2011). Therefore, in order to find a solution to this problem the orientation of the IMU was changed and another axis was used to measure the angle of knee flexion. Shown in Figure 55, is the altered position of the IMU. In this position, the yaw angle of the IMU is used to measure the angle of knee flexion. This new position allowed the IMU to measure the angle accurately without failure.

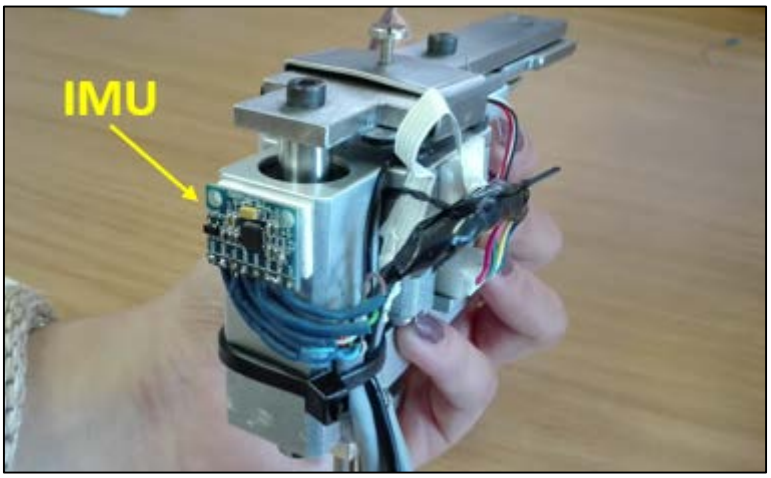

Figure 55: Altered position of IMU on Prototype 2

3.7 Calibration

3.7.1 Introduction

The load cell had to be calibrated in order to relate the digital value of the load cell signal to a force. In this section, the method in which the load cell was calibrated is explained. During calibration, the error on the load cell measurement, the noise in the load cell signal, the hysteresis of the load cell and the response time of the load cell was also quantified. In this section, these quantifications are discussed and summarised in Section 3.7.8. The error in the measurement of the angle is also briefly discussed.

Before the calibration of the load cell is discussed, the configuration of the knee tensioners will be given. Here the configuration of the knee tensioner refers to the parameters of the hardware and software, which influenced the speed and accuracy of data capturing.

3.7.2 Device configuration

The configurations of the knee tensioners are given in Table 3 for each *in-vitro* test the knee tensioners were used in.

Table 3: Configuration of knee tensioners

Parameter	Knee tensioner sampling rate	IMU sampling rate	Data recording rate	Gain of amplifier	Analog f_c	Digital f_c
1st test: Prototype 1	10 Hz	25 Hz	7.5 Hz	337	79.6 Hz	1 Hz
2nd test: Prototype 2	22.5 Hz	100 Hz	7.5 Hz	337	79.6 Hz	1 Hz
3rd test: Prototype 2	22.5 Hz	100 Hz	7.5 Hz	337	18 Hz	1 Hz

3.7.3 Load cell calibration and error

The load cell of Prototype 1 and Prototype 2 was calibrated by loading the knee tensioners with static weights and recording the digital value each weight represented. By doing this, a relationship could be obtained between the force applied to the knee tensioner and the digital value of the load cell signal. A combination of weights with increments of 200 g and adding up to 10 kg were placed on the knee tensioner. In Figure 56, the knee tensioner is shown with a 2 kg weight placed on the femur plate.

Figure 56: Calibrating the load cell with weights

A linear trend line was drawn through the points of a graph showing the mass of the weights versus the digital values of the load cell signal. The gradient of the trend line was used as the overall relationship between the mass of the weights and the load cell signal. In order to quantify an error for the force measurements, the mean absolute error (MAE) was calculated between the data points and the trend line for the ith mass as follows:

$$\boldsymbol{MAE}\ \% = \frac{\boldsymbol{100}}{\boldsymbol{n}} \sum_{\boldsymbol{i=1}}^{\boldsymbol{n}} \left| \frac{\boldsymbol{trend\ line\ value_i - measured\ value_i}}{\boldsymbol{trend\ line\ value_i}} \right| \% \qquad (8)$$

The mean absolute error for the knee tensioners are given in Table 4.

3.7.4 Signal to noise ratio

The signal to noise ratio (SNR) of the load cell signal is a ratio of the strength of the signal to the noise in the signal. Even though it would be ideal to have zero noise in the signal, lowering the cut-off frequency of the filters increases the response time of the load cell. The cut-off frequency of the digital filter was therefore tuned to allow a maximum noise magnitude of 5% of the maximum expected amplitude of the signal. The maximum expected amplitude was determined from the measurements in the first *in*-vitro test. Subsequently, the SNR was only calculated for the second and third *in-vitro* tests in which Prototype 2 was used. This resulted in a cut-off frequency of 1 Hz. The signal to noise ratio was then calculated with the following equation:

$$\boldsymbol{SNR} = \left(\frac{\boldsymbol{A_{signal}}}{\boldsymbol{A_{noise}}} \right)^{\boldsymbol{2}} \qquad (9)$$

In Equation 9, A_{signal} is the maximum expected amplitude of the signal and A_{noise} is the amplitude of the noise in the signal which represents an RMS value of the noise. In Table 4, the signal to noise ratio is given, as well as the magnitude of the noise in the signal.

3.7.5 Response time of load cell

The response time of the load cell determines how accurate the knee tensioner can record a change in tibiofemoral force. The response time of the load cell is defined as the duration of detecting a change in the tibiofemoral force. With this information, it was determined what the rotation speed of the tibia should be that would allow the knee tensioner to measure the tibiofemoral force without error due to the response time of the load cell. The response time was determined by placing a weight on the femur plate and measuring the time it took for the load cell to detect the change in force. This was done for different weights so that a relationship could be obtained between the force ($\Delta\, force_{weight}$) and the time ($\Delta\, time$). This relationship was used together with the maximum expected change in tibiofemoral force ($\Delta\, force_{knee}$) for a change in angle of knee flexion ($\Delta\, angle$), to calculate a maximum allowed angular velocity of the tibia with Equation 10.

$$\frac{1}{\boldsymbol{angular\ velocity}} = \left(\frac{\Delta\, \boldsymbol{force_{knee}}}{\Delta\, \boldsymbol{angle}}\right) \times \left(\frac{\Delta\, \boldsymbol{time}}{\Delta\, \boldsymbol{force_{weight}}}\right) \qquad (10)$$

Since the maximum expected change in tibiofemoral force per angle of knee flexion is used in Equation 10, the angular velocity that was calculated represents the extreme case. In Table 4, the maximum allowed angular velocity of the tibia is given.

The response time of the load cell also plays an important role in the Force Control function of the knee tensioner as it determines how fast the knee tensioner reacts to a change in tibiofemoral force by actuating the femur plate so that the force on the femur plate is kept constant. The response time of the knee tensioner was evaluated by rotating a synthetic femoral condyle on the surface of the femur plate as shown in Figure 57.

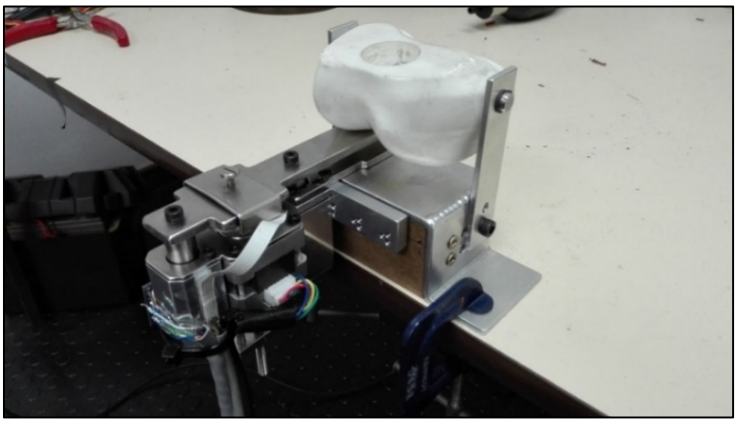

Figure 57: Testing the response time of Prototype 1 with a Synthetic femoral condyle

3.7.6 Hysteresis

The hysteresis percentage error of the load cell, as given in the specification sheet of the load cell in Appendix A, is 0.03 %.

3.7.7 Angle calibration and error

Since the IMU produces an angle in degrees, it was not necessary to calibrate it. In the Appendix A, the specification sheet of the InvenSense MPU-6050 is given which includes its sensitivity and errors with regards to the different measuring axes.

3.7.8 Results of calibration

In Table 4, the results of the calibration of the knee tensioners are presented.

Table 4: Results of calibration

Test and prototype	Load cell MAE	Signal-to-noise ratio	Angular velocity of tibia
1st test: Prototype 1	7.8 %	19357.3	0.17 °/s
2nd test: Prototype 2	6 %	4903.3	3.45 °/s
3rd test: Prototype 3	6 %	4903.3	3.45 °/s

4 In-vitro testing

4.1 Introduction

In order to evaluate the knee tensioners that were designed and manufactured, they were tested on cadaver knees. The objective of the tests was to assess the functionality of the knee tensioner designs, and measure and record, with the knee tensioners, the following characteristics of each knee: The tibiofemoral force (which is equal to the distraction force applied by the knee tensioner), the gap distance and the angle of the knee.

Three tests were conducted. In each test, unicompartmental knee arthroplasty was performed on a cadaver knee. The manufactured knee tensioners were tested with native and prosthetic femoral condyles. Trial prosthetic femoral components were used as the prosthetics. In the first test (Test 1), Prototype 1 was tested and in the second (Test 2) and third test (Test 3), Prototype 2 was tested. In Test 1, it was important to establish design aspects of the knee tensioner related to the following: Whether the knee tensioner could be inserted into and removed from the knee joint, whether the tibia plate fitted onto the resected surface of the tibia plateau, and whether the femoral plate stayed in contact with the femoral condyle at all times. The use of the holding pins for fixing the device to the tibia and the method of creating the required holes for the pins also had to be evaluated. In Test 2 and Test 3, the emphasis was solely on data capturing.

In this chapter, the testing of Prototype 1 and Prototype 2 is discussed. The tests will be discussed in terms of the experimental setups and the methods that were followed.

4.2 Test setup

The tests were conducted in a cadaver laboratory in the Anatomy Building of the Faculty of Health Sciences at the University of Cape Town. Three half-body cadavers were prepared for each test respectively. The half-body cadavers were stored at -30° beforehand. In total, the knee tensioners were tested on four knees as follows: One in Test 1, two in Test 2 and one in Test 3.

In each case, the unicompartmental knee arthroplasties were performed by Dr Willem van der Merwe, an orthopaedic surgeon practising at the Sports Science Orthopaedic Clinic in Cape Town (Van der Merwe, 2016).

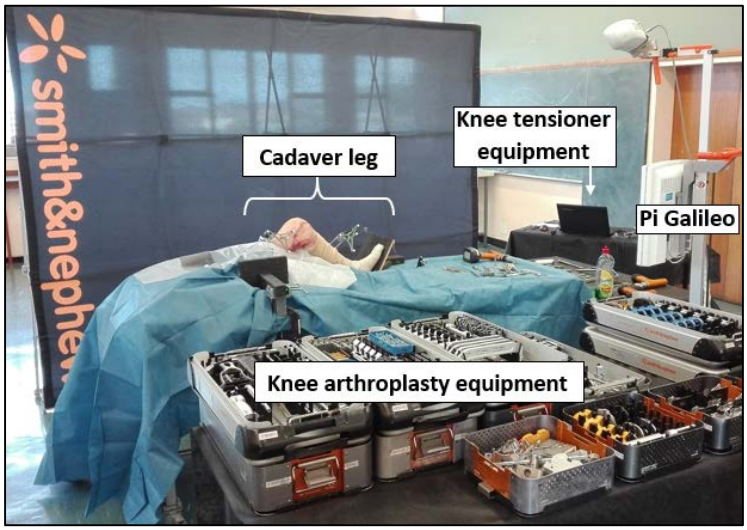

Figure 58: Test equipment layout

In Figure 58, the layout of the equipment for the test in the laboratory is shown. The equipment for the tests can be divided into two parts: The equipment required for the operation of the knee tensioner, and the equipment required for the performance of the knee arthroplasties. In Appendix E, the list of the equipment for the knee tensioner is given. The knee tensioner equipment was placed on a table in close proximity of the operation table and positioned so that the knee tensioner could be used on the cadaver knee while the Control Box remained stationary on the table. In Figure 59, the table on which the knee tensioner equipment is placed is shown with the PC, Control Box and knee tensioner on it. Notice in Figure 59 and Figure 60, the knee tensioner is covered in plastic with only the femur plate and the tibia plate exposed. This is to protect the electronic components on the knee tensioner from biological material and fluids.

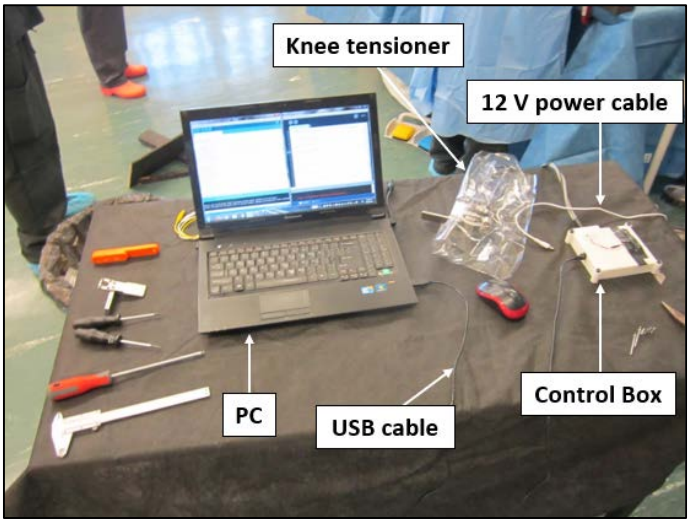

Figure 59: Knee tensioner equipment on laboratory table

In Test 1 and Test 2, the knee arthroplasties were performed with the help of the Smith & Nephew NAVIO Surgery System, a computer assisted surgery (CAS) system (Smith & Nephew, London, United Kingdom) (Lonner, et al., 2015). In Test 3, the Smith & Nephew Pi Galileo CAS system was used, as shown in Figure 58 (Smith & Nephew, London, United Kingdom) (Singh, et al., 2012). The varus and valgus angle of the knee was measured with the NAVIO Surgery System and the Pi Galileo system. However, the varus and valgus angle of the knee was only recorded during Test 3 and correlated with the data measured by Prototype 2.

4.3 Method

In Appendix E, a detailed description of the three tests is given, with steps as to how they can be replicated. Photos of the tests are also included in Appendix E. In general, each test starts with the exposure of the knee joint. Since the combined thickness of the tibia plate and the femur plate is 8.5 mm, 9 mm is then removed from the proximal tibia within the compartment of interest. A hole is then made in the tibia for the holding pin of the knee tensioner. This allows the knee tensioner to be inserted into the knee joint, as shown in Figure 60. The knee tensioner is then used to measure the tibiofemoral force, gap distance and angle of knee flexion with the native femoral condyle. After this, the knee tensioner is removed from the knee joint and the femoral condyle is replaced with the unicompartmental prosthetic component, after which measurements are repeated. In all three tests, the Journey Uni 2 femoral component, manufactured by Smith & Nephew (Smith & Nephew, London, United Kingdom), was used. In Test 3, the Journey Uni 2 femoral component was used as well as a competitor unicompartmental femoral component manufactured by Arthrex (Arthrex, Florida, United States of America) (Arthrex, 2017), which will be referred to as the ‘Arthrex’ prosthesis in this thesis. Therefore, measurements could be compared between the native femoral condyle and the prosthetic femoral condyles.

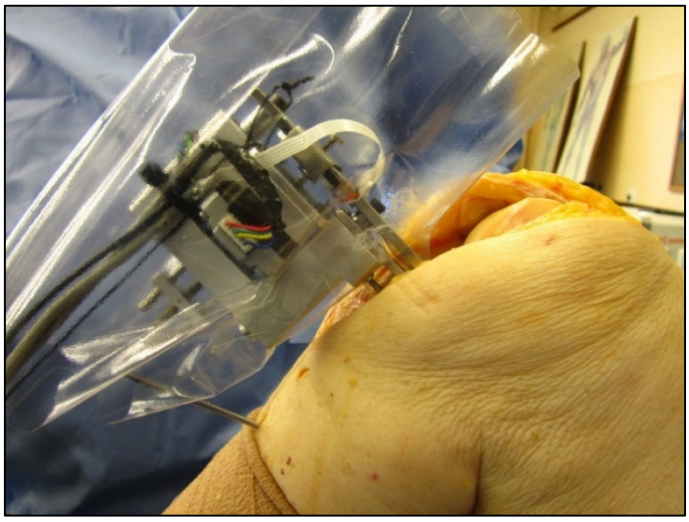

Figure 60: Knee tensioner inserted into the knee joint

Two measurement methods were carried out during the tests: Static measuring and dynamic measuring. In static measuring, the tibiofemoral force and the gap distance of the knee joint was measured at three angles: 0°, 45° and 90° knee flexion. For static measuring, Mode 2 (see Section 3.5.3) of the knee tensioner was used. In dynamic measuring the tibiofemoral force, the gap distance and the angle of the knee joint was measured at all angles between 0° and 90° knee flexion. For dynamic measuring Mode 1 and Mode 4 (see Section 3.5.3) was used.

The operation of the knee tensioner, once inserted into the knee joint, is represented by the flow diagrams in Figure 61 and Figure 62 for static measuring and dynamic measuring respectively.

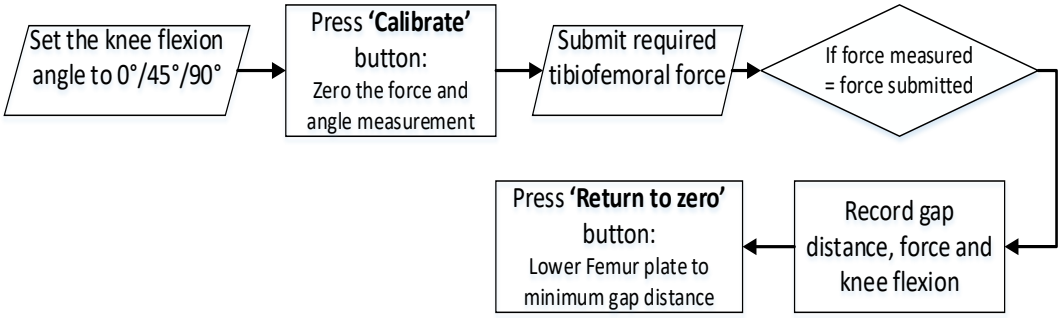

Figure 61: Operation of the knee tensioner in the knee joint for static measuring

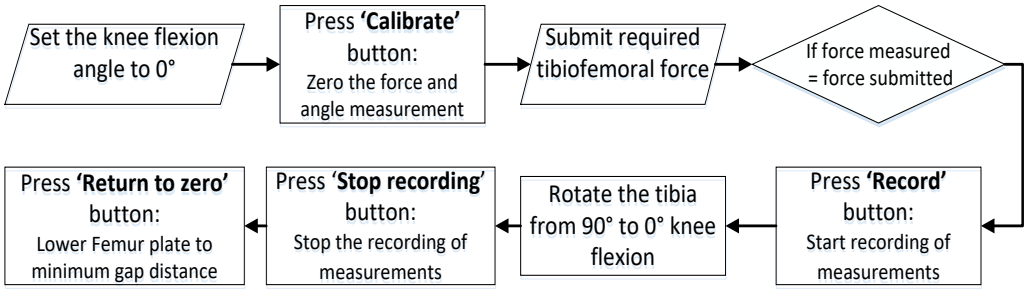

Figure 62: Operation of the knee tensioner in the knee joint for dynamic measuring

The rotation of the lower leg about the knee joint could be handled by any designated person present during the test. During dynamic measuring, the knee joint would be rotated by hand by rotating the lower leg about the knee joint and keeping the upper leg stationary. This allows the knee tensioner to use the starting position of the lower leg as a reference for the measuring of the knee flexion angle. During Test 1, it was noted that the way in which the lower leg of the cadaver was held by hand, during the rotation of the lower leg, influenced the tibiofemoral force measurement. Initially, the lower leg of the cadaver would be held by placing one hand beneath the foot of the cadaver and swinging the lower leg in an upward

motion. However, during the swinging motion of the lower leg, the handler would tend to push the foot towards the knee, thereby applying additional force on the knee tensioner. The risk of this happening was mitigated during Test 2 and Test 3 by placing the hand beneath the calf of the cadaver leg, during the rotation of the lower leg.

In Chapter 5, the measurements are presented that were recorded during the three tests. In Test 1, dynamic measuring was conducted in which a constant gap distance was maintained in the knee joint using Mode 1 of the knee tensioner. In Test 2 and Test 3, both static measuring and dynamic measuring were conducted. During dynamic measuring in Test 2 and Test 3, Mode 1 and Mode 4 of the knee tensioner were used to maintain a constant gap distance and a constant distraction force respectively.

5 Test results

In this chapter the results of the three *in-vitro* tests, as described in Chapter 4, are presented. The results include the assessment of the functionality of the knee tensioners, and the measurements recorded with the knee tensioners during the tests. The results of each test are presented chronologically. Both static and dynamic measurements are given in graphs. With these graphs the knee tensioners can be evaluated on a quantitative level, as discussed in Chapter 6.

5.1 Test 1 results

In Test 1, Prototype 1 was used. It was important to establish certain design aspects of the knee tensioner related to its use during the tests, which will now first be reported on.

The knee tensioner could easily be inserted and removed from the knee joint, by pushing the knee tensioner into the joint and pulling it out by hand. The tibia plate covered the length of the tibia plate in the anterior-posterior direction. The width of the tibia plate was narrow enough so that the tibia plate could be shifted on the resected tibial surface in the medial-lateral direction to align the femur plate with the femoral condyle. It was found that the femur plate was always aligned with the femoral condyle in the transverse plain. Whether the femoral condyle made contact with the femur plate relied on the gap distance the knee tensioner created. Due to the curvature of the tibia, only one holding pin could be utilised. One holding pin was found to be sufficient in securing the knee tensioner to the tibia. In creating the hole of the holding pin in the tibia, the holding pin block (with the holding pin attached) and the tibia plate had to be removed from the knee tensioner and used as the tool for creating the hole. The disassembling and assembling of the knee tensioner, for this purpose, prolonged the test. The solution to this was to create a tool consisting of a duplicate holding pin and tibia plate, as shown in Appendix E in Figure E.4, for the sole purpose of creating the holding pin holes.

In Test 1, the subject of the test was the medial compartment of the right knee of the cadaver. Dynamic measuring was conducted and the Distance Control function of the knee tensioner was used. Three samples were recorded with a gap distance of 10 mm, two with the native femoral condyle and one with the Journey Uni 2 prosthetic femoral condyle.

In Figure 63, one of the samples measured with the native femoral condyle is shown in a graph showing the tibiofemoral force as a function of the angle of knee flexion.

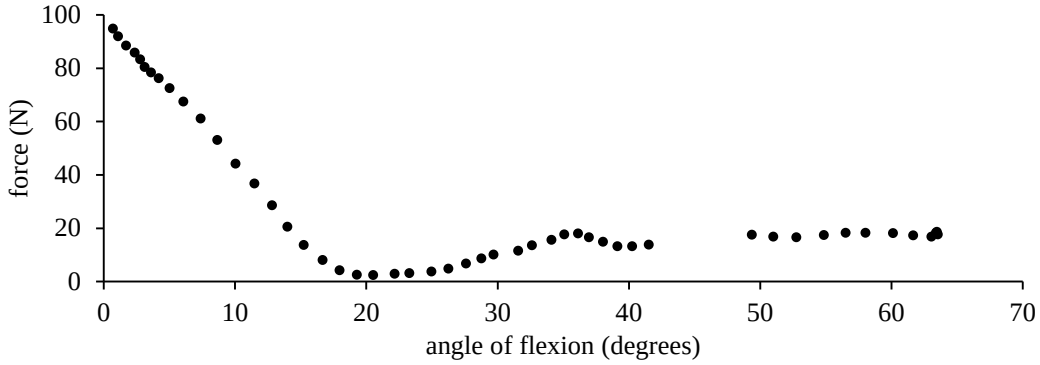

Figure 63: Test 1 result - Tibiofemoral force in native medial compartment of the right knee with a gap distance of 10 mm

5.2 Test 2 results

In Test 2, Prototype 2 was used. In this test both static measuring and dynamic measuring was conducted on both the native and prosthetic femoral condyles. The prosthesis that was used is the Journey Uni 2.

The knee tensioner was tested on two knees from the same cadaver. The subjects of the test were the medial and lateral compartment of the right knee, and the medial compartment of the left knee. With static measuring, measurements from the medial and lateral compartment of the knee and the native and prosthetic femoral condyles could be compared in the right and left knee, respectively. These comparisons are shown in Figure 64 and Figure 65.

Figure 64 shows the results for static measuring on the native right knee. The gap distances were measured for four different tibiofemoral forces applied by the knee tensioner. See Figure 14 for a comparison with the static results from the study by Takayama *et al.* (2015).

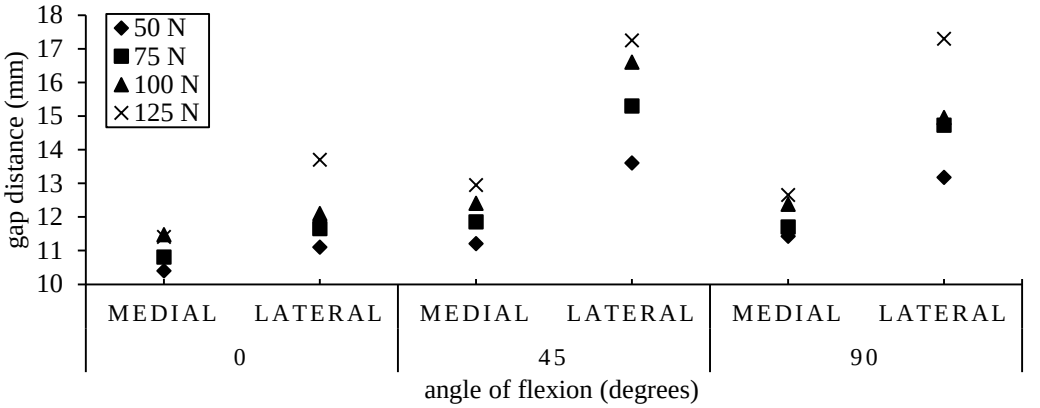

Figure 64: Test 2 result - Gap distances in native right knee

In Figure 65, the results for static measuring on the medial compartment of the left knee are shown for the native and the prosthetic femoral condyle. The gap distances were measured for three different tibiofemoral forces. Note that the gap distance at 45° for the native femoral condyle was not measured. This is due to the time constraint during testing.

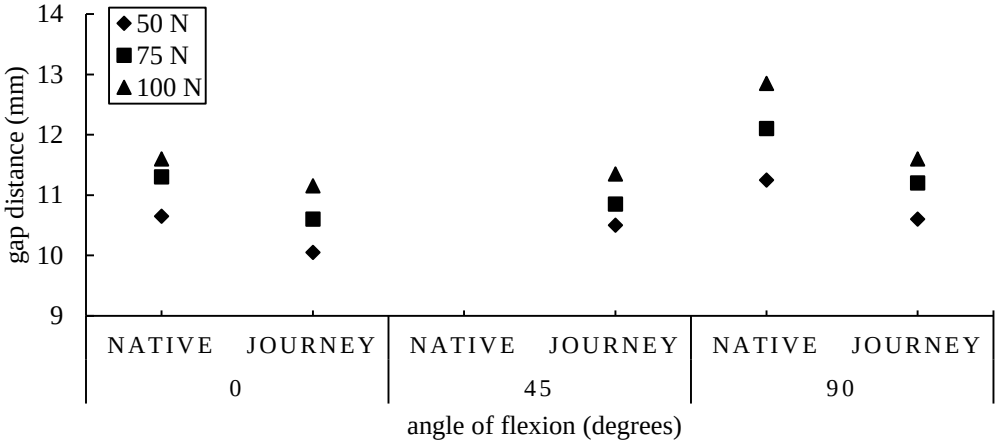

Figure 65: Test 2 result - Gap distances in the medial compartment of the left knee

The next three figures give the results of dynamic measuring. In Figure 66, the average tibiofemoral force measured between two samples obtained with the Distance Control function of the knee tensioner is shown for the prosthetic medial compartment of the left knee. The tibiofemoral force was measured with a gap distance of 10 mm. During this measurement, the IMU failed to measure the angle of knee flexion due to the problem of 'gimbal lock', which is explained in Section 3.6.5. Consequently, assuming the angle of knee flexion changed at a constant rate, the time domain of the measured force was converted to an angle domain from 0° to 90°, which represent the angles of knee flexion.

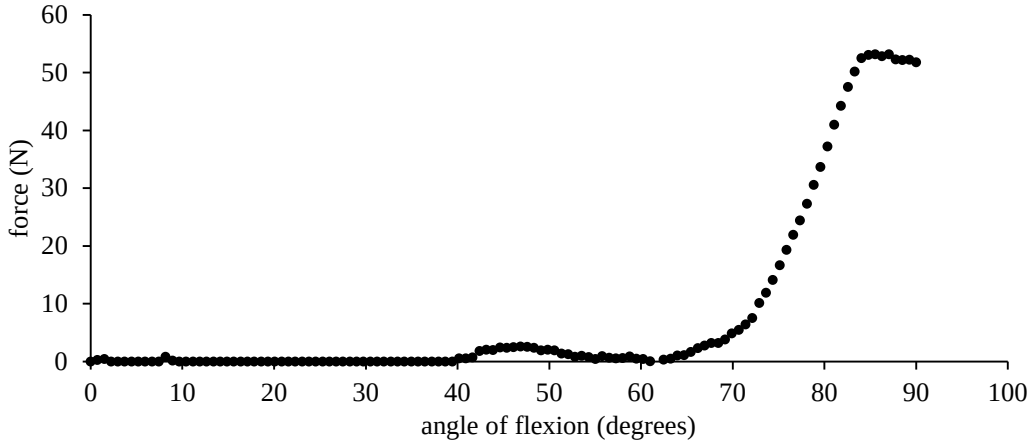

Figure 66: Test 2 result - Tibiofemoral force in the prosthetic medial compartment of the left knee with a gap distance of 10 mm

The gap distances shown in Figure 67 and Figure 68 were measured using the Force Control function of the knee tensioner with a tibiofemoral force of 100 N. In Figure 67, the gap distance in the native medial compartment of the right knee is shown. Unlike the other dynamic measurements, this measurement was conducted with the knee initially in full extension. In Figure 68, the average of the two samples obtained in the prosthetic medial compartment of the left knee is shown. The angle domain of the gap distance in Figure 68 was also converted from the time domain of the measurement, due to the occurrence of 'gimbal lock'. In Appendix G, Figure G.1 and Figure G.2 show how the knee tensioner maintained the tibiofemoral force at 100 N for the corresponding angles of knee flexion.

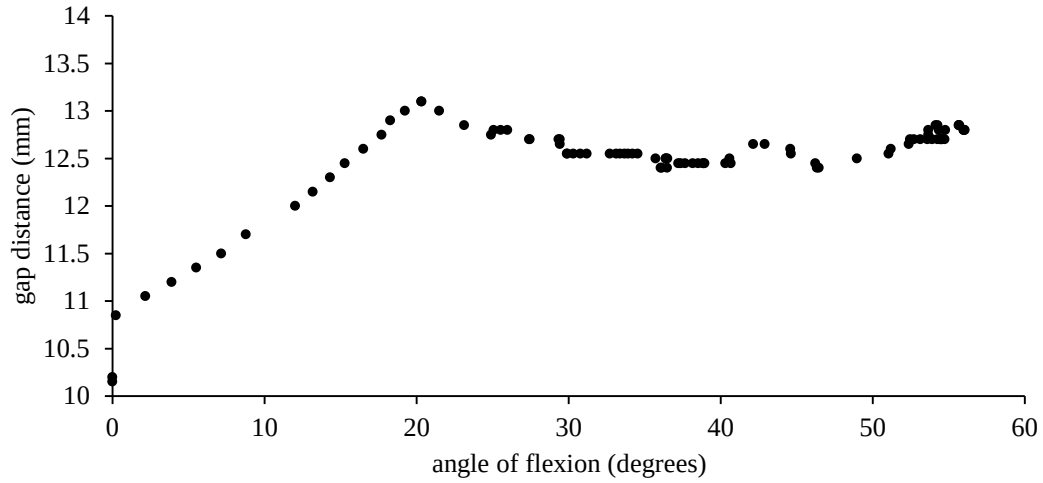

Figure 67: Test 2 result - Gap distance in the native medial compartment of the right knee with a tibiofemoral force of 100 N

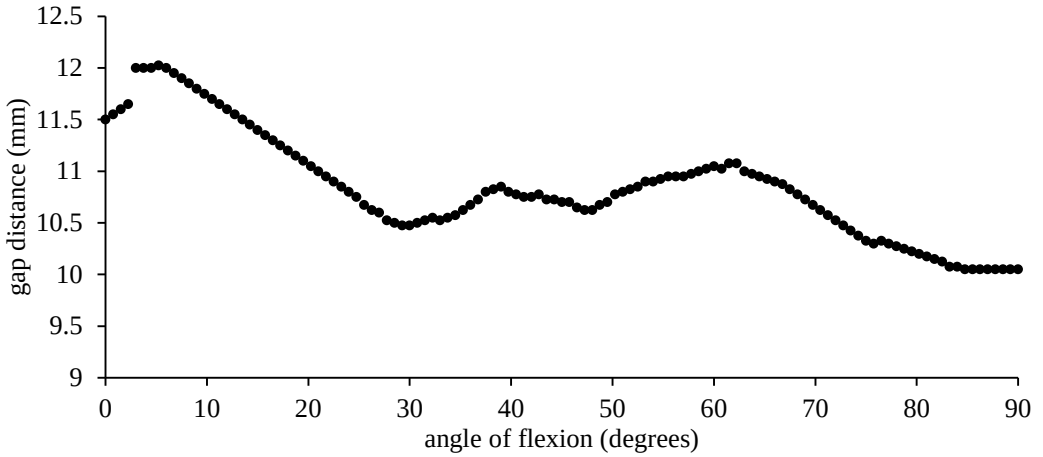

Figure 68: Test 2 result - Gap distance in the prosthetic medial compartment of the left knee with a tibiofemoral force of 100 N

5.3 Test 3 results

In Test 3, Prototype 2 was used with the modified control system in which proportional control was added to the original Knee Tensioner Algorithm. The problem of gimbal lock, which prevented the angle from being measured in Test 2, was also fixed as explained in Section 3.6.5. Again, both static measuring and dynamic measuring were conducted. The knee tensioner was tested with the native femoral condyle as well as with two prosthetic femoral condyles, namely the Journey Uni 2 and the Arthrex. Unlike the trial component of the Journey Uni 2, the Arthrex was 3D printed as a polymer. The subject of the test was the medial compartment of the left knee.

The gap distance obtained with static measuring is shown in Figure 69 for two different tibiofemoral forces. In this case, the measurements were obtained with the native femoral condyle and the Journey Uni 2 prosthetic femoral condyle.

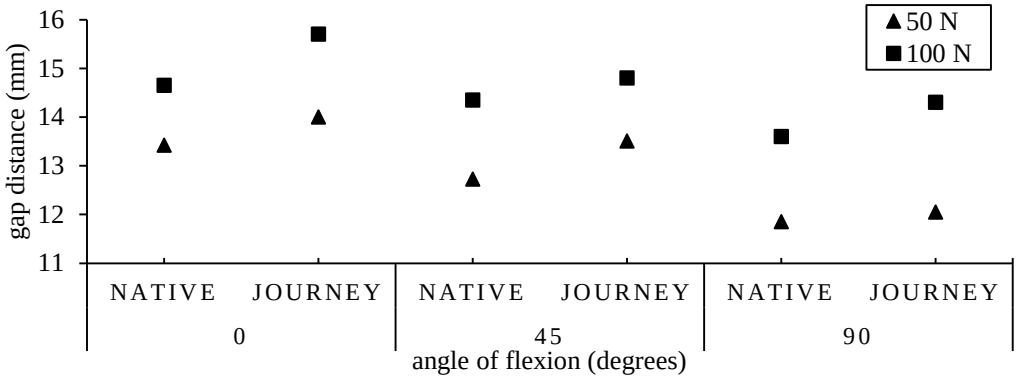

Figure 69: Test 3 result - Gap distances in the medial compartment of the left knee

In Figure 70 and Figure 71, the results of dynamic measuring are given. Figure 70 shows the tibiofemoral forces obtained using the Distance Control function of the knee tensioner with the Arthrex prosthetic femoral condyle. The tibiofemoral forces were measured with four different gap distances. During these measurements, the varus and valgus angle of the knee were also measured simultaneously using the Smith & Nephew Pi Galileo CAS system. The varus and valgus angle that correspond with the measurements in Figure 70 are given in Appendix G in Figure G.6, Figure G.7, Figure G.8 and Figure G.9.

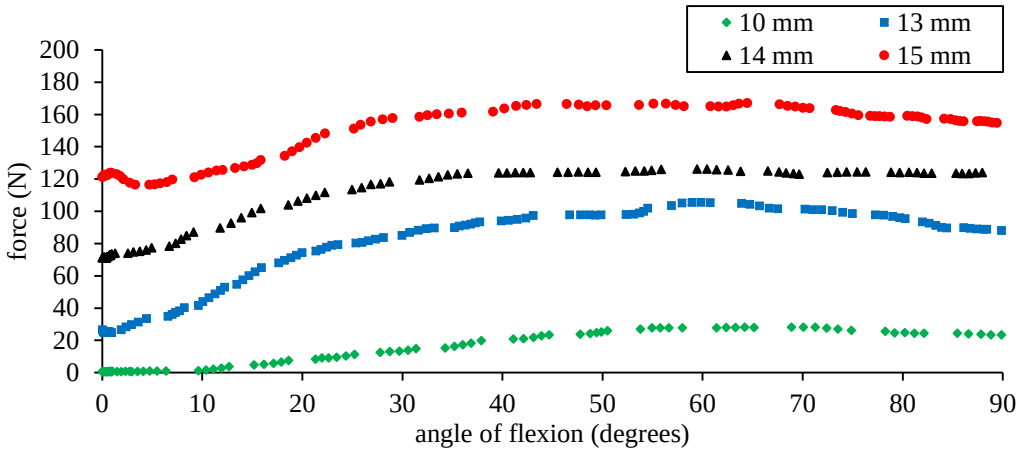

Figure 70: Test 3 result - Tibiofemoral forces in the prosthetic medial compartment of the left knee

Figure 71 shows the gap distances for the native, Journey Uni 2 prosthetic and Arthrex prosthetic femoral condyles with a tibiofemoral force of 100 N in each case. The measurement on the native femoral condyle shown in Figure 71 is one of two samples that were obtained. In Appendix G, Figure G.3, Figure G.4 and Figure G.5 show how the knee tensioner maintained the tibiofemoral force at 100 N for the corresponding angle of knee flexion.

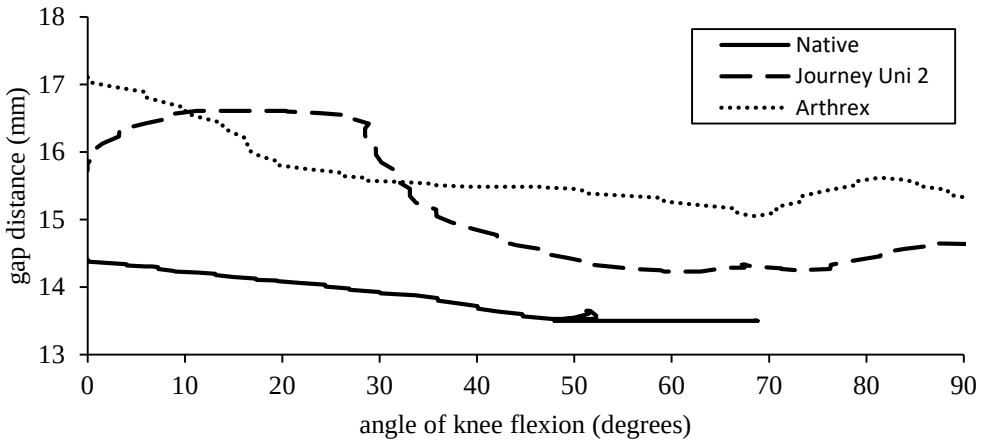

Figure 71: Test 3 result - Gap distances in the medial compartment of the left knee with a tibiofemoral force of 100 N

6 Discussion

In this chapter, the results of the *in-vitro* tests are discussed. The results are discussed with respect to each test and with reference to the graphs given in Chapter 5. Thereafter, the practical use of the knee tensioners during the *in-vitro* tests will be critically evaluated in terms of their feasibility for use in the operation theatre.

6.1 Test 1 results

In Figure 63, the tibiofemoral force in the native medial compartment of the right knee is shown between 0° and 63.47° knee flexion. The initial angle of the knee was judged by the surgeon and therefore the angle of knee flexion does not range exactly between 0° and 90°. The exact initial angle of the knee can be determined using the NAVIO Surgery System. Even though the NAVIO Surgery System was used during the performance of the knee arthroplasty, the position trackers in the tibia had to be removed to provide space for the insertion of the knee tensioner into the knee joint. Therefore, the exact angle of the knee could not be determined.

The increase in the tibiofemoral force from 20° to 0° can be ascribed to the way the surgeon swings the lower leg towards 0° knee flexion, as described in Section 4.3, in which additional force is applied to the knee tensioner. Thus, there arises uncertainty around the extent to which the geometric profile and kinematics of the knee, and the additional force applied by the surgeon contributes to the tibiofemoral force measured.

The friction force on the guide rods of Prototype 1 also influence the magnitude of the force measured by the knee tensioner, as mentioned in Section 3.6.2. The friction force impedes the vertical movement of the femur plate. Thus, in this case the strain measured by the strain gauge of the load cell is not proportional to the tibiofemoral force. The femur plate also tends to ‘lock’ under higher-end loads, preventing the load cell from measuring a change in tibiofemoral force. However, from Figure 63, it can be seen that ‘locking’ did not occur during this measurement, since there are no successive points which are equal in force.

The average interval between the data points in Figure 63 is 1.27°. Between 40° and 50° knee flexion there is a visibly large interval between two points. The interval between these two points is 7.84°. Based on the sampling rate of the measurement, this would mean the angle of the knee changed at a rate of 58.71° per second. This is improbable and indicates that the reason for the large interval is due to a technical malfunction. The technical malfunction can possibly be ascribed to either the Arduino Nano, which froze for a brief period, or an artefact offset in the IMU measurement. This technical malfunction only occurred during Test 1 and was most likely prevented by the modifications made to Prototype 1 with the development of Prototype 2.

6.2 Test 2 results

In Test 2, the two issues identified in Section 6.1 that influence the accuracy of the force measured by the knee tensioner were addressed. Prototype 2 was used in which the plain linear bearings were replaced by linear ball bearings, thereby reducing the friction force on the guide rods and preventing the femur plate from 'locking'. The surgeon was also advised to alter the way in which the lower leg of the cadaver is held when it is swung, as explained in Section 4.3, thereby mitigating the risk of the surgeon applying additional force on the knee tensioner. The results of Test 2 include the results of static measuring and dynamic measuring.

6.2.1 Static results

The results of static measuring give a simplified overview of the stiffness of the knee. In Test 2, it was used to compare the native medial and lateral compartments, and the native and prosthetic femoral condyles, respectively.

With regards to Figure 64, the range of the gap distances at each angle of the lateral compartment is larger than that of the medial compartment. The range of the lateral compartment is 141.86 %, 108.57 % and 236.73 % more than that of the medial compartment at 0°, 45° and 90° knee flexion, respectively. This indicates that the medial compartment of the knee is stiffer than the lateral compartment.

The smaller gap distances at 0° knee flexion and the increase of the gap distances towards 90° knee flexion indicate a similar trend to the results of Takayama *et al.* (2015) in their study of the "component gap". The results of this study are given in Section 2.5. According to Takayama *et al.* (2015), the smaller gap distances at 0° knee flexion can be ascribed to a knee having flexion contracture (a knee unable to be fully straightened) before knee arthroplasty, which results in a tightening of the posterior capsule by the posterior condyle at 0° knee flexion. A study by Sugama *et al.* (2005) also confirmed that the posterior soft tissue structures influence the extension gap in their investigation of how the extension gap changes after the flexion gap is prepared. The results of the study by Matsumoto *et al.* (2009) of the gap distances in TKA, as shown in Section 2.5, also show a decreased gap distance at 0° knee flexion. Matsumoto *et al.* (2009) pointed out that this is due to the tightening of the posterior capsule by the posterior condyles.

In Figure 65, the native and prosthetic femoral condyles are compared in the medial compartment of the left knee. At 0° and 90°, it is shown that the gap distances are larger for the native femoral condyle for each force. Therefore, the insertion of the prosthesis decreased the gap distance, which results in higher tibiofemoral forces. Higher tibiofemoral forces reduce the risk of lift-off, in which the femoral condyle loses contact with the polyethylene component of the joint replacement, and results in a more stable knee joint.

Even though there is a slight increase in the gap distances from 0° knee flexion towards 90° knee flexion, it is not as prominent as in the gap distances shown in Figure 64. However, it is possible that flexion contracture existed in both knees of the cadaver and that the posterior soft tissue structures were tighter at 0° knee flexion (Takayama, et al., 2015). The absence of the gap distances at 45° knee flexion for the native medial compartment adds uncertainty.

6.2.2 Dynamic results

The results of three dynamic measurements are given in Figure 66, Figure 67 and Figure 68. Figure 66 exemplifies the improper use of the knee tensioner in measuring the tibiofemoral force. It shows that in order to assess the tibiofemoral force, the correct gap distance must be chosen. The graph shows that for most of the angles between 0° and 60° knee flexion, the tibiofemoral force that was measured is zero. This indicates that between 0° and 60°, the prosthetic femoral condyle did not exert a force on the femur plate due to laxity in the knee. The ligaments weren't tensioned enough to keep the bones in contact with the plates of the knee tensioner. Therefore, with a gap distance of 10 mm it was impossible to generate a profile of the tibiofemoral force. Increasing the gap distance to a distance at which the tibiofemoral force remains above zero for all angles between 0° and 90° knee flexion, would ensure that the profile of the tibiofemoral force could be assessed between these angles.

The gap distance shown in Figure 67 was measured with the angle of knee flexion initially at 0°. Once again, the position trackers of the NAVIO Surgery System had to be removed to provide space for the insertion of the knee tensioner into the knee joint. The final angle of the knee was judged by the surgeon, which explains why the range of the angle only extends from 0° to 56° knee flexion.

In Appendix G in Figure G.1, the corresponding tibiofemoral force for the gap distance shown in Figure 67 is given. The measured force deviates 3.44 % above and 11.75 % below the desired force of 100 N. Between 0° and 20°, the response of the knee tensioner is demonstrated. In Figure G.1, the measured force is below 100 N at 0° knee flexion. The knee tensioner then responds by increasing the gap distance in order to increase the tibiofemoral force to 100 N. This is reflected in Figure 67 where it is shown how the gap distance increases between 0° and 20° knee flexion. The deviation in the tibiofemoral force above and below the desired force of 100 N can be ascribed to the distance of the increments the knee tensioner changes the gap distance by and the speed at which it does so. The gap distance is increased and decreased in increments of 0.2 mm. Reducing the increment distance would result in finer adjustments of the gap distance, reducing the amount of overshoot. In addition, reducing the speed at which the gap distance is adjusted would also result in less overshoot. However, smaller increments and slower speeds require a slower angular velocity of the knee, increasing the duration of the measurement. For these reasons, the modified control system was developed and implemented in Test 3.

When comparing the gap distance in Figure 67 to the static measuring results in Figure 64, the gap distances at 100 N correspond well. In both measurements, there is a slight increase in the gap distance from 0° to 45°, where after it remains constant close to 12.5 mm.

In Appendix G in Figure G.2, the corresponding tibiofemoral force for the gap distance shown in Figure 68 is given. Between 20° and 90°, the force deviates 5.02 % above and 7.46 % below the desired force of 100 N. Between 0° and 20° the force deviates 15.19 % above and 24.42 % below 100 N. The larger deviations can be ascribed to a steep increase and decrease in the gap distance caused by the geometric profile and kinematics of the femoral condyle in which the knee tensioner responded too slowly to the change in the tibiofemoral force. As explained for Figure 67, the distance of the increments the knee tensioner changes the gap distance by, and the speed at which it does so, also cause deviations in the measured force.

The profile of the gap distance in Figure 68 difference greatly from the profile of the gap distance in Figure 68. The replacement of the femoral condyle seems to have alleviated the tightness of the posterior soft tissue structures, which can be ascribed to the posterior prosthetic femoral condyle which moved the articulating surface of the condyle in the proximal direction at 0° knee flexion.

6.3 Test 3 results

The results of Test 3 include the results of static measuring and dynamic measuring. The measurements obtained in Test 3 are similar to those obtained in Test 2 and were conducted in order to prove the repeatability of Prototype 2. In addition, the aim was to improve on the results of the Force Control function by implementing the modified control system. With the modified control system, smoother graphs for the gap distance were expected as well as smaller deviations from the desired tibiofemoral force.

6.3.1 Static results

In Figure 69, gap distances with the native femoral condyle and the Smith & Nephew Journey Uni 2 prosthetic femoral condyle are compared in the medial compartment of the left knee. For the prosthetic femoral condyle, the gap distances are larger than the gap distances for the native femoral condyle at all angles for 50 N and 100 N, respectively. Therefore, the prosthesis relieves force in the ligaments.

The larger gap distances at 0° knee flexion and the decrease of the gap distances towards 90° knee flexion, as shown in Figure 69, indicate the absence of preoperative flexion contracture (Takayama, et al., 2015). Matsumoto *et al.* (2013) refer to previous studies in which the *in-situ* forces of the cruciate ligaments were

investigated over the range of motion of the knee. It was found that when comparing the posterior cruciate ligament (PCL) to the anterior cruciate ligament (ACL), between 0° and 90° knee flexion, the PCL was tensed between midrange and 90° knee flexion, while the ACL was tensed between 0° and midrange knee flexion. The decrease of the gap distances towards 90 ° knee flexion can be ascribed to this phenomenon and it can be deduced that the PCL exhibits greater tension when tensed in comparison to the tension of the ACL when tensed.

6.3.2 Dynamic results

Figure 70 and Figure 71 give the results of dynamic measuring. In Figure 70, the tibiofemoral force in the prosthetic medial compartment of the left knee is shown. The prosthesis that was used is the 3D printed Arthrex. The trends of the forces shown in the graph are the same for each gap distance and shows that choosing a gap distance that results in a measured force above zero for all angles can generate an insightful profile of the tibiofemoral force in the knee.

In Appendix G in Figure G.6, Figure G.7, Figure G.8 and Figure G.9, the varus-valgus angle of the knee is shown for the 10 mm, 13 mm, 14 mm and 15 mm gap distances, respectively. Since the lower leg was swung without applying forces in the lateral direction, the varus-valgus angle exists due to the natural kinematics of the knee. The varus-valgus angle measured by the Pi Galileo CAS system can provide proof for the legitimacy of the trend of the tibiofemoral forces measured by the knee tensioner. As the knee changes from a valgus angle to a varus angle, the distance between the medial femoral condyle and the proximal tibia decreases, thereby applying increased force on the femur plate of the knee tensioner.

In Figure 71, the gap distance is shown for the native femoral condyle and the two prosthetic femoral condyles. When compared with the results obtained with the Force Control function in Test 2, the measurements in Figure 71 show gradients that are more gradual. This is attributed to the modified control system in which the knee tensioner adjusts the gap distance proportionally to the magnitude of the deviation from the desired force in terms of distance and speed. Since the gap distance can be controlled more precisely than before, the knee tensioner overreacts less to small changes in force and reacts faster to large changes. Therefore, the gap distance can be measured more accurately and fluctuations around the desired force are decreased.

In Appendix G in Figure G.3, Figure G.4 and Figure G.5, the corresponding tibiofemoral forces are shown for the gap distances in Figure 71. The range of the deviations from the desired force for the native femoral condyle, the Journey Uni 2 femoral condyle and the Arthrex femoral condyle is 6.65%, 32.1% and 12.16 %, respectively. For the native femoral condyle and the Arthrex femoral condyle, this is an improvement on the deviations in Test 2.

Once again the gap distances in Figure 71 indicate an absence of flexion contracture as explained in Section 6.2.1 and can be explained by the tension of the PCL and

ACL as discussed in Section 6.3.1. The gap distances correspond with the tibiofemoral forces shown in Figure 70 in which both the gap distances and the tibiofemoral forces level out from approximately 50° to 90° knee flexion.

6.4 Significance of results

The results, as given in the previous section, have proven that the knee tensioners developed in this study are capable of providing insight into certain characteristics of the knee, which include knee stiffness, spatial geometry, and articulating surface geometry of either the medial or the lateral compartments. The results also show how these characteristics differ between the native knee and a knee with a prosthetic femoral component. The novelty of the knee tensioners is displayed in the results of dynamic measuring. Unlike previous knee tensioners, Prototype 1 and Prototype 2 are capable of measuring the tibiofemoral force and the gap distance continuously as the knee is flexed from 0° to 90° knee flexion or vice versa. They can also differentiate between the medial and the lateral compartments. In addition, the capability of measuring either the gap distance at a constant tibiofemoral force or the tibiofemoral force at a constant gap distance sets these knee tensioners apart from previously developed tensioners. The combination of the tibiofemoral force and the gap distance measurements, from one knee compartment, provides greater insight than what previously developed knee tensioner have provided.

The results show the measurements of the tibiofemoral force and the gap distance after soft tissue balancing has been performed by the surgeon. There are still no set standards for soft tissue balancing and the technique varies between practitioners (Matsuda & Ito, 2015). The first step that can be taken towards improving soft tissue balancing is the intra-operative evaluation of soft tissue balancing with the knee tensioners, which can indicate if adjustments need to be made before the final prosthetic components are inserted. However, this would first require that the knee tensioners be modified for clinical knee arthroplasty.

The knee tensioners developed in this study assess the outcome of soft tissue balancing on a quantitative level which can be correlated to postoperative results. This may lead to the standardisation of soft tissue balancing which lies beyond surgeons' own subjective standards. However, standardisation must still account for patient-specific paraments.

6.5 Practical use of the knee tensioners

Even though the knee tensioners were tested in a laboratory setup, the layout of the equipment and the staff present create similarities to the environment of an operation theatre, with the exception of having regulations for sterility and additional equipment for the monitoring of patient vitals. Therefore, it can be determined whether the use of the knee tensioners in the operation theatre will be feasible, based on the laboratory tests. In this section the feasibility of the use of the

knee tensioners is discussed with reference to the implementation of the equipment in the laboratory, the compatibility of the knee tensioners with the knees that were tested, the handling of the knee tensioners, and the control of the knee tensioners.

6.5.1 Equipment layout

The addition of the knee tensioner equipment to the knee arthroplasty equipment in the cadaver laboratory did not hinder the performance of the knee arthroplasty and was ergonomically satisfactory. The length of the cable connecting the knee tensioner to the Control Box, allowed the table on which the Control Box and PC was placed (knee tensioner table) to be positioned a distance away from the operating table such that it did not hinder the movement of the surgeon or theatre nurses.

6.5.2 Compatibility with knees

Both Prototype 1 and Prototype 2 fit within the knees they were tested. The goal was to size the femur plate and the tibia plate so that the femoral condyle remained within contact of the femur plate throughout all angles of knee flexion between 0° and 90°. This goal was met in all three tests.

The only modification that was made to accommodate the geometry of the tibias in the tests was the reduction in the number of holding pins in Prototype 1. During Test 1 it was found that the use of two holding pins was not feasible, due to the curvature of the tibia. However, the use of one holding pin was found to be sufficient for both Prototype 1 and Prototype 2 and secured the knee tensioner to the tibia. For future use in which the original femur plate and tibia plate do not fit the knee they are tested in, the plates can easily be replaced by appropriate plate sizes. This can either be done by basing the size of the plates on MRI scans of the test knee and attaching the correct sizes before the test, or by having different plate sizes at hand during the test and attaching them to the knee tensioner through trial and error. Therefore, the knee tensioners that were manufactured can be used in all knee sizes.

6.5.3 Handling

Since the wires of the IMU, load cell and stepper motor were exposed on the surface of the knee tensioners, holding the knee tensioners by hand posed the risk of detaching the wires as the fingers would grip the knee tensioners and press onto the wires. Even though no wires detached during the tests, care should be taken when handling the knee tensioner, especially while inserting it into the knee joint where it is forced into the tibia. The knee tensioner should be gripped while touching the least amount of wires or none if possible. Alternatively, a way should be sought to protect the wires.

6.5.4 Interface and control

The knee tensioners responded to all commands through the GUI. The GUI allowed the use of all four Modes of the knee tensioners, of which three were used during the tests. All buttons and input fields on the GUI were labelled clearly to enable untrained operators to control the device. Therefore, the GUI provided a suitable interface for the control of the knee tensioner.

6.5.5 Conclusion

It can be concluded that the concept of the knee tensioners developed in this study are suitable for use in clinical knee arthroplasty if they are further modified to meet the regulations for sterilisation. The modifications that will allow the use for clinical knee arthroplasty could include the following: The implementation of a detachable cable between the knee tensioner and the Control Box (that can be sterilised) and a casing for the knee tensioner that prevents fluids or organic material from coming into contact with the knee tensioner. The method in which the knee tensioner can be sterilised is given in the recommendations for the knee tensioner in Section 7.4.

7 Conclusion

In this chapter, a summary is presented of the work completed in this study. This is followed by a discussion of the aim and objectives of the study and an evaluation thereof. The limitations of the study are then given along with recommendations for future use of the knee tensioners.

7.1 Summary

In this study, two prototypes were developed for a dynamic knee tensioning device and were tested on cadaver knees. The knee tensioners, as the prototypes are known, can measure the joint gap stiffness of the knee in terms of the gap distance, the distraction force, and the angle of knee flexion. In contrast to previously developed knee tensioning devices, the knee tensioners can measure the joint gap stiffness dynamically, i.e. as the angle of knee flexion changes between 0° and 90°, either by maintaining a constant distraction force or a constant gap distance.

Four concepts were considered for the design of the knee tensioning device, out of which the design of Prototype 1 was chosen as the final design. A physical model of Prototype 1 was then manufactured. After Test 1, in which Prototype 1 was tested on a cadaver knee, Prototype 2 was manufactured which improved on the shortcomings of Prototype 1. The design of Prototype 1 was improved by replacing the plain linear bearings with linear ball bearings and manufacturing a body which forms a unit in which the bearings are housed. The number of holding pins were also reduced from two to one. Prototype 2 was then tested in another *in-vitro* test, Test 2, in which measurements were recorded in the two knees of a cadaver. After Test 2, the Force Control function of Prototype 2 was improved by implementing proportional control in the control system. The position of the IMU was also altered to improve the reliability of the measurement of the angle of knee flexion. In Test 3, Prototype 2 was tested on one cadaver knee with these two modifications.

Test 1 produced results of dynamic measuring with the use of the Distance Control function. In Test 2 and Test 3, the Distance Control function and the Force Control function was used to produce results of dynamic measuring and static measuring. The results provide insight into the joint gap produced during the assessment of soft tissue balance, which was previously limited to a few intermediate angles between 0° and 90° knee flexion.

7.2 Aims and objectives

The aim of this study was to provide a proof of concept for a dynamic knee tensioning device capable of measuring the joint gap stiffness during knee arthroplasty at all angles between 0° and 90° knee flexion, and to quantify the necessary distraction force. In order to ensure that the aim of the study was accomplished, certain objectives were identified as given in Chapter 1. In Table 5, an evaluation of these objectives is given. It is shown that all the objectives have been achieved. The letters in the 'Detail of objective' column, refer to the letters in Section 1.3.

Table 5: Evaluation of the objectives of the study

Objective	Detail of objective	Evaluation	
		Achieved?	Discussion
Perform a litearture study	a	Yes	The literature on soft tissue balance was reviewed as well as the methods of assessing it, which include: Mechanical alignment, kinematic alignment and ligament balancing. Refer to section 2.4.
	b	Yes	Studies were reviewed in which devices have been developed for the quantification of joint gap stiffness. Refer to section 2.5.
Develop a knee tensioning device capable of quantifying joint gap stiffnes	c	Yes	A stepper motor was used in the knee tensioner to actuate the Femur plate, thereby applying a force between the tibia and the femur. Refer to section 3.5.4.
	d	Yes	A load cell was used to measure the distraction force applied by the knee tensioner. Refer to section 3.5.5.
	e	Yes	The steps of the stepper motor was used to calculate the gap distance. Refer to section 3.5.7.
	f	Yes	An IMU was used to measure the angle of knee flexion. Refer to section 3.5.6.
	g	Yes	The Knee Tensioner Algorithm integrates the signal from the load cell and the IMU, and calculates the gap distance simulteneously. Refer to section 3.5.10.
Prove the functionality of the knee tensioning device	h	Yes	Three *in-vitro* tests were conducted in which Prototype 1 and Prototype 2 were tested in cadaver knees. Refer to chapter 4.
	i	Yes	Graphs were generated in which the gap distance and the distraction force are presented as a function of knee flexion, respectively. Refer to chapter 5.

7.3 Limitations

Four aspects of the developed knee tensioners have been identified as limiting factors of the extent to which the knee tensioners can be used. The factors include the following: The sterilisation of the knee tensioners, the response time of the load cell, the maximum distraction force of the knee tensioners, and the method of measuring the angle of knee flexion.

All equipment used during surgical procedures on patients in an operation theatre must be sterilised before being used. Therefore, for the knee tensioners to be tested intraoperatively in clinical knee arthroplasty, they need to be sterilised. The scope of this study did not include the formulation of a strategy for the sterilisation of the knee tensioners. Therefore, the testing of the knee tensioners was limited to *in-vitro* tests in which cadaver knees were used.

In Section 3.7, the angular velocity at which the lower leg must be rotated about the knee, to ensure the tibiofemoral force is measured without error due to the response of the load cell, was calculated. The calculated angular velocity is a requisite for the use of the knee tensioner. This limited the speed at which all measurements were taken within the knee joint using the knee. Even though the duration of the *in-vitro* tests did not have an impact on the outcome of this study, an increase in the duration of clinical knee arthroplasty can result in financial implications.

Prototype 2 could exert a maximum distraction force of 160 N during *in-vitro* testing. Commanding the knee tensioner to exert a force higher than 160 N causes the stepper motor to stall while the Knee Tensioner Algorithm continues to send commands to the stepper motor. Therefore, even though the actual gap distance cannot be increased to achieve a distraction force of 160 N, the algorithm continues to calculate the gap distance based on the steps of the stepper motor which still increases as the commands are being sent to the stepper motor. This results in an incorrect gap distance measurement at forces above 160 N.

As explained in Section 3.4.6, the angle of knee flexion must be measured by keeping the upper leg stationary while the lower leg is rotated about the knee. Therefore, the upper leg must be held still while the lower leg is swung. As the lower leg is swung, the upper leg tends to marginally move as well, which corrupts the angle measurement.

Another limitation to this study is the small sample size of the results of the *in-vitro* tests.

7.4 Recommendations

In this section, recommendations for the future use of the knee tensioners are discussed.

The use of the knee tensioners in clinical knee arthroplasty will allow surgeons to assess the joint gap and tibiofemoral forces intraoperatively before the final prosthetic components are inserted and fixed. It can then be determined whether the knee arthroplasty technique is successfully being performed and whether further bony resections and ligament releases need to be made to improve the joint gap.

As mentioned in Section 7.3, for use in clinical knee arthroplasty, the knee tensioners must be sterilised. Surgical equipment is typically sterilised by placing the equipment in an autoclave in which it is heated by pressurised steam for approximately 30 minutes to temperatures above 100° C (Tuttnauer, 2016). The electronics used in the knee tensioners, which include the stepper motor, the load cell, and the IMU, would be destroyed if the knee tensioners were sterilised in an autoclave, due to the high temperatures in the autoclave. However, the knee tensioners can be sterilised using Ethylene Oxide gas. In cases where heat sensitive surgical equipment must be sterilised, it can be sterilised by exposing it to Ethylene Oxide gas for approximately 60 hours (Eurotherm, 2017).

Two factors influenced the angular velocity at which the lower leg could be rotated to ensure accurate measurements: The speed at which the Arduino executed the Knee Tensioner Algorithm and the cut-off frequencies of the low-pass filters. Each function in the Knee Tensioner Algorithm code costs time. Therefore, optimising the code would result in fewer lines of code, increasing the speed at which the algorithm is executed.

Implementing low-pass filters of a higher order will also improve the response of the load cell. With the first-order low-pass filters, the cut-off frequency was chosen to remove as much noise as possible from the load cell signal. However, this also removed signals with frequencies representing the magnitude of the tibiofemoral force. Higher order low-pass filters are more effective in removing unwanted signals above the cut-off frequency. Therefore, a higher cut-off frequency can be chosen which does not affect the signal representing the tibiofemoral force.

In order to improve the method of measuring the angle of knee flexion with the IMU, a support structure can be created for the upper leg. The support structure can keep the leg stationary without requiring a person to hold it by hand.

As discussed in Section 3.2, two knee tensioners can be used to measure the joint gap stiffness in both compartments of the knee during TKA. For this purpose, it is recommended that a PCB be manufactured that can accommodate two of each of the electronic components on the knee tensioner, and that the Knee Tensioner Algorithm and GUI Algorithm be modified to process the additional sensor signals.

8 References

109JB. (2015, November 27). MPU6050_DMP6 example crashing [Msg 15]. *Message posted to https://github.com/jrowberg/i2cdevlib/issues/154*.

American Academy of Orthopaedic Surgeons. (2016, November 21). *Arthritis of the Knee*. Retrieved from OrthoInfo: http://orthoinfo.aaos.org/topic.cfm?topic=a00212#top

Anastasiadis, A., Magnissalis, E., & Tsakonas, A. (2010, October). A novel intraoperative sensor for soft tissue balancing in total knee arthroplasty. *Journal of Medical Engineering and Technology, 34*(7-8), 448-454.

Arduino. (2017, November 10). *Arduino Nano*. Retrieved from Arduino : https://store.arduino.cc/usa/arduino-nano

Arduino. (2017, August 1). *MPU-6050 Accelerometer + Gyro*. Retrieved August 1, 2017, from Arduino: https://playground.arduino.cc/Main/MPU-6050

Arduino. (2017, July 20). *The Arduino Playground*. Retrieved July 20, 2017, from Arduino: http://playground.arduino.cc/

Arthrex. (2017, November 9). Retrieved from Arhrex: https://www.arthrex.com/

Asano, H., Muneta, T., & Sekiya, I. (2008, November). Soft tissue tension in extension in total knee arthroplasty affects postoperative knee extension and stability. *Knee Surgery, Sports Traumatology, Arthroscopy, 16*(11), 999-1003.

Autodesk Inc. (2015, February 27). Autodesk Inventor 2016 [Computer software]. San Rafael, California, United States: Autodesk Inc.

Babazadeh, S., Stoney, J., Lim, K., & Choong, P. (2009). The relevance of ligament balancing in total knee arthroplasty: how important is it? A systematic review of the literature. *Orthopedic Reviews, 1*(26), 70-78.

Body Planes and Sections. (2016, December 14). Retrieved June 11, 2017, from Boundless Anatomy and Physiology: https://www.boundless.com/physiology/textbooks/boundless-anatomy-and-physiology-textbook/introduction-to-anatomy-and-physiology-1/mapping-the-body-33/body-planes-and-sections-289-1344/

Campbell, D., Schuster, A., Pfluger, D., & Hoffmann, F. (2010, June). Unicondylar knee replacement with a new tensioner device: clinical results of a multicentre

study on 168 cases. *Archives of Orthopaedic and Trauma Surgery, 130*(6), 727-732.

Cheprasov, A. (2017, September 18). *Anatomical Directional Terminology: Lateral, Medial & More*. Retrieved from Study.com: http://study.com/academy/lesson/anatomical-directional-terminology-lateral-medial-more.html

Dion, M., Healey, C., Giddings, S., & Drazen, J. (2015, April). Force measurement across the patellofemoral joint using a smart patellar implant following a total knee arthroplasty. *2015 41st Annual Northeast Biomedical Engineering Conference (NEBEC)*, 1-2.

D'Lima, D., Patil, S., Steklov, N., & Colwell, C. (2007, October). Dynamic intraoperative ligament balancing for total knee arthroplasty. *Clinical Orthopaedics and Related Research*, 208-212.

Dosset, H., Swartz, G., Estrada, N., Lefevre, G., & Kwasman, B. (2012). Kinematically Versus Mechanically Aligned Total Knee Arthroplasty. *Orthopedics, 35*(2), 160-169.

Electronic Tutorials. (2017, August 14). *Passive Low Pass Filter*. Retrieved August 14, 2017, from Electronic Tutorials: http://www.electronics-tutorials.ws/filter/filter_2.html

Engdahl, T. (2013). *Ground loop problems and how to get rid of them*. Retrieved August 15, 2017, from ePanorama.net: http://www.epanorama.net/documents/groundloop/

Eurotherm. (2017, September 28). *Ethylene Oxide (EtO) Sterilization Process*. Retrieved from Eurotherm: http://www.eurotherm.com/eto-sterilization

Foran, J. (2016, November 3). *Total Knee Replacement*. Retrieved from OrthoInfo: http://orthoinfo.aaos.org/topic.cfm?topic=a00389

Fotheringham, M. (2016, July 26). *Function of the kneecap*. Retrieved from Malverin Physiotherapy Clinic: http://www.malvernphysio.com.au/function-of-the-kneecap/

Greengard, S. (2012, April 30). *Knee Replacement: Your Surgical Options*. Retrieved November 23, 2016, from Healthline: http://www.healthline.com/health/total-knee-replacement-surgery/surgical-options

HowToDoIt. (2015, April 18). *Frequency response of the RC low-pass filter (Laplace transform method)*. Retrieved from HowToDoIt:

http://howtodoit.com.ua/en/frequency-response-of-the-rc-low-pass-filter-laplace-transform-method/

Hutt, J., LeBlanc, M., Massé, V., Lavigne, M., & Vendittoli, P. (2016). Kinematic TKA using navigation: Surgical technique and initial results. *Orthopaedics & Traumatology: Surgery & Research, 102*, 99-104.

In, Y., Kim, S., Kim, J., Woo, Y., Choi, N., & Kang, J. (2009, January). Agreements between different methods of gap balance estimation in cruciate-retaining total knee arthroplasty. *Knee Surgery, Sports Traumatology, Arthroscopy, 17*(1), 60-64.

Ishikawa, M., Kuriyama, S., Ito, H., Furu, M., Nakamura, S., & Matsuda, S. (2015, June). Kinematic alignment produces near-normal knee motion but increases contact stress after total knee arthroplasty: A case study on a single implant design. *The Knee, 22*(3), 206-212.

Iwaki, H., Pinskerova, V., & Freeman, M. (2000, November). Tibiofemoral movement 1: the shapes and relative movements of the femur and tibia in the unloaded cadaver knee. *The Journal of bone and joint surgery. British volume., 82*(8), 1189-1195.

Jones, E., & Fjeld, P. (2011, April 29). *Gimbal Angles, Gimbal Lock and a Fourth Gimbal for Christmas*. Retrieved September 24, 2017, from Apollo Lunar Surface Journal: https://www.hq.nasa.gov/alsj/gimbals.html

Knee Anatomy. (2017, June 22). Retrieved June 22, 2017, from Exactech: http://exactech.co.jp/canada/patients-caregivers-en-ca/joint-replacement-surgery/knee-replacement/knee-anatomy

Knee Replacement Implant Materials. (2017, June 11). Retrieved June 11, 2017, from BoneSmart: https://bonesmart.org/knee/knee-replacement-implant-materials/

Kwak, D., Kong, C., Han, S., Kim, D., & In, Y. (2012). Development of a pneumatic tensioning device for gap measurment during total knee arthroplasty. *Clinics in Orthopedic Surgery, 4*(3), 188-192.

Lage, V. (2015, March 29). MPU6050_DMP6 example crashing [Msg 1]. *Message posted to https://github.com/jrowberg/i2cdevlib/issues/154*.

Lonner, J., Smith, J., Picard, F., Hamlin, B., Rowe, P., & Riches, P. (2015, January). High Degree of Accuracy of a Novel Image-free Handheld Robot for Unicondylar Knee Arthroplasty in a Cadaveric Study. *Clinical Orthopaedics and Related Research, 473*(1), 206-212.

Luijkx, T. (2017, September 18). *Valgus vs. varus*. Retrieved from Radiopaedia: https://radiopaedia.org/articles/valgus-vs-varus

Lyons, M., MacDonald, S., Somerville, L., Naudie, D., & McCalden, R. (2012, January). Unicompartmental Versus Total Knee Arthroplasty Database Analysis: Is There a Winner? *Clinical Orthopaedics and Related Research, 470*(1), 84090.

Manner, P. (2016, April). *Knee Replacement Implants*. Retrieved from OrthoInfo: http://orthoinfo.aaos.org/topic.cfm?topic=a00221

Marya, K., & Thukral, R. (2013, September). Outcome of unicompartmental knee arthroplasty in octogenarians with tricompartmental osteoarthritis: A longer followup of previously published report. *Indian Journal of Orthopaedics, 47*(5), 459-468.

Matsuda, S., & Ito, H. (2015). Ligament balancing in total knee arthroplasty - Medial stabilizing technique. *Asia-Pacific Journal of Sports Medicine, Arthroscopy, Rehabilitation and Technology*, 108-113.

Matsumoto, T., Kuroda, R., Kubo, S., Muratsu, H., Mizuno, K., & Kurosaka, M. (2009, April). The intra-operative joint gap in cruciate-retaining compared with posterior-stabilised total knee replacement. *The Journal of Bone & Joint Surgery, 91-B*(4), 475 - 480.

Matsumoto, T., Muratsu, H., Kubo, S., Kuroda, R., & Kurosaka, M. (2013, January). Intra-operative joint gap kinematics in unicompartmental knee arthroplasty. *Clinical Biomechanics, 28*(1), 29-33.

Mediagauge. (2017, June 25). *Digital Protractor Goniometer for Medical applications*. Retrieved June 22, 2017, from Mediagauge: http://www.medigauge.com/digital-protractor-goniometer-for-medical-applications/

Meere, P., Schneider, S., & Walker, P. (2016, September). Accuracy of Balancing at Total Knee Surgery Using an Instrumented Tibial Trial. *The Journal of Arthroplasty, 31*(9), 1938-1942.

Meloni, M., Hoedemaeker, R., Violante, B., & Mazzola, C. (2014). Soft tissue balancing in total knee arthroplasty. *Joints, 2*, 37-40.

Meneghini, R., Ziemba-Davis, M., Lovro, L., Ireland, P., & Damer, B. (2016). Can Intraoperative Sensors Determine the “Target” Ligament Balance? Early Outcomes in Total Knee Arthroplasty. *The Journal of Arthroplasty*, 1-7.

MSC Software Corporation. (2014, December 12). Nastran [Computer sotware]. Newport Beach, California, United States of America.

MSC Software Corporation. (2014, December 12). Patran [Computer software]. Newport Beach, California, United States of America.

National Instruments. (2016, May 25). *Measuring Strain with Strain Gages*. Retrieved July 19, 2017, from National Instruments: http://www.ni.com/white-paper/3642/en/

Noticewala, M., Geller, J., Lee, J., & Macaulay, W. (2012). Unicompartmental Knee Arthroplasty Relieves. *The Journal of Arthroplasty, 27*(8), 99-105.

Nowakowski, A., Majewski, M., Müller-Gerbl, M., & Valderrabano, V. (2011). Development of a force-determining tensor to measure "physiologic knee ligament gaps" without bone resection using a total knee arthroplasty approach. *Journal of Orthopaedic Science, 16*(1), 56-63.

Park, J., & Kim, Y. (2011, November). Simultaneous cemented and cementless total knee replacement in the same patients. *The Bone & Joint Journal, 93-B*(11), 1479 - 1486.

(2017, July 26). Personal communication. (W. van der Merwe, Interviewer) Cape Town, Western Cape , South Africa.

Promoco. (2017, November 11). *Linear Actuators*. Retrieved from Promoco: http://www.promoco-motors.com/products/StepperMotors/linearActuators.php

Ries, M., Haas, S. B., & Windsor, R. (2003). Soft-Tissue Balance in Revision Total Knee Arthroplasty. *Journal of Bone and Joint Surgery-American*, 38-42.

Rossi, R., Bruzzone, M., Fantino, G., Dettoni, F., Bonasia, D., & Castoldi, F. (2012). Primary Total Knee Arthroplasty: Surgical Technique. In R. Rossi, & M. Bruzzone, *Soft Tissue Balancing in Primary Total Knee Arthroplasty* (pp. 5-6). Turin: Edizioni Minerva Medica.

Rowberg, J. (2017, August 1). *MPU6050 library*. Retrieved from GitHub, Inc.: https://github.com/jrowberg/i2cdevlib/tree/master/Arduino/MPU6050

Schmidler, C. (2017, April 14). *Anatomy Terms*. Retrieved June 12, 2017, from HealthPages.org: https://www.healthpages.org/anatomy-function/anatomy-terms/

Schmidler, C. (2017, June 4). *Knee Replacement Surgery*. Retrieved July 12, 2017, from HealthPages.org: https://www.healthpages.org/surgical-care/knee-replacement-surgery/

Seedhom, B., Longton, E., & Wright, V. D. (1972, February). Dimensions of the knee. Radiographic and autopsy study of sizes required by a knee prosthesis. *Annals of the Rheumatic Diseases, 31*(1), 54-58.

Singh, V., Varkey, R., Trehan, R., Kamat, Y., Raghavan, R., & Adhikari, A. (2012, December). Functional outcome after computer-assisted total knee arthroplasty using measured resection versus gap balancing techniques: a randomised controlled study. *Journal of Orthopaedic Surgery, 20*(3), 344-347.

SKF. (2017, November 11). *Linear ball bearings LBBR*. Retrieved from SKF: http://www.skf.com/group/products/linear-motion/linear-guides-and-tables/linear-ball-bearings/linear-ball-bearing-lbbr/index.html

Smith & Nephew. (2017, September 23). *Legion TKS*. Retrieved from Smith & Nephew US Professional: http://www.smith-nephew.com/professional/products/all-products/legion/

Soft tissue balancing in total knee arthroplasty. (2014, May 8). *Joints*, 37-40.

Sparkfun. (2017, November 11). *Load Sensor - 50 kg*. Retrieved from Sparkfun: https://www.sparkfun.com/products/10245

Sports Medicine Australia. (n.d.). *Soft Tissue Injuries*. Retrieved Oktober 25, 2016, from Sports Medicine Australia: http://sma.org.au/resources-advice/injury-fact-sheets/soft-tissue-injuries/

Stephens, B., Hakki, S., Saleh, K., & Mihalko, W. (2014, October). Clinical alignment variations in total knee arthroplasty with different navigation methods. *The Knee, 21*(5), 971-974.

Sugama, R., Kadoya, Y., Kobayashi, A., & Takaoka, K. (2005). Preparation of the Flexion Gap Affects the Extension Gap in Total Knee Arthroplasty. *The Journal of Arthroplasty , 20*(5), 602-607.

Takayama, K., Matsumoto, T., Muratsu, H., Uefuji, A., Nakano, N., Nagai, K., . . . Kurosaka, M. (2015, January). Joint gap assessment with a tensor is useful for the selection of insert thickness in unicompartmental knee arthroplasty. *Clinical Biomechanics2015, 30*(1), 95-99.

TDK InvenSense. (2017, August 1). *MPU-6050 Six-Axis (Gyro + Accelerometer) MEMS MotionTracking™ Devices*. Retrieved from TDK InvenSense: https://www.invensense.com/products/motion-tracking/6-axis/mpu-6050/

Texas Instruments. (2017, November 11). *INA125 Instrumentation Amplifier with Precision Voltage Reference*. Retrieved from Texas Instruments: http://www.ti.com/product/INA125

Tuttnauer. (2016, September 21). *Introduction to Autoclave Sterilization Process*. Retrieved from News Medical: https://www.news-medical.net/whitepaper/20160921/Introduction-to-Autoclave-Sterilization-Process.aspx

Types of Total Knee Implants. (2017, June 11). Retrieved June 11, 2017, from BoneSmart: https://bonesmart.org/knee/types-of-total-knee-implants/

Van der Merwe, W. (2016, February 19). Personal communication. (D. Wium, Interviewer)

Viskontas, D., Skrinskas, T., Johnson, J., King, G., Winemaker, M., & Chess, D. (2007, April). Computer-assisted gap equalization in total knee arthroplasty. *The Journal of Arthroplasty, 22*(3), 334-342.

Woolhead, G. D. (2005, August 1). Outcomes of total knee replacement: a qualitaive study. *Rheumatology, 44*(8), 1032-1037.

Yoon, J., Jeong, H. O., & Yang, J. (2013, December). In Vivo Gap Analysis in Various Knee Flexion Angles During Navigation-Assisted Total Knee Arthroplasty. *The Journal of Arthroplasty, 28*(10), 1796-1800.

Zimmer. (2017, September 23). *Knee Replacement Products*. Retrieved September 23, 2017, from Zimmer: http://www.zimmer.com/medical-professionals/products/knee.html

Appendix A. Specifications

A.1 Arduino Nano specifications

The following specification were obtained from store.arduino.cc (Arduino, 2017):

Microcontroller:	ATmega328
Operating Voltage:	5 V
Flash Memory:	32 KB of which 2 KB used by bootloader
Architecture:	AVR
SRAM:	2 KB
Clock Speed:	16 MHz
EEPROM:	1 KB
Analog I/O Pins:	8
DC Current per I/O pins:	40 mA (I/O Pins)
Input Voltage:	7-12 V
Digital I/O Pins:	22
PWM Output:	6
Power Consumption:	19 mA
PCB Size:	18 x 34 mm
Weight:	7 g
Product Code:	A000005

A.2 Stepper motor specifications

Hybrid Linear Actuators

39BYGL Series

Hybrid Stepping Motor Series

General Specifications

Step Accuracy	±5%
Temperature Rise	80°C Max
Ambient Temperature Range	-20°C ~ +50°C
Insulation Resistance	100 MΩ Min. 500 VDC
Dielectric Strength	500 VAC 1s

Customized solutions on request.

Hetai Motor

Electrical Specifications

Model	Step distance	Motor Length	Rate Voltage	Rate Current	Phase Resistance	Phase Inductance	Holding Torque	Detent Torque	Rotor Inertia	Lead Wire	Motor Weight
	mm/step	L (mm)	V	A	Ω	mH	mNm	mNm	kgmc²	NO.	kg
39BYGL215A	0.01	34	12	0.4	30	42	210	11.8	0.02	4	0.18

Mechanical Dimensions

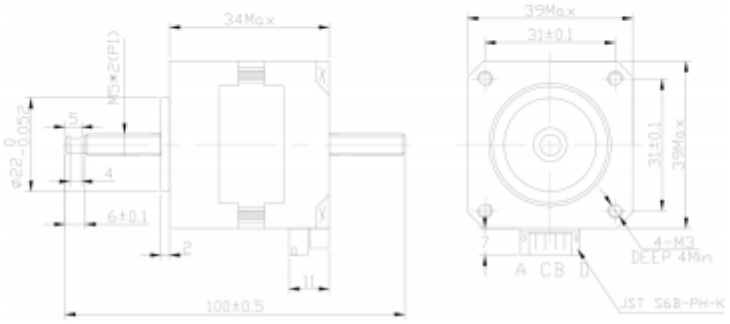

Connection Diagram

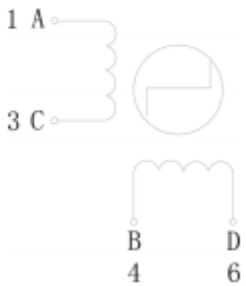

Figure A.1: Stepper motor specifications (Promoco, 2017)

A.3 Load cell specifications

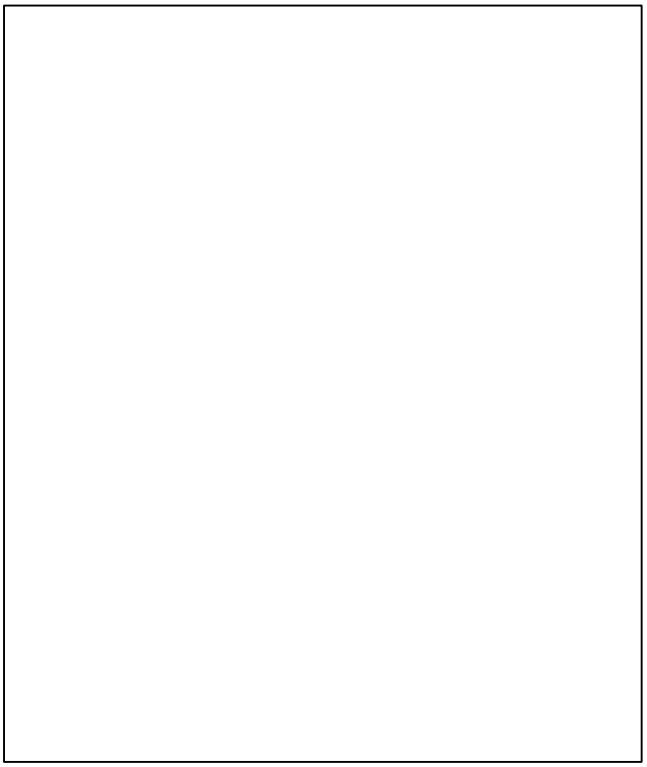

Figure A.2: Specifications of load cell (Sparkfun, 2017)

A.4 INA125 Instrumentation amplifier specifications

SPECIFICATIONS: V_S = ±15V

At T_A = +25°C, V_S = ±15V, IA common = 0V, V_{REF} common = 0V, and R_L = 10kΩ, unless otherwise noted.

PARAMETER	CONDITIONS	INA125P, U			INA125PA, UA			UNITS
		MIN	TYP	MAX	MIN	TYP	MAX	
INPUT								
Offset Voltage, RTI								
Initial			±50	±250		*	±500	µV
vs Temperature			±0.25	±2		*	±5	µV/°C
vs Power Supply	V_S = ±1.35V to ±18V, G = 4		±3	±20		*	±50	µV/V
Long-Term Stability			±0.2			*		µV/mo
Impedance, Differential			10^{11} || 2			*		Ω || pF
Common-Mode			10^{11} || 9			*		Ω || pF
Safe Input Voltage				±40			*	V

Figure A.3 Extract 1 of INA125 datasheet (Texas Instruments, 2017)

SPECIFICATIONS: V_S = ±15V (CONT)

At T_A = +25°C, V_S = ±15V, IA common = 0V, V_{REF} common = 0V, and R_L = 10kΩ, unless otherwise noted.

PARAMETER	CONDITIONS	INA125P, U MIN	INA125P, U TYP	INA125P, U MAX	INA125PA, UA MIN	INA125PA, UA TYP	INA125PA, UA MAX	UNITS
FREQUENCY RESPONSE								
Bandwidth, –3dB	G = 4		150			*		kHz
	G = 10		45			*		kHz
	G = 100		4.5			*		kHz
	G = 500		0.9			*		kHz
Slew Rate	G = 4, 10V Step		0.2			*		V/µs
Settling Time, 0.01%	G = 4, 10V Step		60			*		µs
	G = 10, 10V Step		83			*		µs
	G = 100, 10V Step		375			*		µs
	G = 500, 10V Step		1700			*		µs

Figure A.4: Extract 2 of INA125 datasheet (Texas Instruments, 2017)

APPLICATION INFORMATION

Figure 1 shows the basic connections required for operation of the INA125. Applications with noisy or high impedance power supplies may require decoupling capacitors close to the device pins as shown.

The output is referred to the instrumentation amplifier reference (IA_{REF}) terminal which is normally grounded. This must be a low impedance connection to assure good common-mode rejection. A resistance of 12Ω in series with the IA_{REF} pin will cause a typical device to degrade to approximately 80dB CMR (G = 4).

Connecting V_{REF}OUT (pin 4) to one of the four available reference voltage pins (V_{REF}BG, V_{REF}2.5, V_{REF}5, or V_{REF}10) provides an accurate voltage source for bridge applications. For example, in Figure 1 V_{REF}OUT is connected to V_{REF}10 thus supplying 10V to the bridge. It is recommended that V_{REF}OUT be connected to one of the reference voltage pins even when the reference is not being utilized to avoid saturating the reference amplifier. Driving the $\overline{\text{SLEEP}}$ pin LOW puts the INA125 in a shutdown mode.

SETTING THE GAIN

Gain of the INA125 is set by connecting a single external resistor, R_G, between pins 8 and 9:

$$G = 4 + \frac{60k\Omega}{R_G} \quad (1)$$

Commonly used gains and R_G resistor values are shown in Figure 1.

Figure A.5: Extract 3 of INA125 datasheet (Texas Instruments, 2017)

A.5 Linear ball bearing specifications

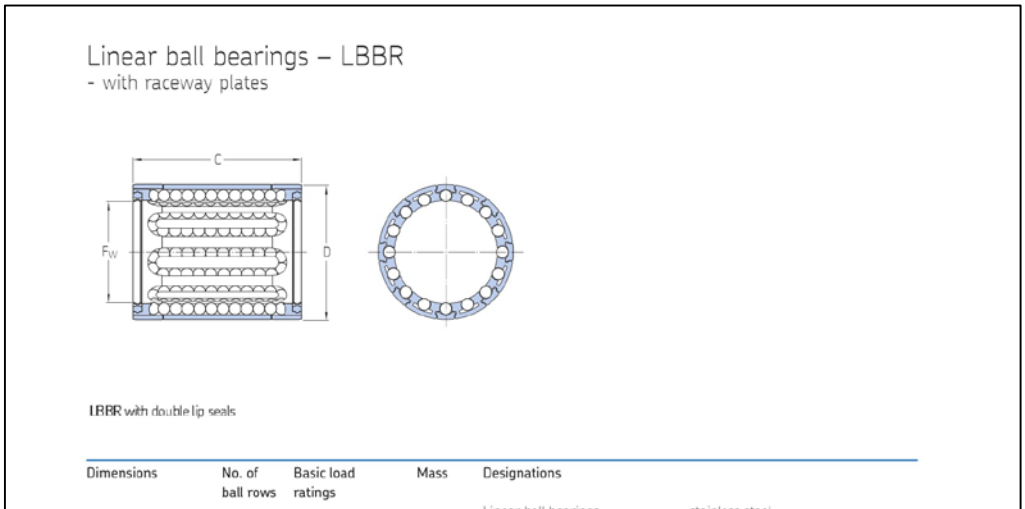

Linear ball bearings – LBBR
- with raceway plates

C
F_w
D

LBBR with double lip seals

Dimensions	No. of ball rows	Basic load ratings	Mass	Designations

Figure A.6: Linear ball bearings specifications (SKF, 2017)

A.6 InvenSense MPU-6050 specifications

Due to the size of the document, the speficiations of the IMU is not included in this thesis. The spefications document of the IMU can be found in attached CD or in the website of the manufacturers of the IMU: www.invensense.com (TDK InvenSense, 2017)

Appendix B. Engineering drawings

In this appendix, the engineering drawings of the parts of both Prototype 1 and Prototype 2. The assembly drawing of both prototypes are given along with the drawings of a selection of the most prominent parts. All the drawings were created in Autodesk Inventor (Version: Professional 2016, San Rafael, 2015).

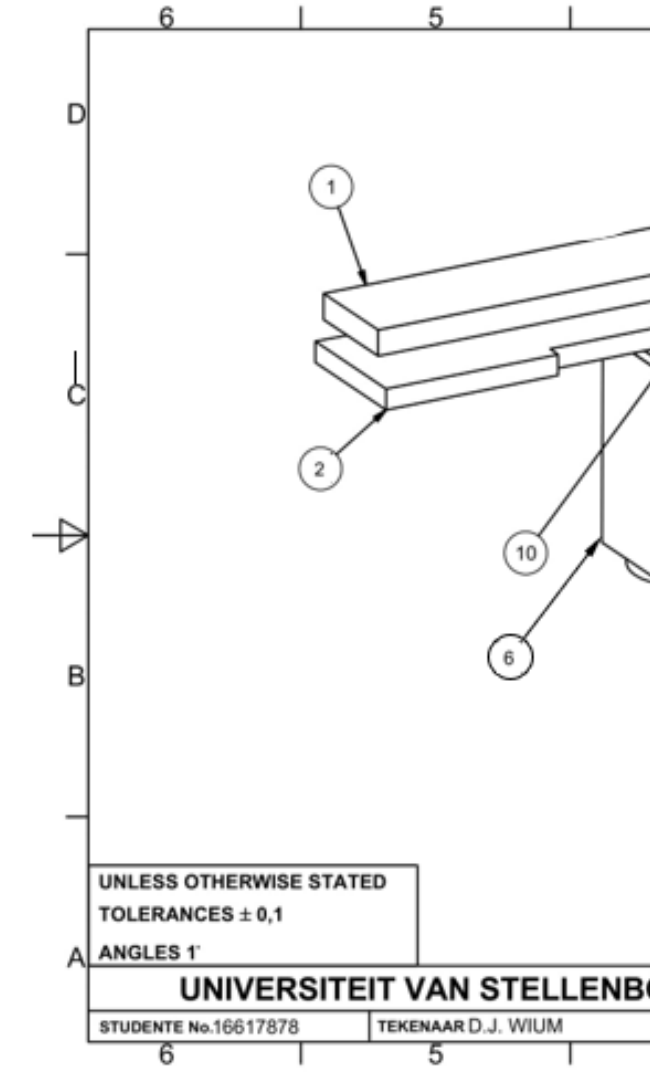

Figure B.1: Prototype 1 assembly

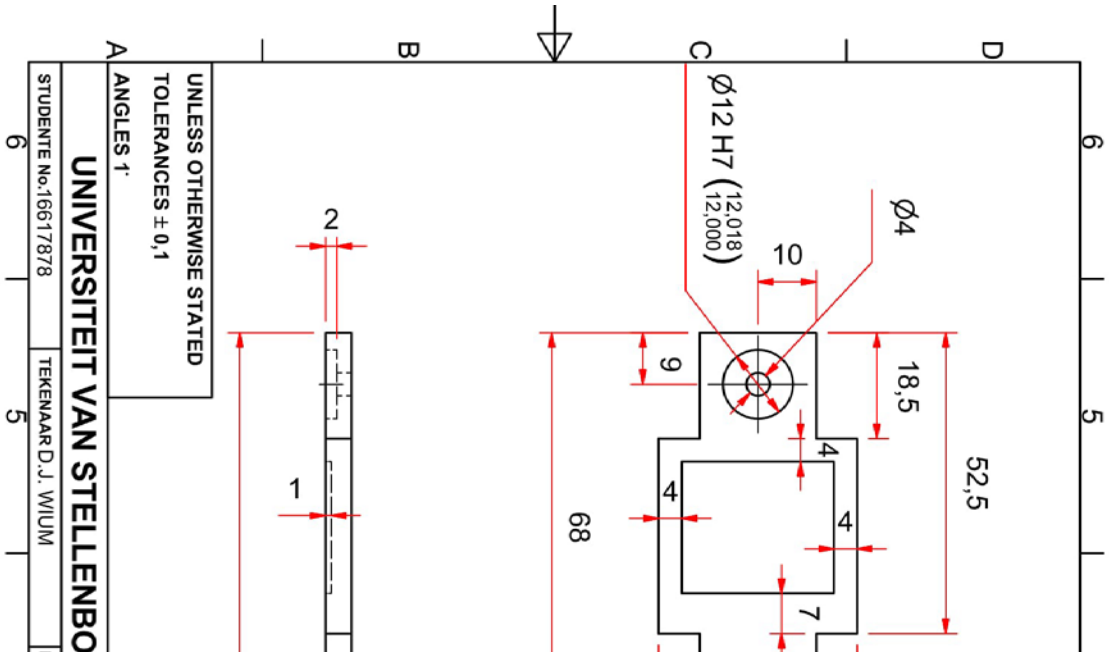

Figure B.2: Femur plate (Prototype 1)

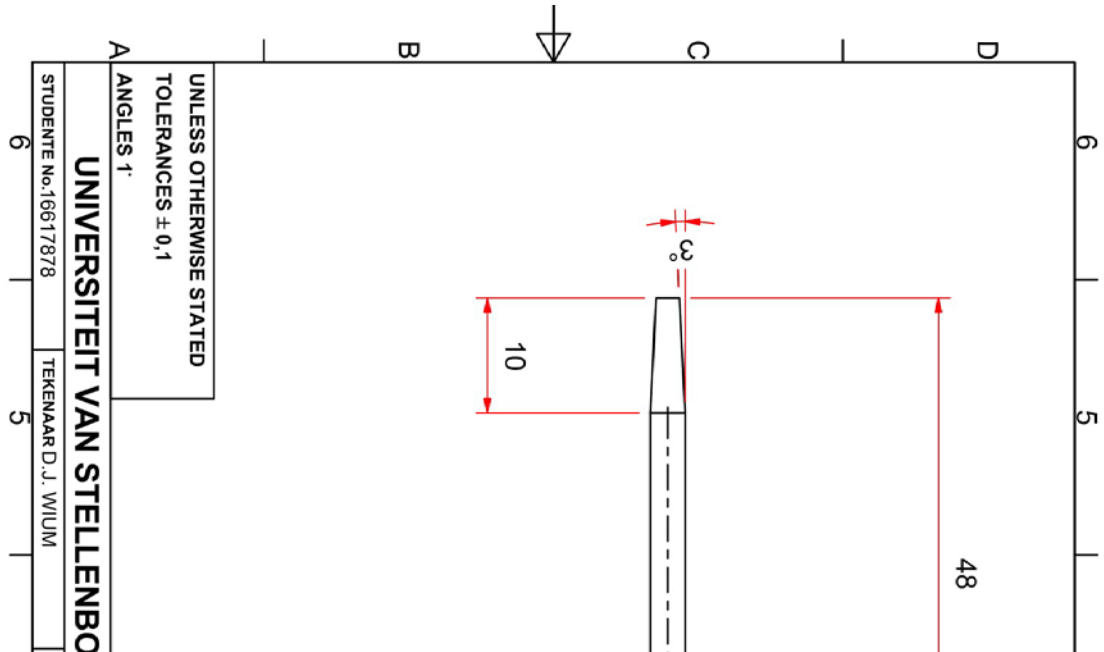

Figure B.3: Holding pin

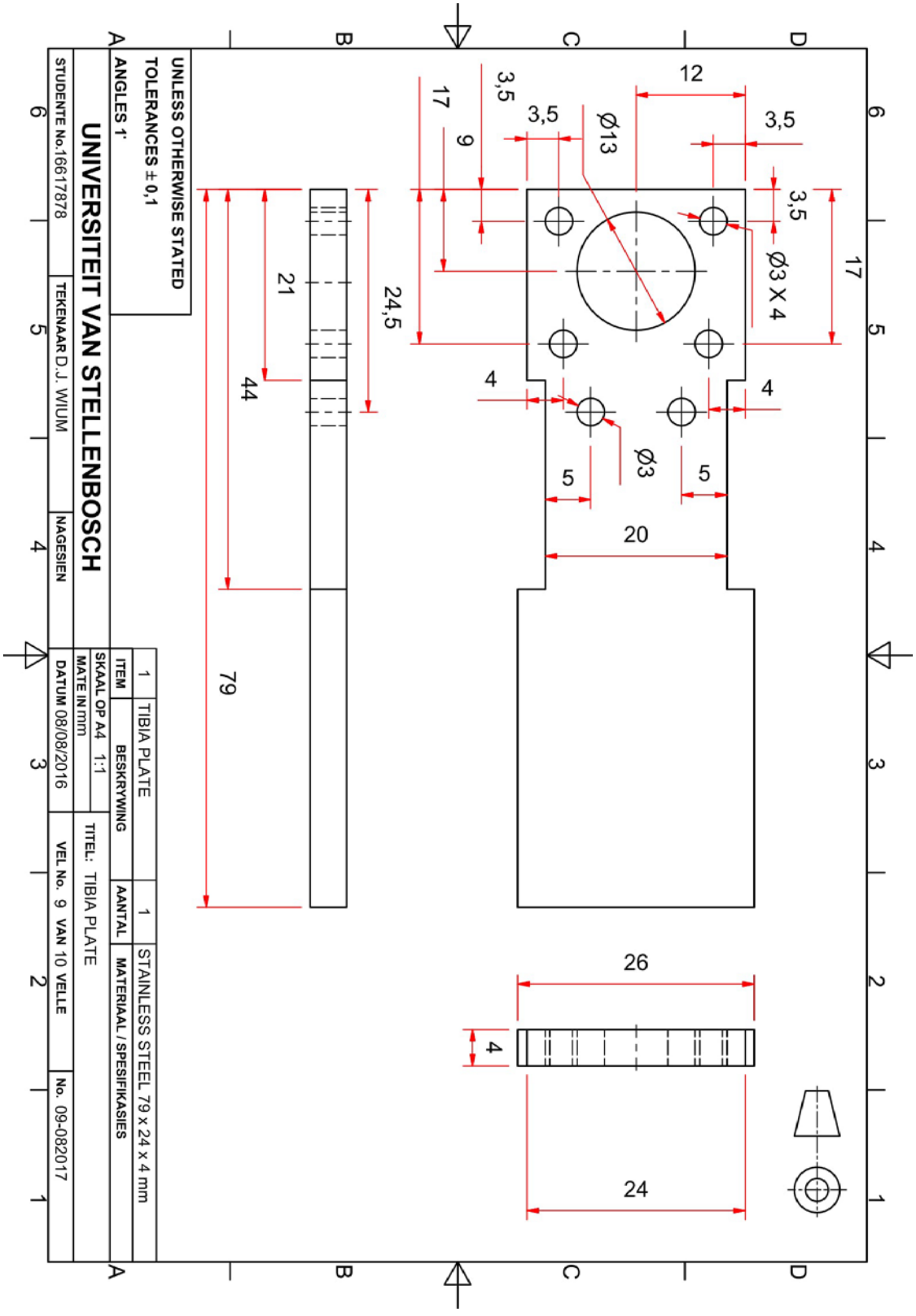

Figure B.4: Tibia plate

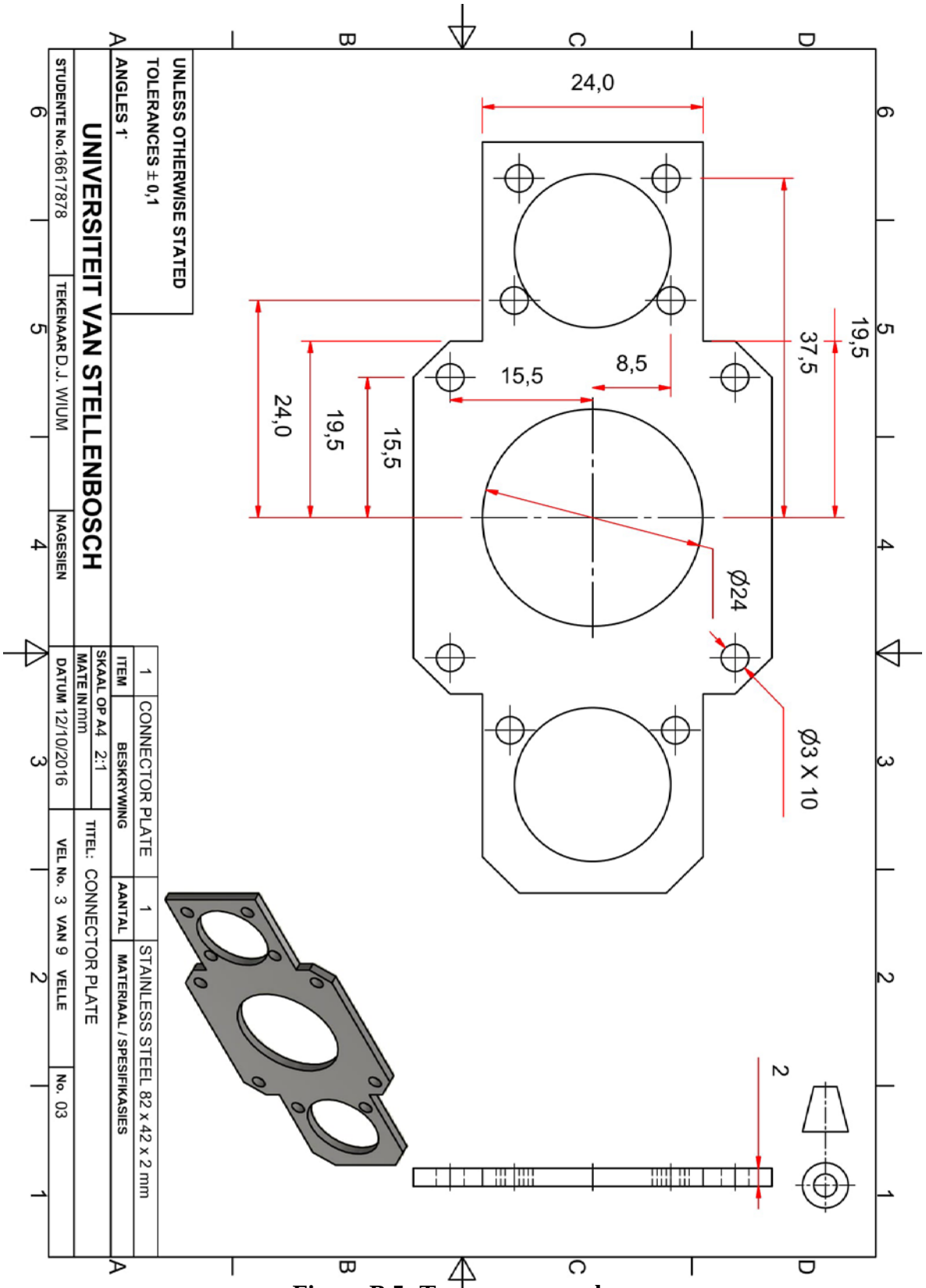

Figure B.5: Top connector plate

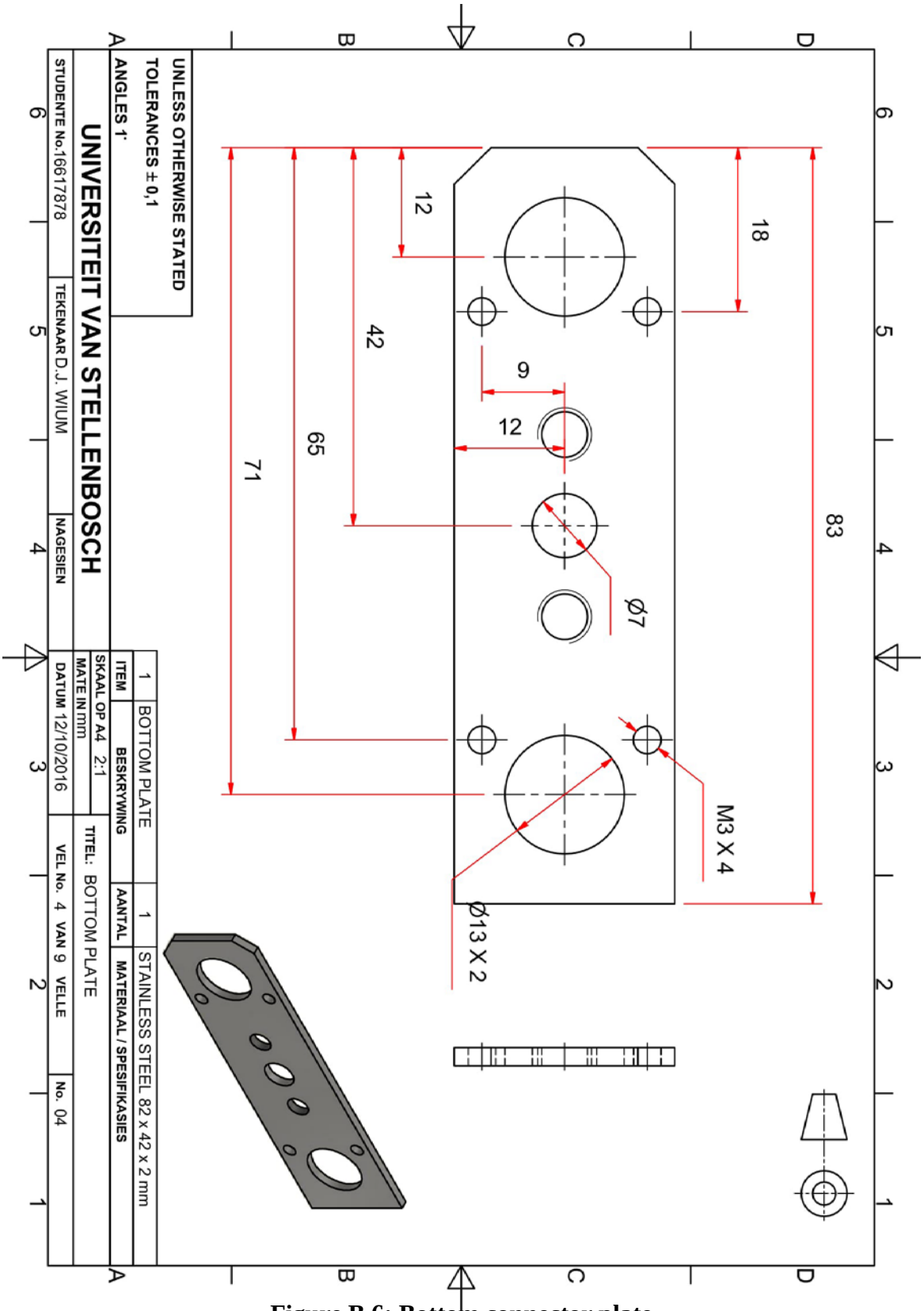

Figure B.6: Bottom connector plate

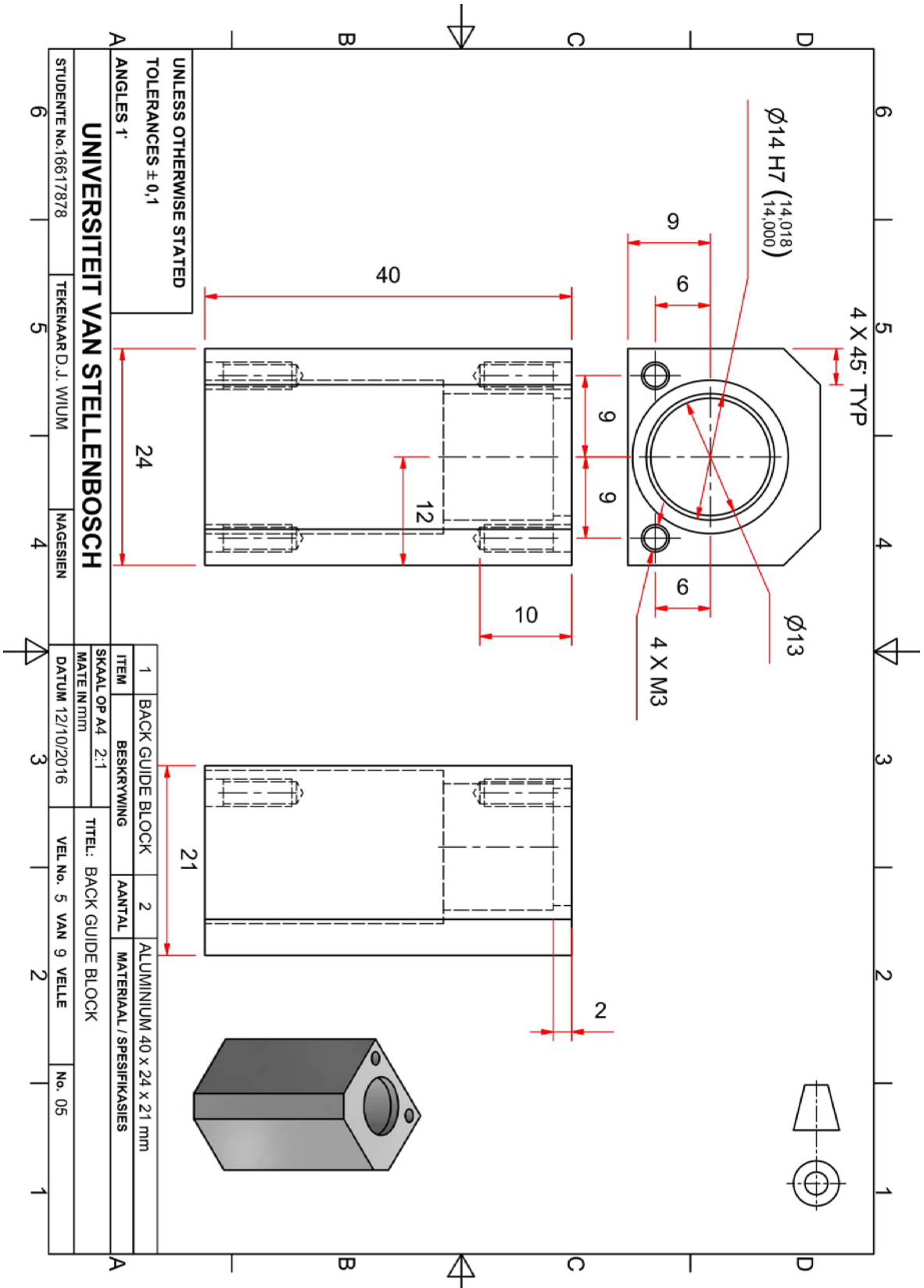

Figure B.7: Back plain linear bearing block

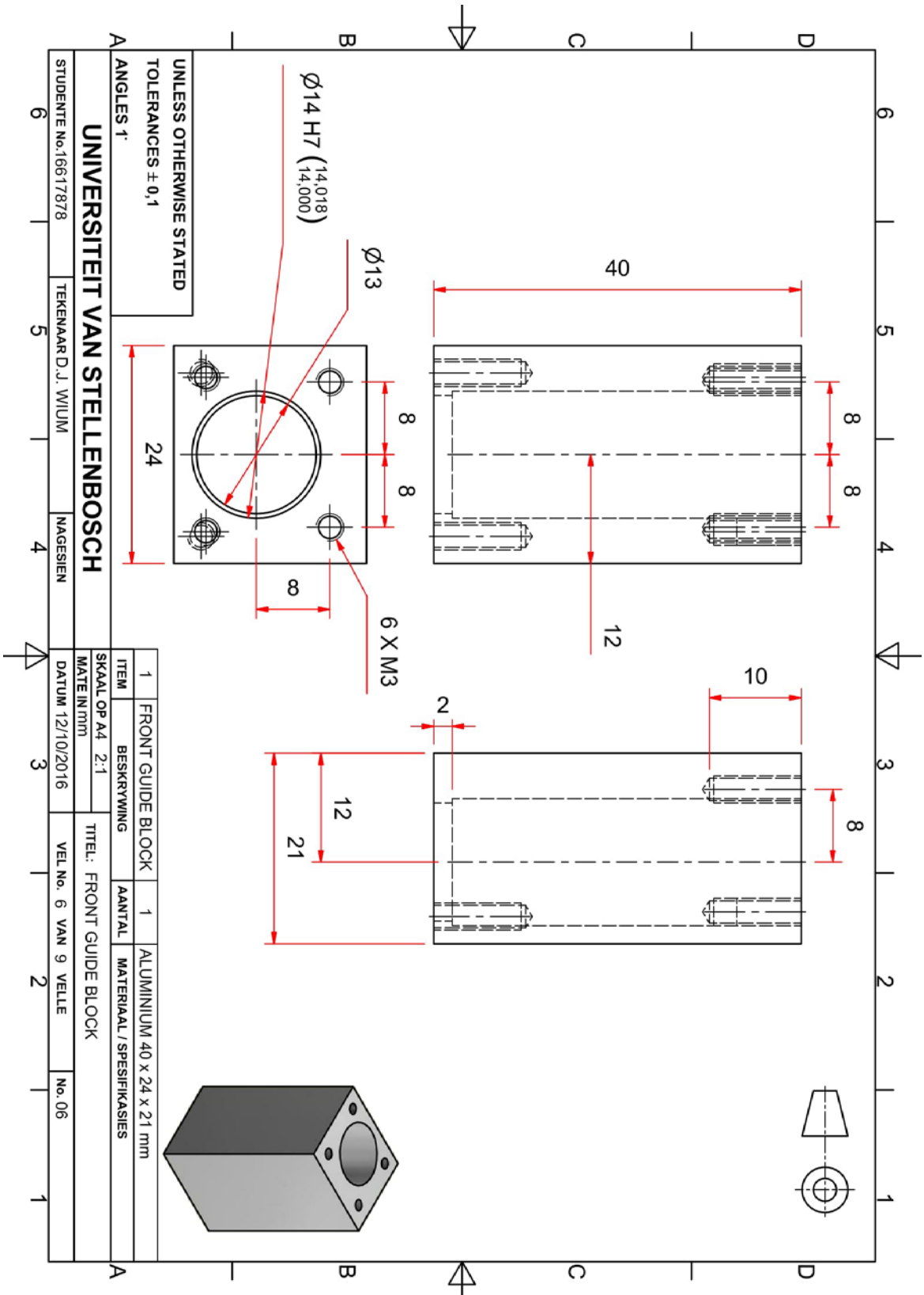

Figure B.8: Front plain linear bearing block view 1

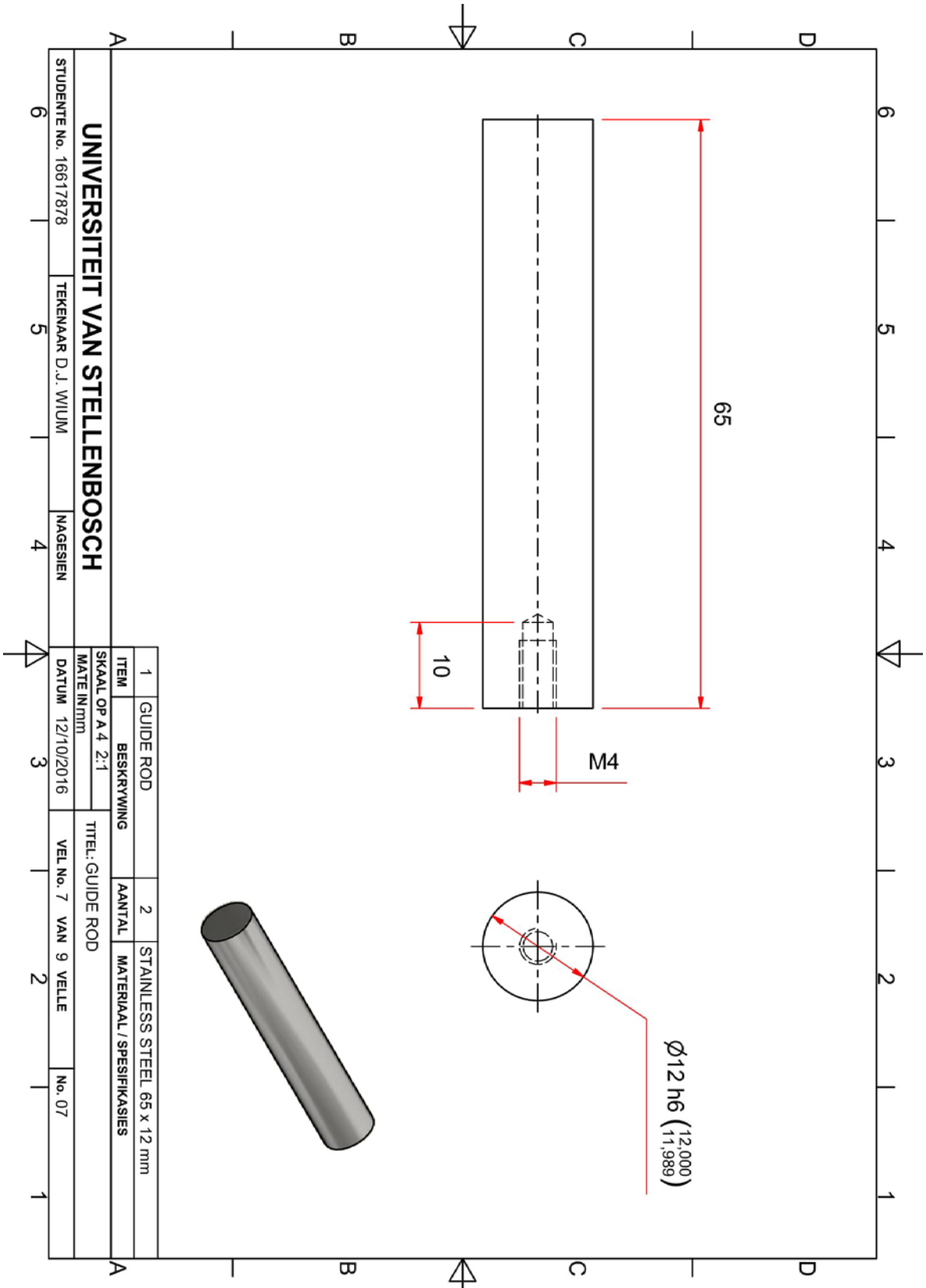

Figure B.9: Guide rod

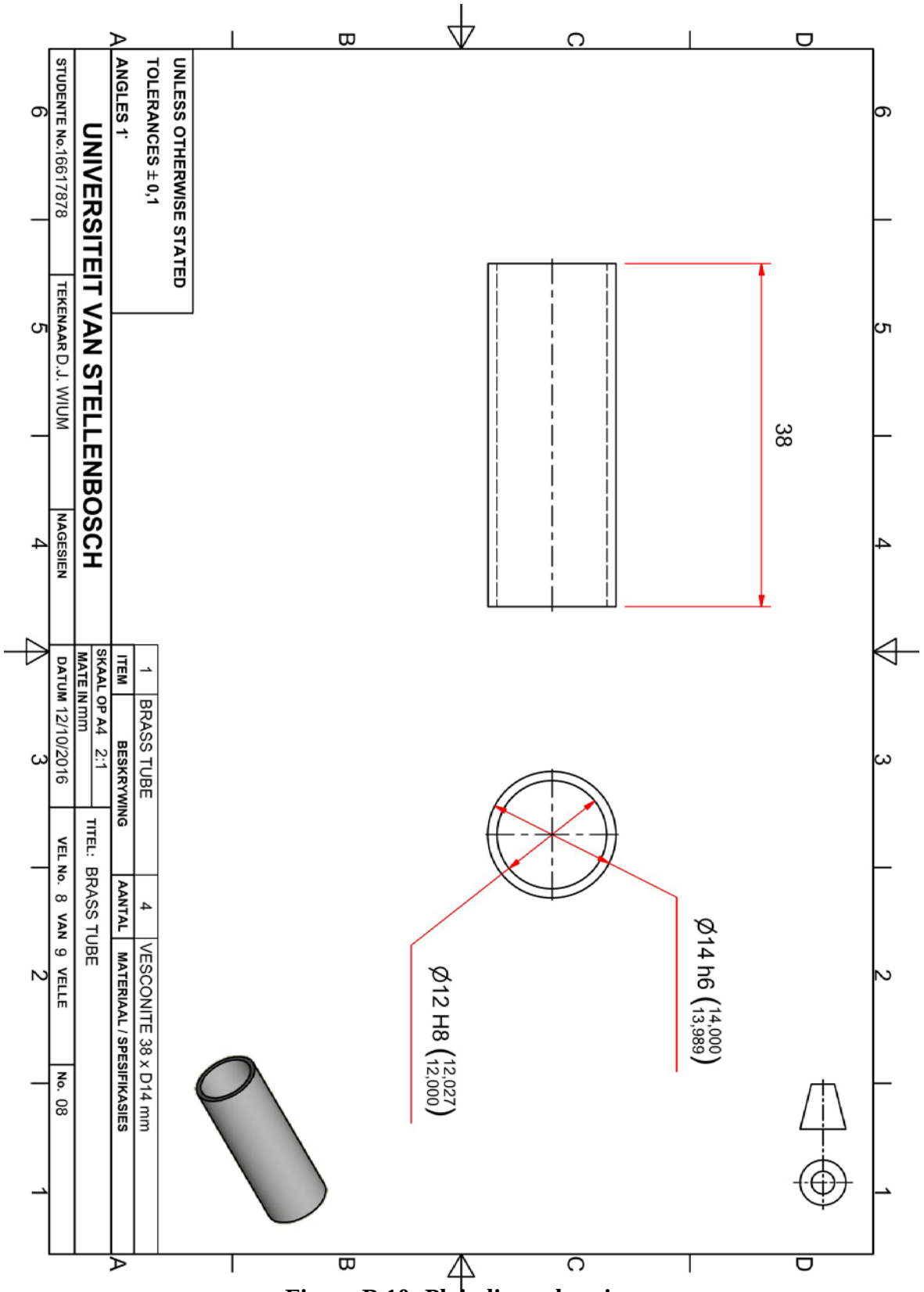

Figure B.10: Plain linear bearing

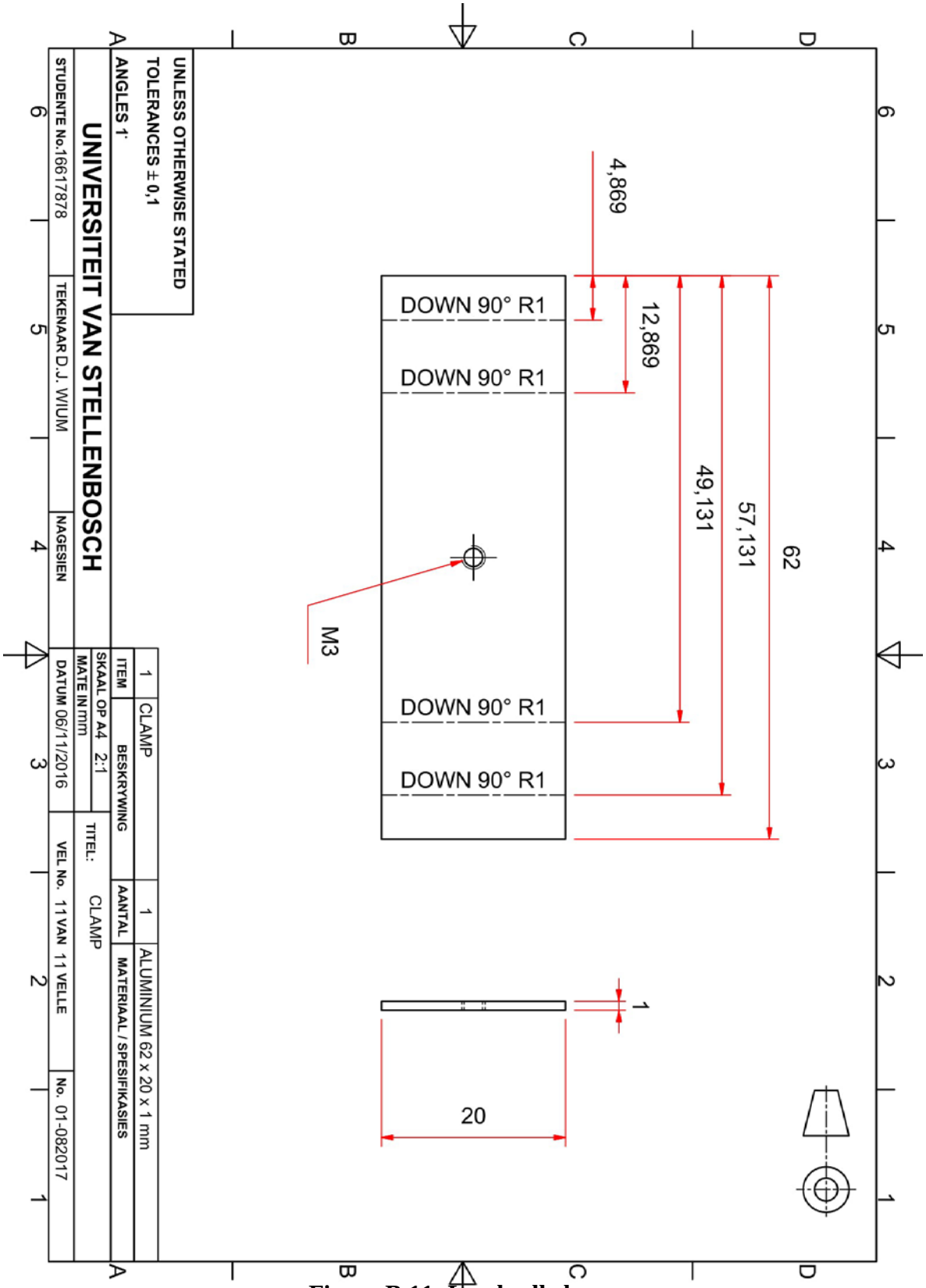

Figure B.11: Load cell clamp

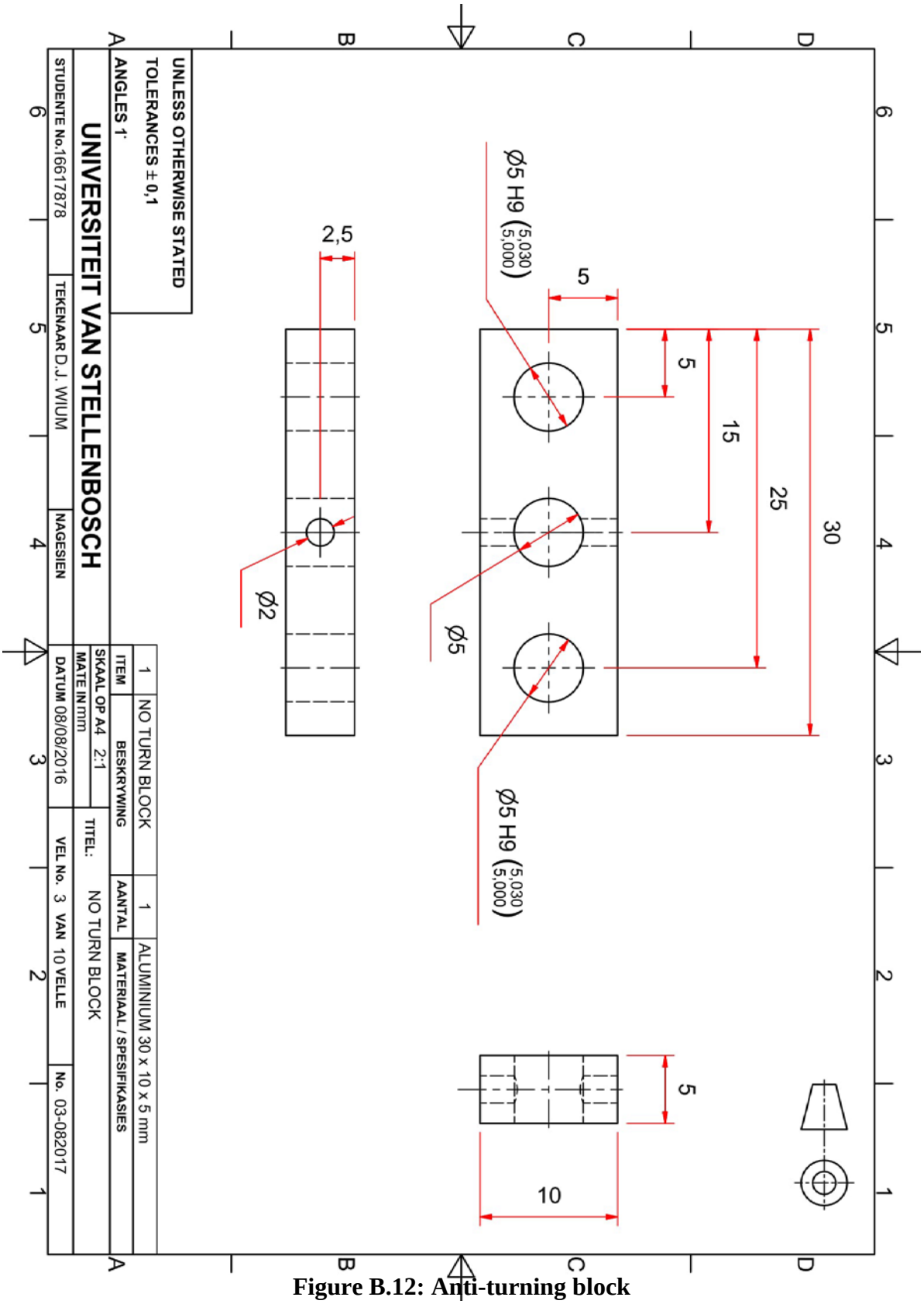

Figure B.12: Anti-turning block

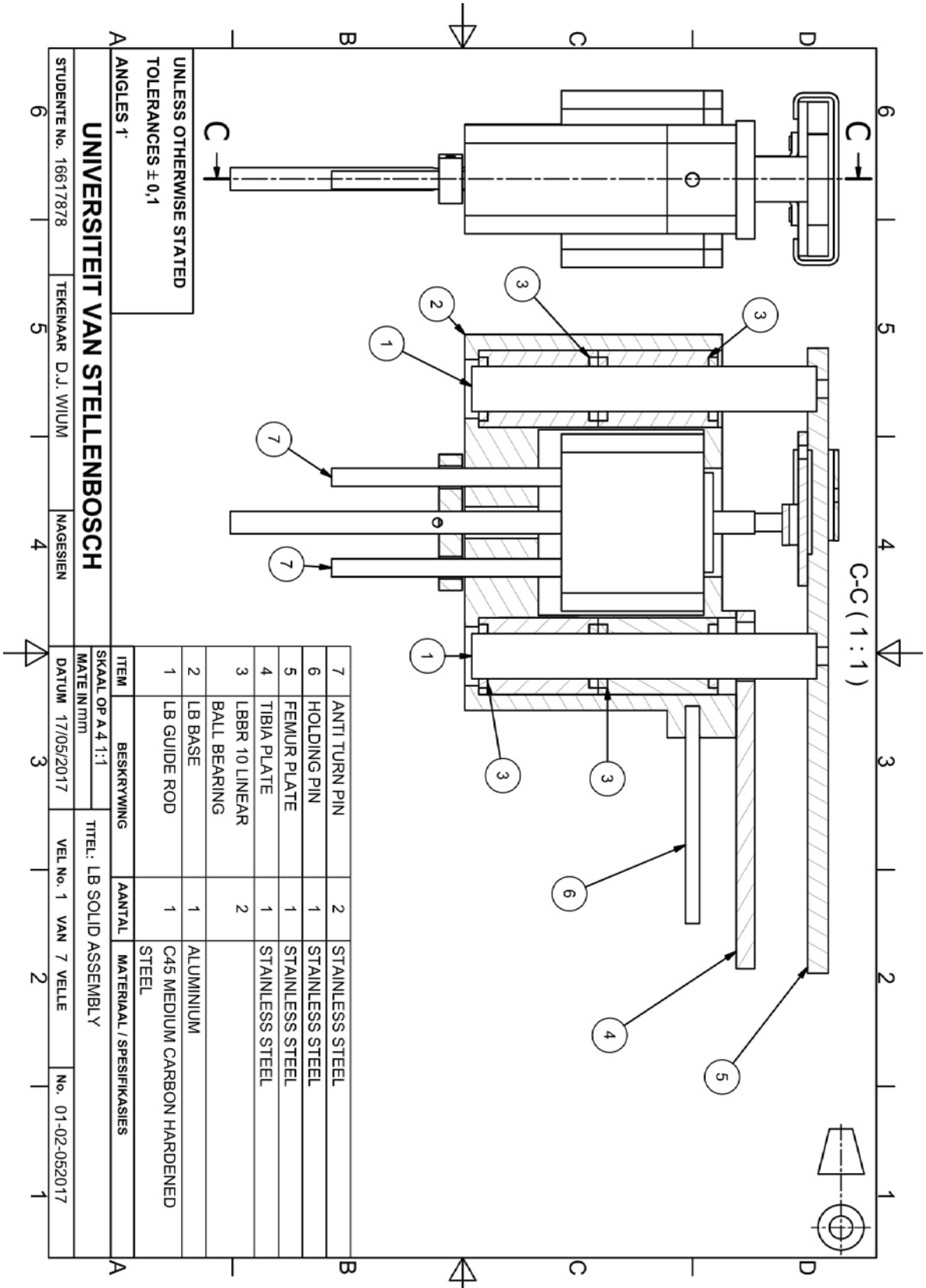

Figure B.13: Prototype 2 assembly

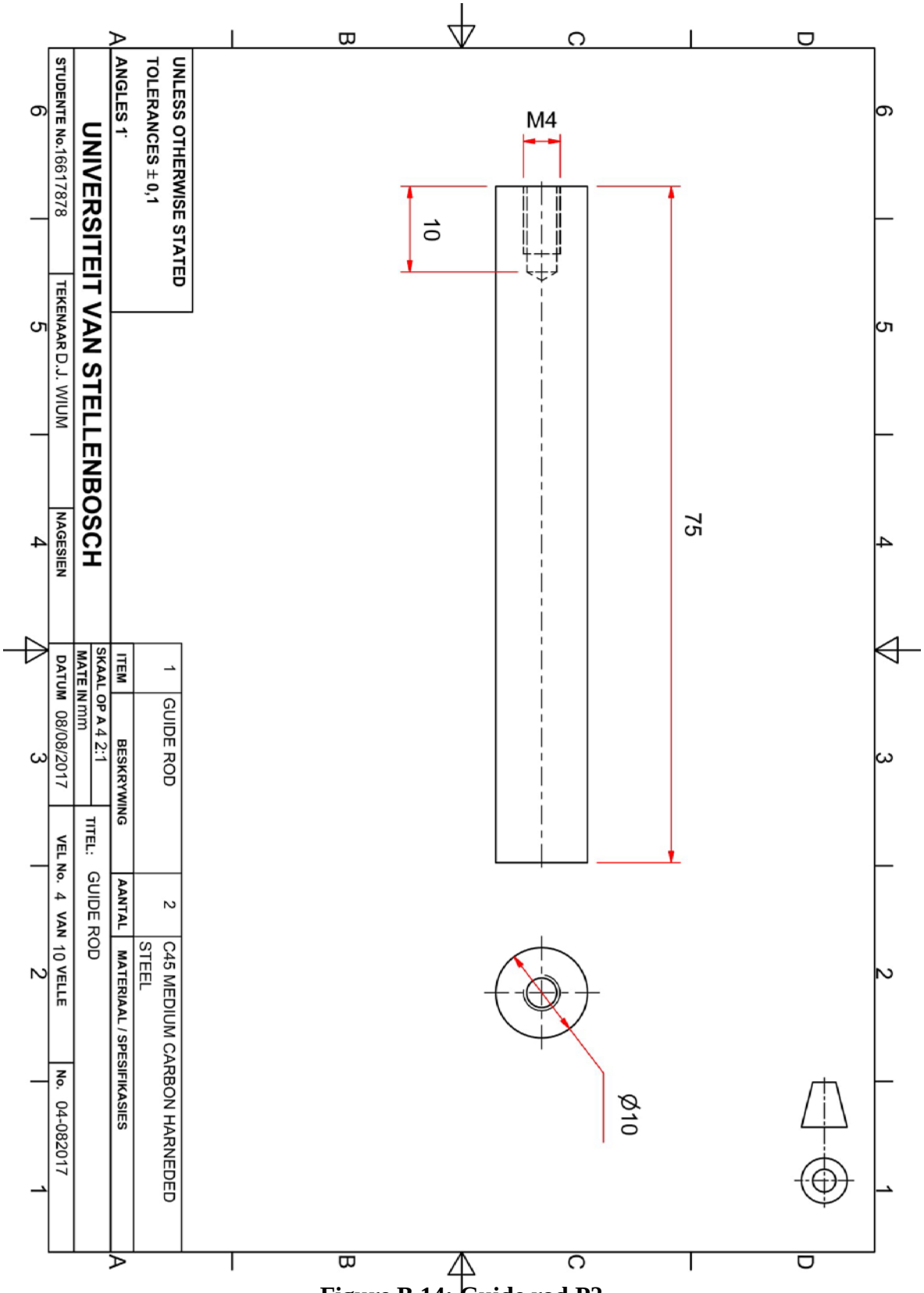

Figure B.14: Guide rod P2

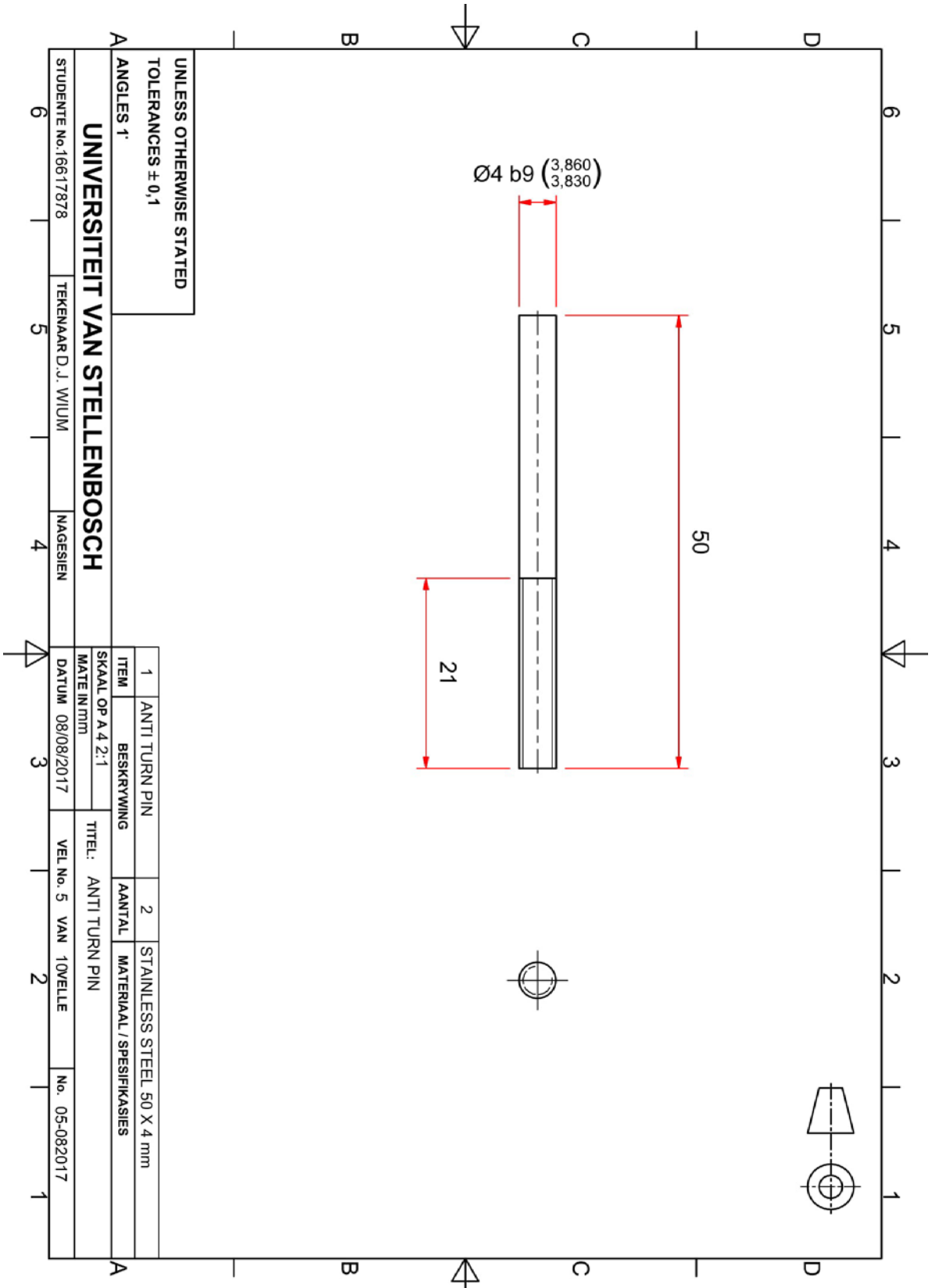

Figure B.15: Anti-turning pin

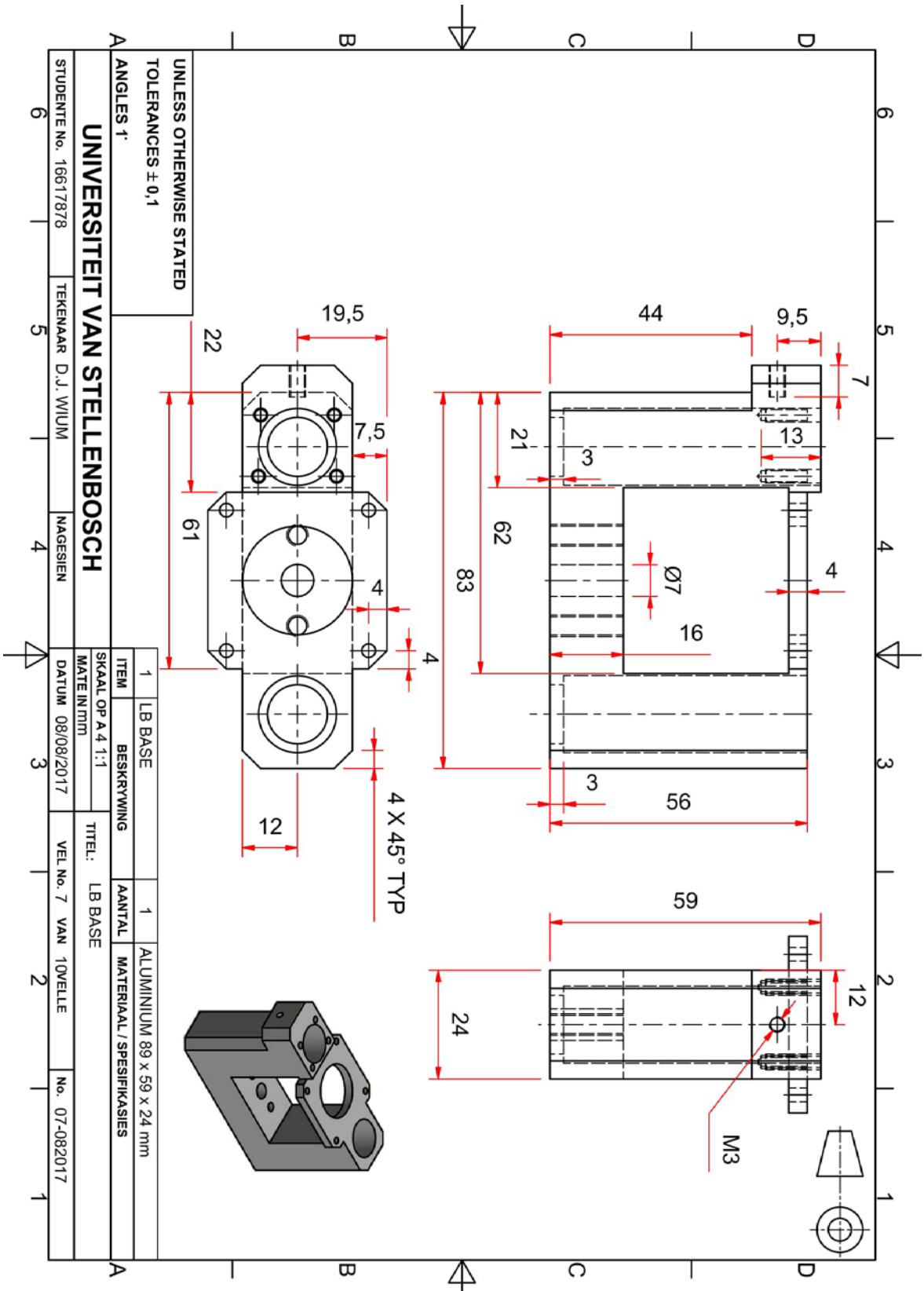

Figure B.16: Prototype 2 solid body view 1

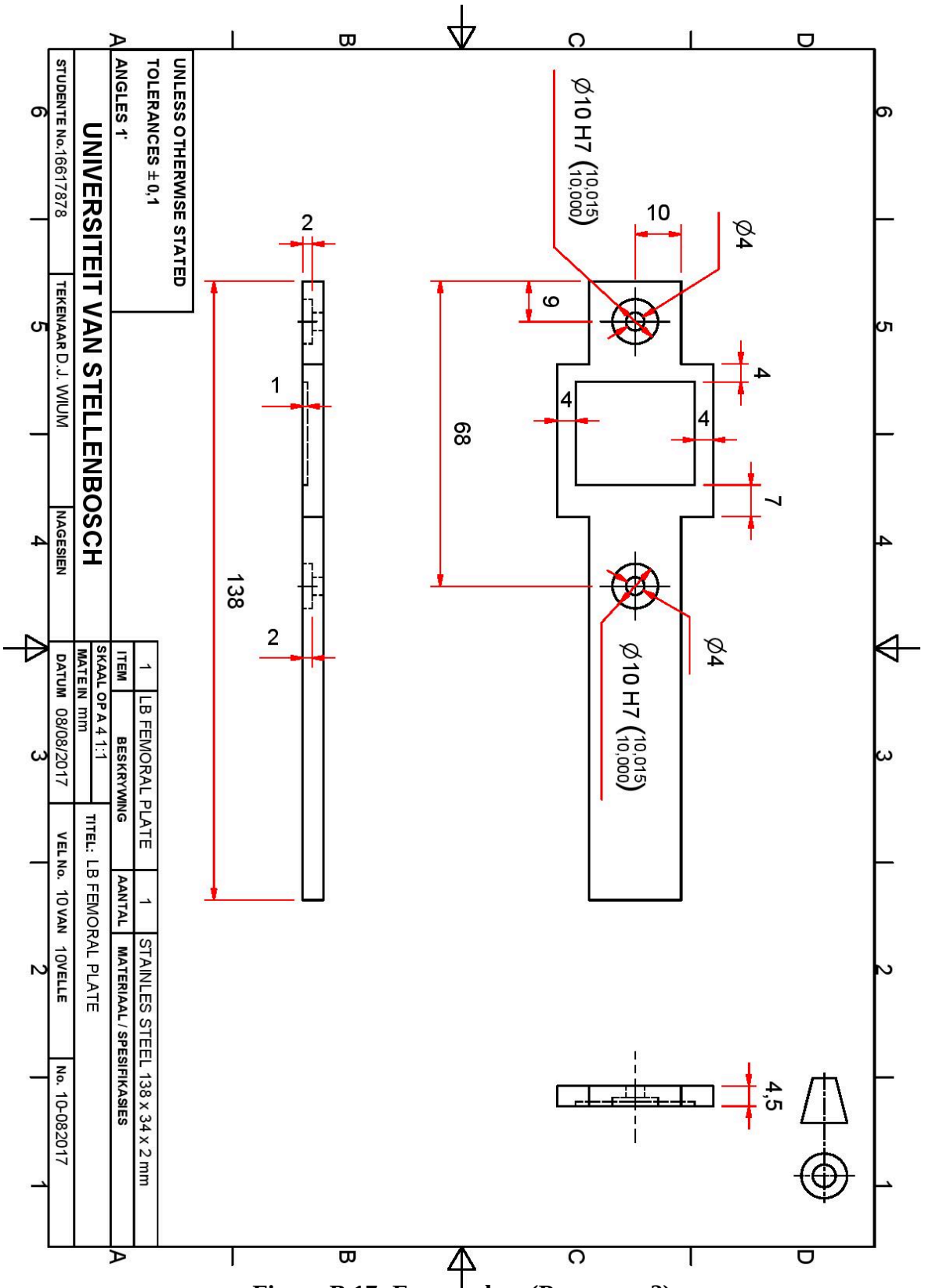

Figure B.17: Femur plate (Prototype 2)

Appendix C. GUI screenshot

In Figure C.1, a screenshot of the GUI is shown.

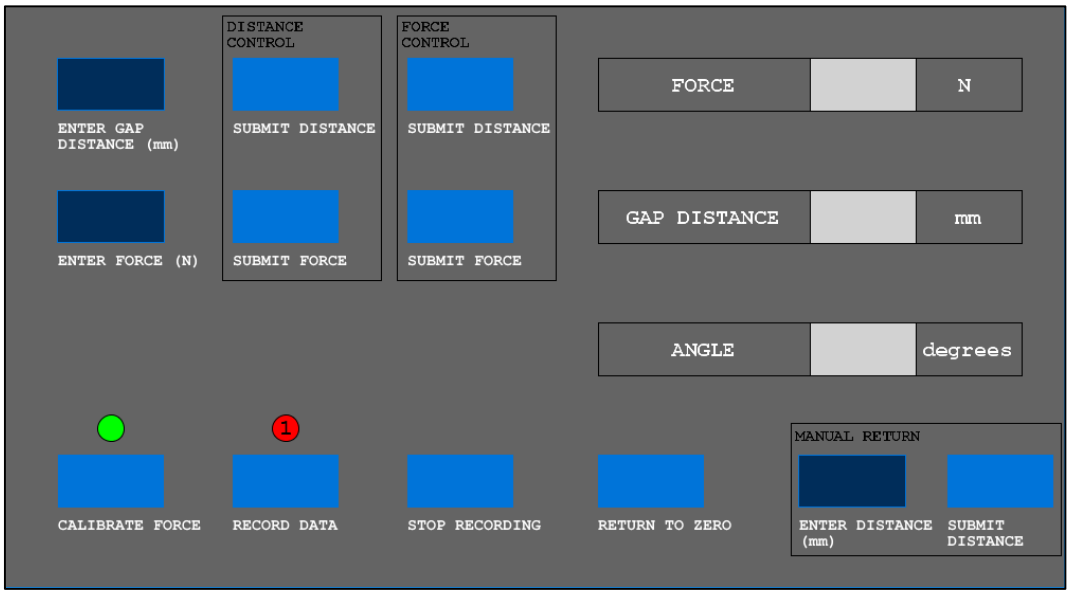

Figure C.1: Screenshot of the GUI created in Processing

Appendix D. PCB configuration

In this appendix, the components of the printed circuit board (PCB) are given along with the schematic of the PCB. The PCB was designed using the software Autodesk Eagle (Version 8.3.2, San Rafael, 2017). Even though only one knee tensioner was used in this study, the PCB was designed to accommodate the components of two knee tensioners which can be used during total knee arthroplasty (TKA) in the future. For this study, the components of one knee tensioner were placed on the PCB.

Three errors were discovered after the PCB was designed and manufactured. They were solved with practical solutions. The errors and their solutions, with reference to the pin numbers and labels in the schematic in Figure D.1, are as follows:

1. Pin 4 and pin 15 of the INA125P IC2 were not connected to pin 1 and pin 3 of the Header Pins.
   Solution: A wire was soldered to connect the pins.
2. Pin 4 and pin 15 of the INA125P IC2 were both connected to pin 4 and pin 15 pf the INA125P IC1.
   Solution: The track connecting pin 4 and pin 15 of the INA125P IC1 to pin 4 and pin 15 of the INA125P IC2 was physically scratched to as to split the track to prevent the current flow in the track.
3. Pin 4 and pin 15 of the INA125P IC1 are not connected to a Header Pin.
   Solution: Not required for this study.

Since the errors were discovered after the PCB was manufactured, the PCB layout will not be given here, so as not to mislead the reader. However, the schematic of the PCB circuit, which has been corrected for errors 1 and 2, is shown in Figure D.1. The files required for the design of a new PCB based on the schematic is provided in the attached CD.

Here follows a list of the components on the PCB in this study:

1. Arduino Nano
2. 12 row female header pins (x2)
3. DRV8825 stepper drive
4. INA125 instrumentation amplifier
5. Pushbutton (2x)
6. 180 Ω resistor
7. 20 Ω resistor
8. 10 kΩ resistor
9. 100 µF capacitor
10. Load cell (not indicated in schematic)

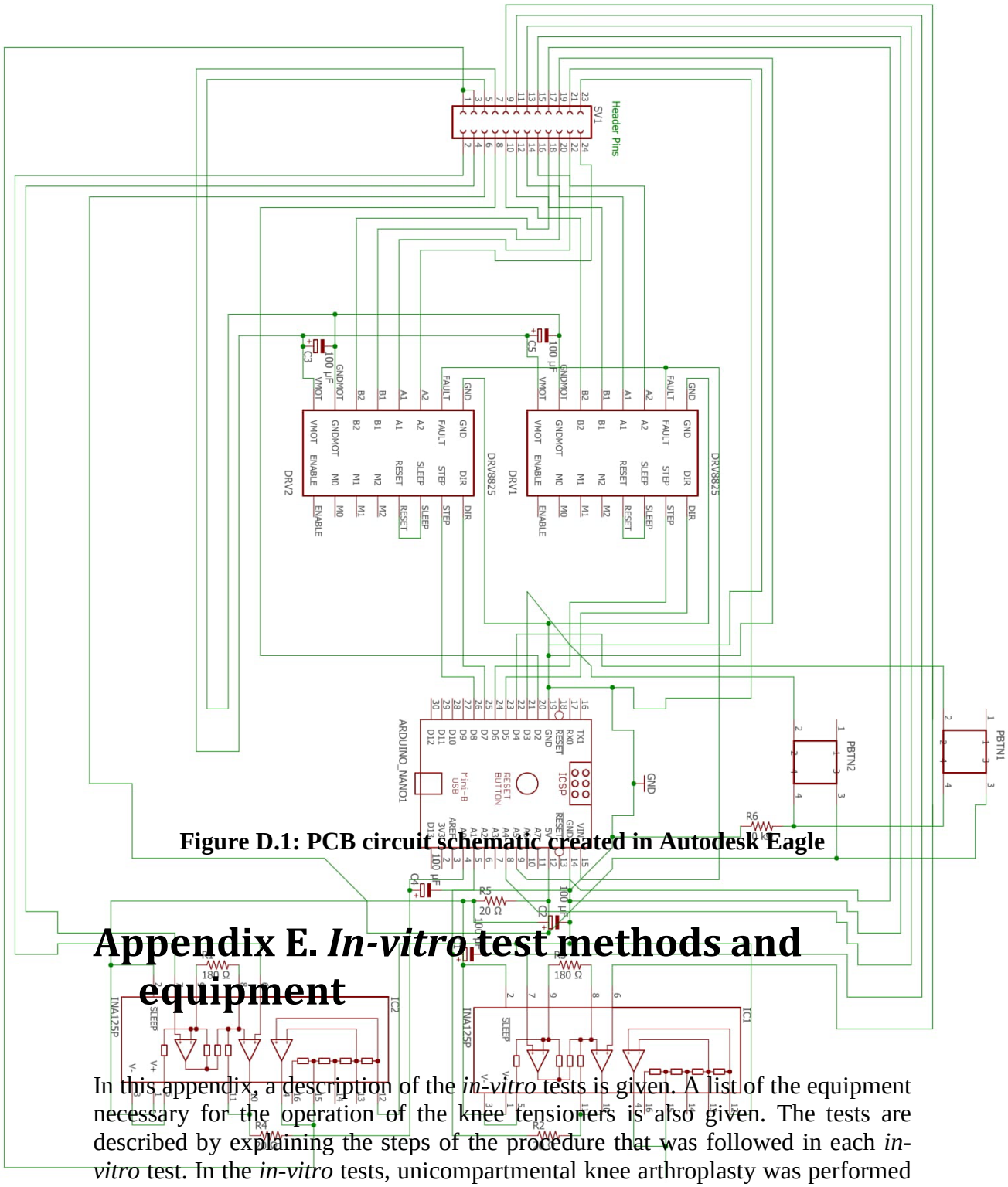

Figure D.1: PCB circuit schematic created in Autodesk Eagle

Appendix E. *In-vitro* test methods and equipment

In this appendix, a description of the *in-vitro* tests is given. A list of the equipment necessary for the operation of the knee tensioners is also given. The tests are described by explaining the steps of the procedure that was followed in each *in-vitro* test. In the *in-vitro* tests, unicompartmental knee arthroplasty was performed on cadaver knees in which the knee tensioners developed in this study were tested.

Apart from the knee tensioners themselves, additional equipment was required to operate the knee tensioners. Here follows a list of all equipment necessary to operate the knee tensioners during the *in-vitro* tests:

1. Knee tensioner device
2. Control box
3. Cables connecting
4. 12 V, 1 A wall adapter power supply
5. USB A male to mini-B cable
6. 2-point to 3-point power adapter (x2)
7. Flat-blade screwdriver
8. 4 mm Allen key
9. 2 mm Allen key
10. 3 mm Allen key
11. Small plier
12. Covering plastic roll
13. Fine point needle
14. Vernier Caliper
15. Soldering iron
16. Solder wire
17. Laptop
18. Laptop power cable
19. Scissors
20. Transparent tape
21. Small croc cables (x2)

In the following steps, the procedure of the tests is explained. These steps are not specifically based on previously defined steps of knee arthroplasty.

Step 1: Preparation

The half-body cadaver is defrosted before knee arthroplasty is performed. The cadaver is laid on the surgical table and covered in surgical draping while the leg to be operated on remains exposed. All equipment necessary for the performance unicompartmental knee arthroplasty on the cadaver is placed around the surgical table. The knee tensioners and its equipment are set up on a table in close proximity to the surgical table, as shown in Figure 58. The laptop is plugged into a wall socket via its power adapter cable. The Control Box and the Laptop are also connected via the USB cable. The Arduino code is then uploaded to the Arduino Nano and the GUI is opened with Processing on the laptop. The 12V adapter cable is then plugged into a wall power socket and connected to the Control Box. Using the GUI, a simple up and down movement of the femur plate is commanded to test whether the stepper motor works correctly.

Step 2: Computer navigation preparation (if applicable)

The position trackers of the Smith & Nephew NAVIO Surgery System or the Smith & Nephew Pi Galileo CAS system are attached to the tibia and the femur which

enables the tracking of the movement of the bones in three-dimensional space. The position trackers are inserted into holes drilled into the tibia and the femur.

Step 3: Exposing the knee

The unicompartmental knee arthroplasty procedure is initiated by the surgeon making a vertical incision on the subject knee to expose the knee, as shown in Figure E.1. The tissue on either the medial or lateral side of the knee is then pulled open. If the NAVIO Surgery System is used, the location of points on the bone is then captured by the NAVIO Surgery System in three-dimensional space. This is to allow the NAVIO Surgery System to create a 3D model of the bones. The points on the knee are also used to calibrate the NAVIO Surgery System in terms of the size of the knee, the angle of knee flexion, the varus-valgus angle, and the kinematic axis.

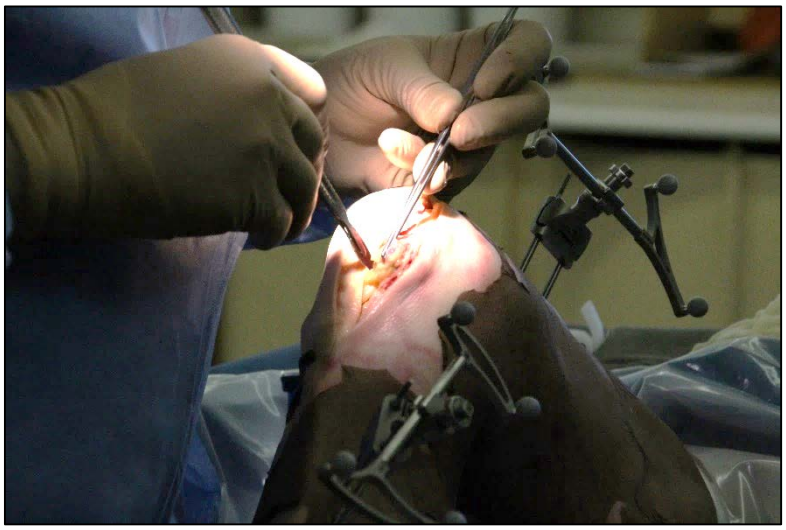

Figure E.1: Exposing the lateral side of the right knee

Step 4: Tibial resection

In order to allow the femur plate and the tibia plate to fit into the tibiofemoral gap, a gap of at least 9 mm is required between the femoral condyle and the resected surface of the tibia. Therefore, 9 mm is removed from the tibia. The surface of the resected surface has to be flat to allow all of the bottom surface of the tibia plate to be in contact with the tibia. In Figure E.2, it is shown how the tibia is resected using the NAVIO Surgery System drill. The knee after the tibial resection has been made is shown in Figure E.3.

Figure E.2: Resecting the tibia with the NAVIO Surgery System drill

Figure E.3: The knee after the tibia resection has been made

Step 5: Holding pin holes

In order to create the holes for the holding pins of the knee tensioner, the duplicate tibia plate and holding pin tool, as shown in Figure E.4, is used. The duplicate tibia plate is positioned underneath the femoral condyle and in the position where the tibia plate of the knee tensioner is to be placed. A hammer is then used to force the duplicate holding pin into the tibia to create the hole. Once the hole has been created the duplicate tibia plate and holding pin tool is removed from the bone. It may be required to strengthen the bone with bone cement before the holding pin holes are made. The bone cement is then absorbed into the bone by creating a vacuum in the bone. This prevents the tibia from disintegrating once the knee tensioner is inserted into the knee joint.

Figure E.4: Duplicate tibia plate and holding pin tool

Step 6: Knee tensioner insertion

The knee tensioner is inserted either with the knee in 0° or 90° knee flexion. The knee tensioner is inserted by hand. In Figure E.5, the knee tensioner is shown in the knee.

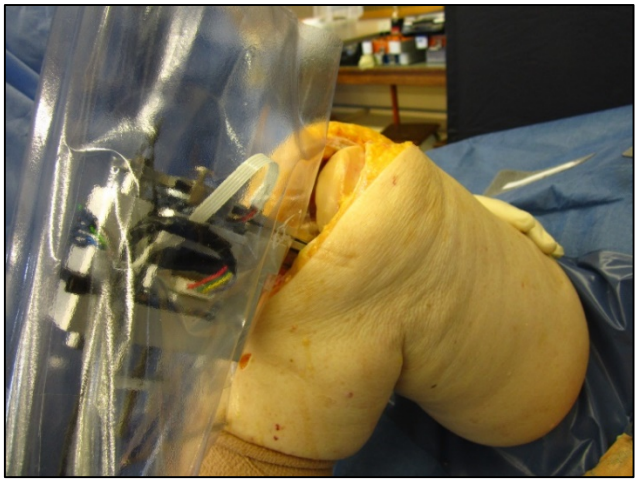

Figure E.5: Knee tensioner in knee

Step 7: Native femur data capturing

The knee tensioner is then used to measure the tibiofemoral force, the gap distance and the angle of knee flexion with the native femur as described in Section 4.3. During this step, the Pi Galileo CAS system or the NAVIO Surgery System can be used to measure the varus-valgus angle of the knee while the knee tensioner records the measurements if the position trackers do not interfere with the position of the knee tensioner in the knee.

Step 8: Replacing the femoral condyle

After the knee tensioner is removed, the femoral resections are made. The femoral resection prepares the femoral condyles for the insertion of the trial prosthetic femoral component.

Step 9: Insertion of the prosthetic femur

The correct prosthetic femoral component is chosen. The trial prosthetic femoral component is then inserted and fixed without any cement. The trial component allows the surgeon to assess whether the size of the prosthesis is correct and also whether further bone resections or ligament releases have to be made. The trail component can be removed after being inserted. In Figure E.6, the trail prosthetic femoral component is shown in the knee.

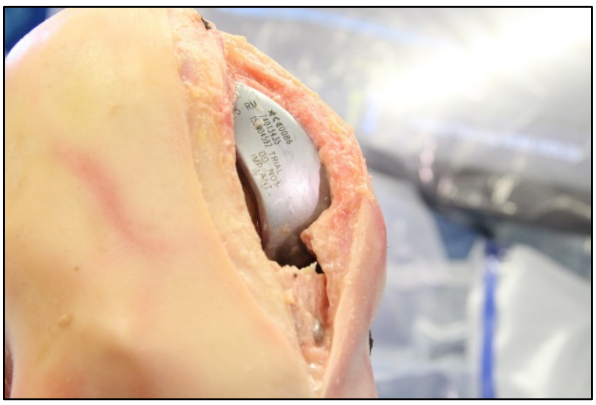

Figure E.6: Trial prosthetic femoral component

Step 10: Prosthetic femur data capturing

The knee tensioner is then again inserted into the knee joint and the measurements are recorded as described in Section 4.3.

Step 11: Test Conclusion

After measurements are recorded with the prosthetic femoral component, the knee tensioner is removed from the knee joint. All equipment is then cleaned and stored in respective packaging. The measurements recorded during the test is then briefly reviewed and discussed.

Appendix F. Femur plate analytical calculations

F.1 Femur plate deflection

In calculating the deflection of the end of the femur plate, the femur plate can be modelled as a cantilever beam. In Figure F.1, the length of the femur plate is shown that extends from the end of the plate, that is inserted into the knee, to the first guide rod. It can be assumed that the plate has a fixed end and that a point load of 150 N is exerted on the end of the plate.

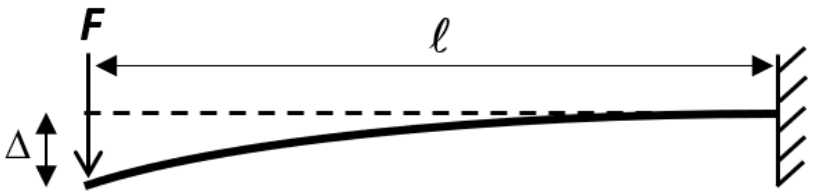

Figure F.1: Femur plate, modelled as a fixed end cantilever beam, with the force (*F*) applied at the end of the plate and deflection of the end of the plate (Δ)

The deflection of the end of the plate (Δ) is calculated with the following equation:

$$\Delta = \frac{F\ell^3}{3EI} \tag{11}$$

E is the Young's Modulus of the steel and *I* is the are moment of inertia of the plate which is calculated as follows, with *b* as the width of the plate and *h* the height of the plate:

$$I = \frac{bh^3}{12} \tag{12}$$

With $F = 150$ N, $\ell = 70$ mm, $E = 200$ GPa, $b = 20$ mm and $h = 4.5$ mm, the deflection is:

$$\Delta = \frac{(150)(0.07^3)}{3(200 \times 10^9)(\frac{(0.02)(0.0045^3)}{12})} = 0.56\ mm$$

F.2 Femur plate stress

The stress in the femur plate due to bending and shear can be calculated with the femur plate modelled as a cantilever beam, as shown in Figure F.1.

The maximum stress (σ) due to bending is calculated with the following equation:

$$\sigma = \frac{F\ell h}{2I} \tag{13}$$

For the parameters used to calculate the deflection of the end of the plate in Appendix F.1, the maximum bending stress is:

$$\sigma = \frac{(150)(0.07)(0.0045)}{2\left(\frac{(0.02)(0.0045^3)}{12}\right)} = 155.56\ MPa$$

The maximum stress due to shear force in the plate is calculated with the following equation:

$$\tau_{xy} = \frac{3F}{2bh} \tag{14}$$

Then for the same parameters used for the maximum bending stress, the maximum shear stress is:

$$\tau_{xy} = \frac{3(150)}{2(0.02)(0.0045)} = 2.5\ MPa$$

To test whether the beam will yield, Tresca's Maximum Shear Stress failure theory is applied. The failure theory states that yielding will occur if the maximum shear stress (τ_{xy}) is larger or equal to half the yielding stress (σ_y) of the material:

$$\tau_{max} \geq \frac{\sigma_y}{2} \tag{15}$$

The maximum shear stress is calculated as follows:

$$\begin{aligned} \tau_{max} &= \sqrt{\left(\frac{\sigma}{2}\right)^2 + \tau_{xy}^2} \\ &= \sqrt{\left(\frac{155.56}{2}\right)^2 + 2.5^2} \\ &= 77.82\ MPa \end{aligned} \tag{16}$$

With the yield stress of steel is approximately 215 MPa:

$$\frac{\sigma_y}{2} = 107.5\ MPa > \tau_{max}$$

Therefore, yielding will not occur.

Appendix G. Additional *in-vitro* test results

G.1 Tibiofemoral forces with Fore Control function

In this appendix, the tibiofemoral forces are shown for the Force Control function which correlate with the results given and explained in Chapter 5.

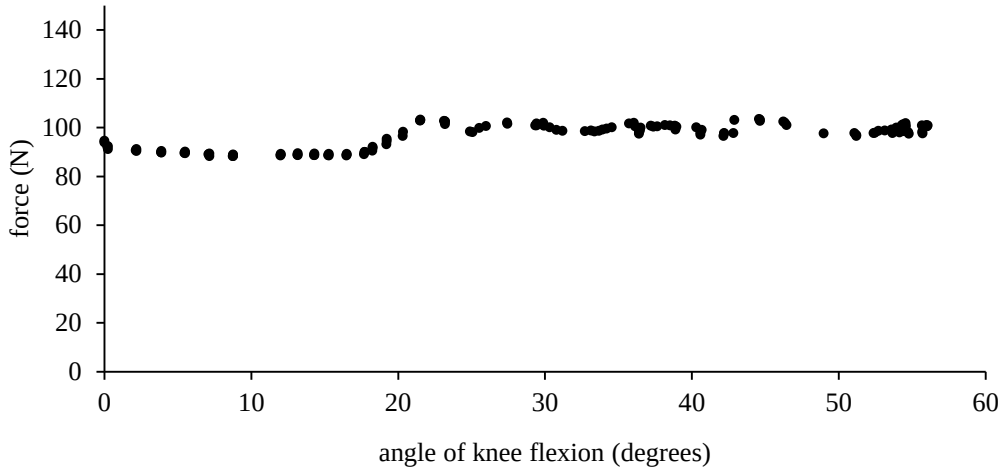

Figure G.1: Test 2 result - Tibiofemoral force in the native medial compartment of the right knee

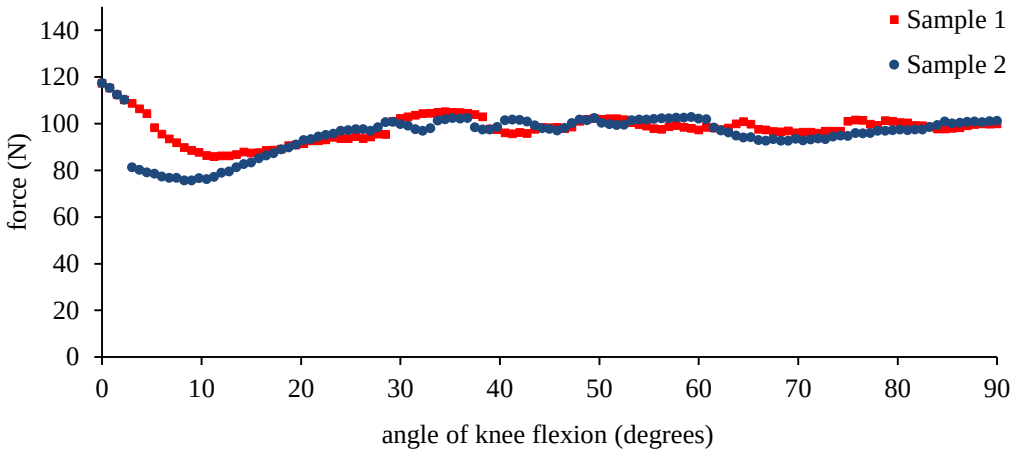

Figure G.2: Test 2 result - Tibiofemoral force in the prosthetic medial compartment of the left knee

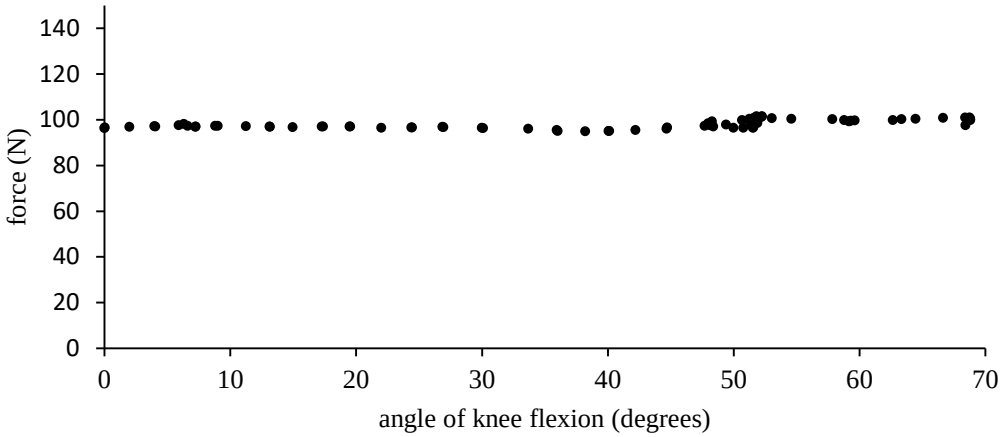

Figure G.3: Test 3 result - Tibiofemoral force in the native medial compartment of the left knee

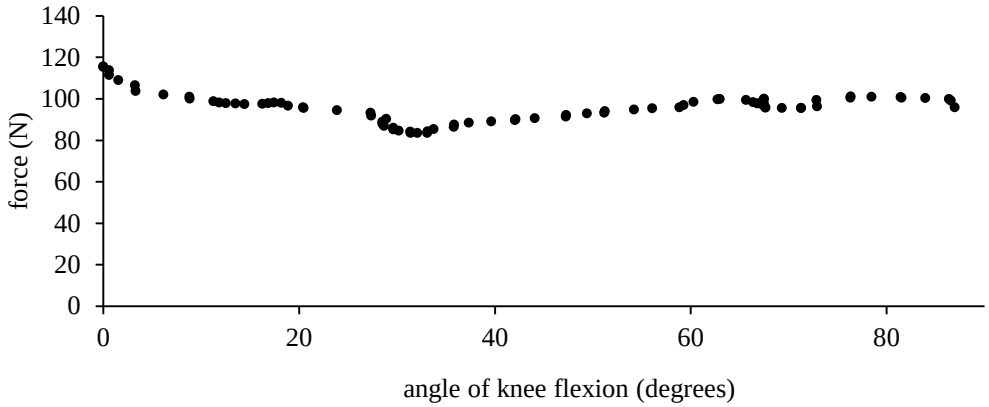

Figure G.4: Test 3 result - Tibiofemoral force in the Journey Uni 2 medial compartment of the left knee

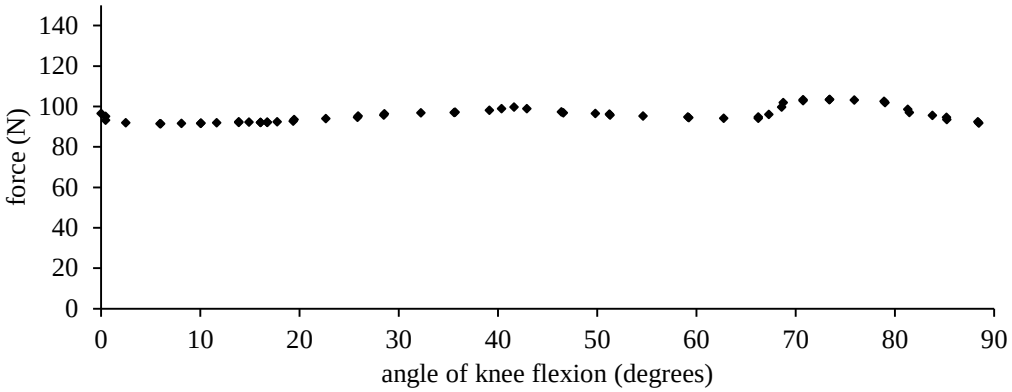

Figure G.5: Test 3 result - Tibiofemoral force in the Arthrex medial compartment of the left knee

G.2 Varus-valgus angle

In this appendix, the varus-valgus angle of the prosthetic medial compartment of the left knee during dynamic measuring with the Constant Distance function is given. These results correlate with the results of Test 3 as given and explained in Chapter 5.

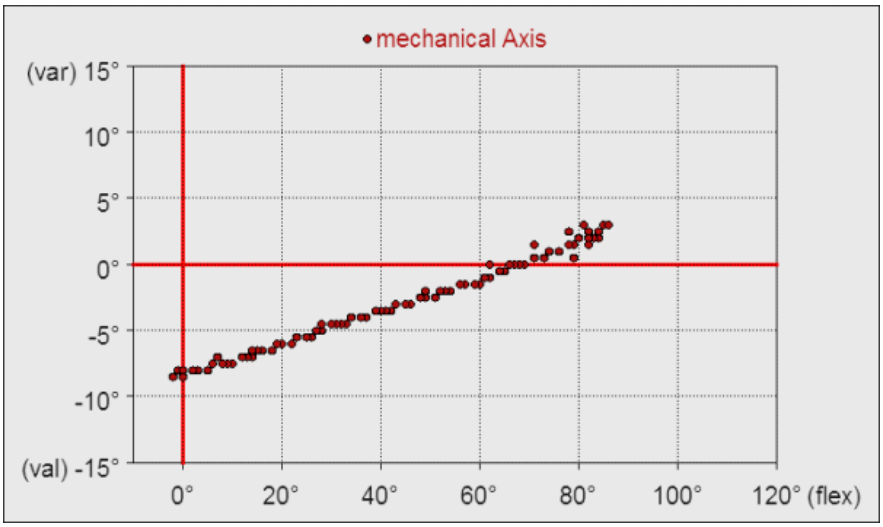

Figure G.6: Test 3 result - Varus-valgus angle with constant gap distance of 10 mm

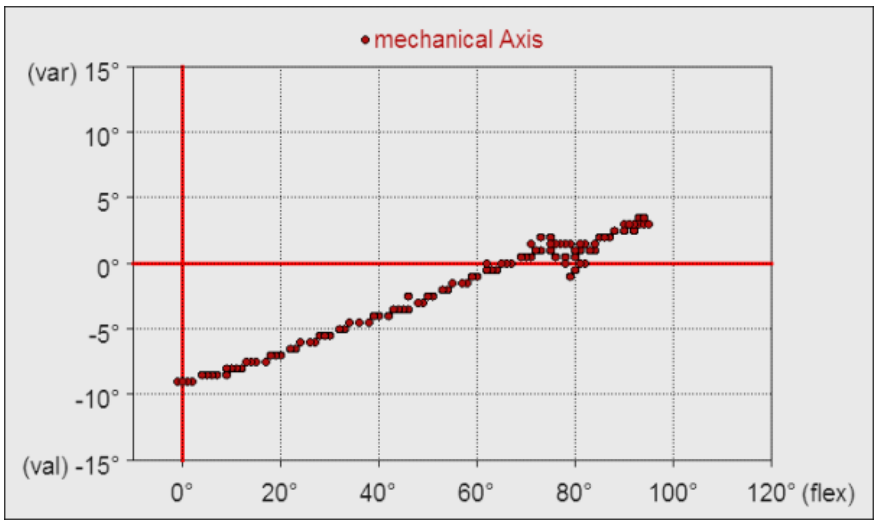

Figure G.7: Test 3 result - Varus-valgus angle with constant gap distance of 13 mm

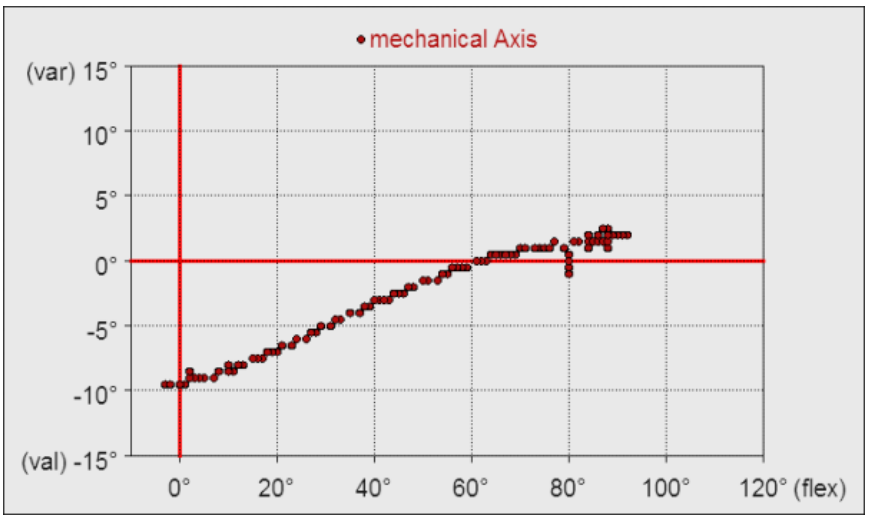

Figure G.8: Test 3 result - Varus-valgus angle with constant gap distance of 14 mm

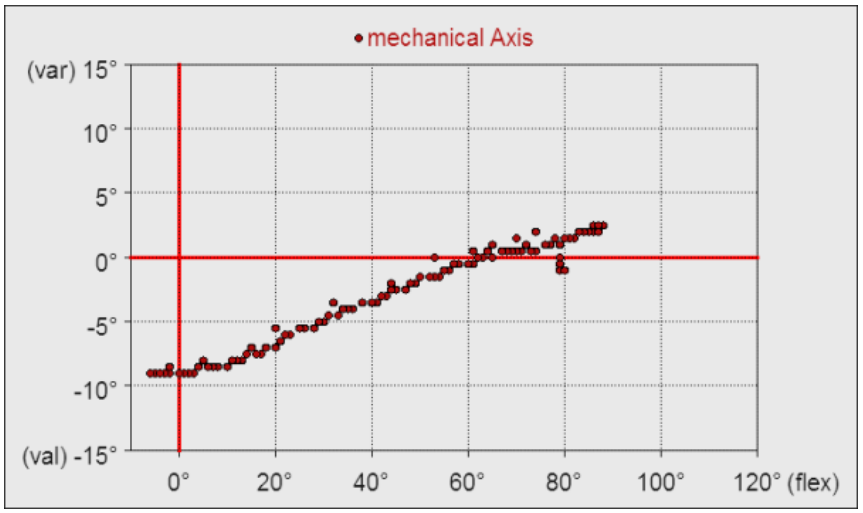

Figure G.9: Test 3 result - Varus-valgus angle with constant gap distance of 15 mm